UNIVERSITY OF SOUTHAMPON

The WaveGyro

Gebhard Waizmann

gebhard@mohrenstetten.de

Master of Science

SCHOOL OF ENGINEERING SCIENCE

September 2011

Abstract

Climate change, environmental pollution and the proceeding resource depletion give awareness of the necessity towards more sustainable energy economics. Energy from ocean waves may once play a contributing role towards this step but is as yet in its fledgling stages. This is mainly due to the harsh sea environment, which implies the need for simple and robust wave energy converter. The work presented in this thesis picks up this thought when dealing with the so-called WaveGyro. Introductory chapters explain how this novel concept arose, followed by a detailed explanation of the working principle.

The WavGyro utilizes gyroscopes to provide an internal reaction moment against the wave excitation. This internal reaction permits designing a completely enclosed and thus environmentally resistant device. The gyroscopic precession is used to convert the wave-induced moment into a moment that accelerates the flywheels. Equations of motion, which describe the gyroscope kinetics, are deduced. The gyroscopic motions and moment is then implemented into the first-order wave hydrodynamics. Two main approaches to describe the wave excitation are presented. The first approach is superposition of radiation and excitation and the second approach makes use of the relative motion principle, which relates the excitation to the extent of displacement. Both approaches are employed to deduce the maximum power capture condition in relation to the device's dimensions and operational parameters.

The influence of real sea state, analytically expressed by the Pierson-Moskowitz spectrum, on the optimum power analysis is considered and implementation methods are developed. Subsequently the spin-up mechanism is explained and examined; this is the mechanism converting the precession moment into torque accelerating the flywheel. It is shown that a simple configuration, composed of an ordinary cogwheel and a sprag-clutch only is not sufficient for this mechanism. Ideas for alternative mechanisms are considered but require further investigation to allow conclusive results.

Finally, an approximate plan for the design of model is developed, which includes basic considerations of scaling laws. Recommendations for further theoretical and practical work on the WaveGyro are provided.

Contents

Abbreviations

DOF	Degree Of Freedom
FROG	French's Reactionless Oceanic Generator
ISWEC	Inertial Sea Wave Energy Converter
MHD	Magneto Hydrodynamic
OWC	Oscillating Water Column
OWSC	Oscillating Wave Surge Converter
PTO	Power Take-Off
SEAREV	Système Électrique Autonome de Récupération d'Énergie des Vagues (autonomous power system for the recovery of energy from waves)
WEC	Wave Energy Converter
CG	Center of Gravity

Glossary

capture ratio	is the power captured relative to the incoming power (usually per width).
Gantt Chart	is a special bar type chart that illustrates the schedule of a project.
gimbal	is a pivoted suspension that allows the rotation of a body about a single axis.
gimbal lock	is the loss of one degree of freedom that can occur by three gimbal systems. When two of the gimbals are driven into a parallel configuration, one direction of rotation will be 'looked'. This can lead to mathematical as well as actual mechanical issues.
nutation	is a nodding, periodic oscillating motion of the rotation axis of a largely axially symmetric object, such as a gyroscope or even a planet.
precession	is generally the change of orientation of the rotation axis of a rotating body, induced by externally applied torque moments.
Wells turbine	is a low-pressure air turbine, initially developed by Prof. Alan Arthur Wells of Queen's University Belfast in the late 1970s for the use in OWC. The blade profile of the turbine is completely symmetrical in a fixed zero pitch position. This allows the turbine to rotate continuously in one direction regardless of of the direction of the air flow. Its efficiency is compared low but with the benefit of robustness and simplicity.

List of Tables

List of Figures

Nomenclature

For ease of comprehension distinctive typographical styles are used throughout this document. Vectors, which are mainly triple-spaced, are all identified by an arrow above the variable as for example: $\vec{x}$ or $\vec{X}$. Matrices, in contrast, are characterized by upper case letters written in boldface, for example: **A**. Scalar variables are mainly, but not always, written in lower case letters. Following listed variables are used:

Latin:

(x_d, y_d, z_d)		device fixed coordinate frame
(X_i, Y_i, Z_i)		inertial coordinate frame
(x_g, y_g, z_g)		gimbal or gyro fixed coordinate frame
$\mathbf{A_{gd}}$		rotation matrix from gimbal to device coordinates
A_{11}	$[kg]$	added mass' in surge
C_P	$[N/rad]$	stiffness against pitch
C_w^*	$[N/m]$	quasi wave stiffness in surge
F_B	$[N]$	buoyancy force
F_G	$[N]$	gravity force
F_{rel}	$[N]$	relative excitation force
F_{res}	$[N]$	resultant force
H_S	$[m]$	significant wave height
I_{fy}	$[kgm^2]$	moment of inertia
M_C	$[Nm]$	cogwheel moment
P_{abs}	$[W]$	absorbed power
$P_{abs}^{cos^2}$	$[W]$	cos²-amplitude of the absorbed power
$P_{abs}^{sin\,cos}$	$[W]$	sin-cos-amplitude of the absorbed power
$P_{abs}^{sin^2}$	$[W]$	sin²-amplitude of the absorbed power
P_{ave}	$[W]$	available wave power
P_{max}	$[W]$	maximum power capture
R_1, R_2, R_3	$[m]$	semi-axes of ellipsoid, respectively cuboid
S_p	$[mm^4]$	polar section modulus
V_e	$[m^3]$	volume of the ellipsoid
$X_w = H/2$	$[m]$	maximum amplitude of the water particle displacement
f_D		diffraction factor
f_p	$[1/s]$	peak wave frequency

k^*		relative wavenumber; $k^* = kl_y$
l_P	$[m]$	positive depth about which P is beneath the still water level
l_P^*		relative l_P
l_{Py}	$[m]$	distance from point *P* to the lower end of the device
l_x	$[m]$	
l_y	$[m]$	height of the device
l_z	$[m]$	width of the device
m_D	$[kg]$	device's real mass
r_A	$[m]$	radius of the axis
r_C	$[m]$	radius of the cogwheel
r_G	$[m]$	radius of the groove
A	$[kg]$	coefficient for added mass
B	$[T]$	magnetic flux density [just in chapter 2.1 "MHD Direct Wave Converter"]
B	$[kg/s]$	coefficient for fluid damping
C	$[N/rad]$	coefficient for hydrostatic stiffness (or restoration)
H	$[m]$	wave height
I	$[Nm \cdot s]$	moment of inertia (or rotational inertia)
L	$[Nm \cdot s]$	angular momentum (or rotational momentum)
M	$[Nm]$	applied torque or moment
M_p	$[Nm]$	power take-off moment of one gyroscope
$S(f)$		Pierson-Moskowitz Spectrum
T	$[Nm]$	torque
g	$[m/s^2]$	gravity constant
k	$[1/m]$	wavenumber
m	$[kg]$	mass
p	$[N/m^2]$	dynamic wave pressure
r	$[m]$	distance or radius
u	$[m/s]$	flow rate

Greek:

$\dot{\varphi}_y$	$[rad/s]$	spin rate
$\boldsymbol{\Theta}^{\mathbf{x}}$		skew-symmetric expression of θ (instead of cross product)
Φ_D		diffraction wave velocity potential
Φ_I		incident wave velocity potential
θ	$[rad]$	rotational displacement between device and inertial system
λ	$[m]$	wavelength

σ	$[S/m]$	conductivity
τ	$[s]$	periodic time; **or:** torsional stress
	$[N/mm^2]$	
φ	$[rad]$	rotational displacement between gyroscope and device
ω	$[1/s]$	angular velocity

Acknowledgement

This project was made possible through support and assistance from others to whom bestow shall be given at this point. First of all thanks appertains to my supervisor, Prof. Grant E. Hearn who gave me guidance and support during this project. Further I would like to express my gratitude to Nicholas Townsend for discussions which helped to find back to the thread and to come up with new approaches.

I also would like to express my sincere thanks to my friends who gave my endorsement and motivation. Not only during the work on the project, but throughout the whole duration of the master course, a time full of elated experiences.

Last but not least I would like to thank my whole family who supported me from home with love, faith and trust, specially my parents who gave me all the tools without which I would have never reached the stage where I am now.

1 Introduction and Motivation

Conventional energy sources, such as gas, oil and coal will be depleted in the no too distant future. Sources such as nuclear energy entail, as recently shown once again by the accident in Fukushima (Japan, March 2011), a high potential of hazards. Global warming by greenhouse gases leads to more and more alertness. These issues have recently led to an increasing attraction towards more sustainable and renewable energy sources capable of providing long term solutions for a secure and safe energy supply. However, difficulties arise that have to be addressed. Most of the renewable energy sources have comparatively low energy densities and often fluctuations of availability. The first issue primarily afflicts the economics of energy capture, whilst the second implies a need for several different energy sources at the same time and a well-thought-out power controlling and transmission.

Due to the geographic position of the UK the renewable energies in question are mainly wind, tidal and wave energy. Wind energy is already developed up to a competitive state and tidal energy is probably making the breakthrough in the next years (recently, in March 2011, the Scottish government approved the construction of 10 tidal turbines in the Sound of Islay [1]). The technology for capturing wave energy, however, is still in its fledgling stage. The reason why the development of wave power harvesting is behind is not the availability or low energy density of the wave power itself. Quite the contrary, for UK coastlines the average wave power is fairly high (up to 70 kW/m crest width) and the availability is estimated to be well predictable and hence wave energy has the potential to contribute up to 12% of UK's electricity generation [2].

The challenge for harvesting wave power though, is the rough and harsh sea environment. This includes, beside chemical and biological corrosive and derogating processes, particularly the extreme high wave loads which can occur in heavy sea states. The load, which the structure of an energy harvesting device has to withstand in such circumstances, can easily be a hundred times the load under standard operation conditions. This is by no means an unsolvable technological or engineering problem; however it reflects high capital and maintenance costs for any wave energy device. To bring down the capital cost without loosing efficiency is therefore the challenge of economic wave energy harvesting on a grand scale. Herein lies the cause why so many completely different device designs have already been proposed and tested.

This work will come up with a novel principle of wave energy harvesting device which is thought-out to keep the capital cost as low as possible from the outset, but still leads to a good power capture ratio. Before the working principle is discussed in more detail a brief explanation as to why this principle is thought to have the stated advantages is given, and how this idea came about.

Distinct tasks and activities for this project, their time schedule and interconnection, as well as their progress, were planned by dint of a Gantt Chart. The aim was, to see the progress of the project, to identify arising problems and to ensure appropriate working time distribution throughout the project. The intention was to ensure that objectives are not forgotten and that unnecessary trouble and stress towards the end of the project is avoided. However, it has to be mentioned that not all objectives could and were addressed exactly as initially planned.

2 Steps Towards a Novel Concept

As mentioned a lot of different concepts for wave energy capture have been developed in the last decades. There are several possible criteria available to subdivide and classify each device. One is the intended placing of the device, onshore, near-shore or offshore. Water waves change their internal physical behaviour when propagating, towards the main land, towards shallower water. Thus the site in question can similarly be subdivided into its wave condition classified in deep, intermediate and shallow water waves. Whilst the operation in deep water, and thus usually far offshore entails the need of expensive power transmission, an onshore installation in shallow water has less wave energy available. This is due to the loss of wave energy by reflection and bottom friction during their propagation towards the coast.

Another rough classification can be done using the working principles as follows:

(a) Attenuator: Several floating structures connected by joints. Wave induced heave and pitch motion leads to a relative motion used to extract, mainly hydraulically, energy.

(b) Overtopping: A water reservoir charged by the overflow of waves. Discharge through low head hydro turbines generates electricity.

(c) Oscillating Water Column (OWC): An air containing closed chamber just opened beneath the still water level. Incoming waves rise, through the opening, the water level in the chamber and thus compress the air which is used, e.g. by discharge trough turbines, to generate electricity.

(d) Oscillating Wave Surge Converter (OWSC): The wave surge motion is used (mainly near shore) to oscillate a structure which is usually connected by a joint to a fixed mooring. Typically hydraulic pumps are used to extract the energy from the motion.

(e) Point Absorber: Single buoys moving, often with just one degree of freedom in heave or surge motion in the waves. Linear generators or hydraulic systems are used for energy extraction.

All of those main principles of wave energy conversion entail certain advantages as well as disadvantages.

When looking towards a new concept which overcomes the mentioned issues with the ocean environment and the related economical competitiveness it was thought about devices which stick out due to their simplicity. Entailing less or even no joint or bearing moving in the sea water and thus high reliability and longevity, as well as robustness under hard sea conditions. In this view, the first concept thought about was the MHD Direct Wave Converter which will briefly be outlined next.

2.1 MHD Direct Wave Converter

The MHD in the name stands for Magneto Hydrodynamic. The basic working principle of this concept is the separation of solved salt ions, and thus charge, due to the wave induced water motion in a strong magnetic field. To achieve a reasonable efficiency, a high water flow rates are required. Thus the incoming waves have to be transformed into an almost pure translational oscillating motion. This can be done by a smooth slope which acts like a beach. As the waves approach the shallow water at the slope, the irrotational cyclic water oscillation is transformed into a translational oscillation along the slope.

According to Faradays Law a magnetic field perpendicular to the flow of a charged particle will lead to a deflexion of its flow. The deflexion force is orthogonal to both, the magnetic field as well as the flow. Thus an artificial magnetic field has to be incorporated in the slope with field lines penetrating perpendicular its surface. For sea water propagating upwards the slope this entails a sidewise separation of its flowing charge, the solved salt ions (Na^+ and Cl^-). Due to the charge separation an electrical field is generated. The energy from the electrical field can then be withdrawn by electrodes placed in small distances along the slope, parallel to the flow direction. Because the water flow follows an oscillating motion the resultant electrical field will oscillate as well and lead to an alternating voltage. Thus capacitor placed beneath the surface of the slope, as charge collector, can also be considered and they would not suffer from a direct contact with the hostile sea environment (oxidation etc.).

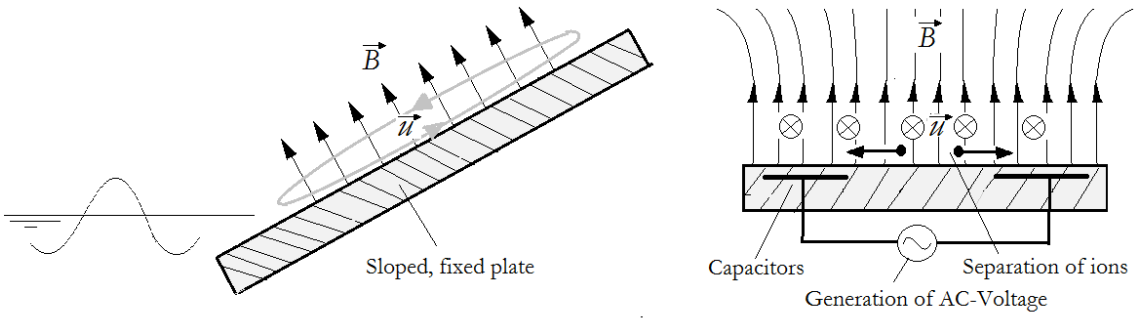

Figure 2.1: Side and front view of the MHD concept

Given by Faradays Law the maximum power density can be roughly estimated by [3]:

$$p\,[W/m^3] = \frac{1}{4}\sigma\, u^2\, B^2 \tag{2.1}$$

As it was already mentioned a sufficient flow rate u is necessary. However it can bee seen from the equation that the magnetic field B is crucial as well. To get this principle working a magnetic field in the order of Tesla is required. This is technological feasible, e.g. by superconductive coils or permanent magnets (e.g. NdFeB-Magnets) but it implies high costs. The conductivity σ dose not go with higher power into the equation, nevertheless first investigation yield to issues with the low conductivity of sea water, which comes from its, for this propose, low salinity.

Some of these issues can probably be overcome or diluted. Nevertheless, despite the amenity and ease of its operation principle, it is not very likely to get it to an economical stage. Neptune Systems, a Dutch company, made investigation on tidal current power generation, generally based on the same magneto hydrodynamic principle. In 2004 they estimated for their device energy costs of 3 €/kWh and got thus to the evident conclusion that this is currently (2004) of about the factor 30 to expensive for a competitive operation [4]. It follows similarly for the explained MHD Direct Wave Converter that it is a fascinating concept but with state of the art technology not competitive and promising enough validate deeper investigations. Development of new magnet materially may perhaps, at someday in the future, lead to a new view and evaluation of the given concerns.

2.2 Hydraulic Pumping OWC

In terms of simplifying a wave harvesting device a second concept arose. The general idea here is based on the principles of the oscillating water column (OWC), as used in the Lim-

pet wave energy device, as an example amongst many others. In an OWC device, the up and down motion of the water waves produces inside a, towards the atmosphere closed, chamber an oscillating water column. In common OWC devices a Wells turbine is used to extract electrical energy from the compressed air generated above the moving water column. This principle is already based on simplicity by means of using a concrete structure for the chamber which is directly facing the rough sea and just for the part of the power take-off (PTO), the turbine, which is not in direct contact with the open sea, a more complex technology. For sufficient performance it is necessary to keep the volume of compressed air low as well as its way towards the turbine. In other words one chamber can not be arbitrary long (practical order is about 20 m) and it follows in turn that for several chambers an according number of turbines are required.

The suggested concept tries to avoid the use of several such turbines, and general the use of complex technique at all. Instead of running a turbine with the compressed air, this pressure will be used to pump up water to a higher hydrostatic potential. This can be done without a lot of mechanical or electrical parts which are related with costs and which would need maintenance. Even when placing several of such devices along an appropriate shoreline, the generated hydrostatic potential of each device can be connected straightforward. And the hydrostatic pressure is then used to run just one, already commonly used and well understood off-the-shelf hydraulic turbine (for low pressure heads).

The hydrostatic potential of the waves depends just on their height. Hence, to form a higher hydrostatic potential a conversion is required (flow rate to pressure). This is quite common in hydraulics where rams with different cylinder diameters are used to convert acting force (pressure) and velocity (flow rate). However to keep simplicity a non mechanical conversion will be used, means just the compressed air above the OWC will be the converting medium. Except some flaps this concept is based on a simple concrete structure.

The concept is schematically shown in Figure 2.2. The water (1) in the OWC is moving up and down and compresses or respectively decompresses the air (2) above. Considering an incoming wave and thus rising water column the air above will transfer the induced pressure to the water column on the rear of the chamber (3). At initial position this rear water column has already a higher hydrostatic potential which is balanced by the water column outside the chamber of the device (4), called the hydrostatic storage. Balancing takes place through a connection (5) on the bottom end between the rear column and the hydro-

static storage. This aperture is controlled by flaps. Starting from the origin balanced situation an applied pressure on the rear water column, induced by the compressed air, will lower its level and transfer water to the hydrostatic storage. The surface area of the rear column is compared to the one of the OWC quite small, thus the change in height of the rear column will be accordingly great. Because the hydrostatic storage column has again a quite large surface area, and furthermore this storage is constantly discharged by a turbine, its height will stay almost constant. If the device is designed and controlled in a proper way the maximum height of the rear water column (3) is almost completely displaced by an incoming wave crest.

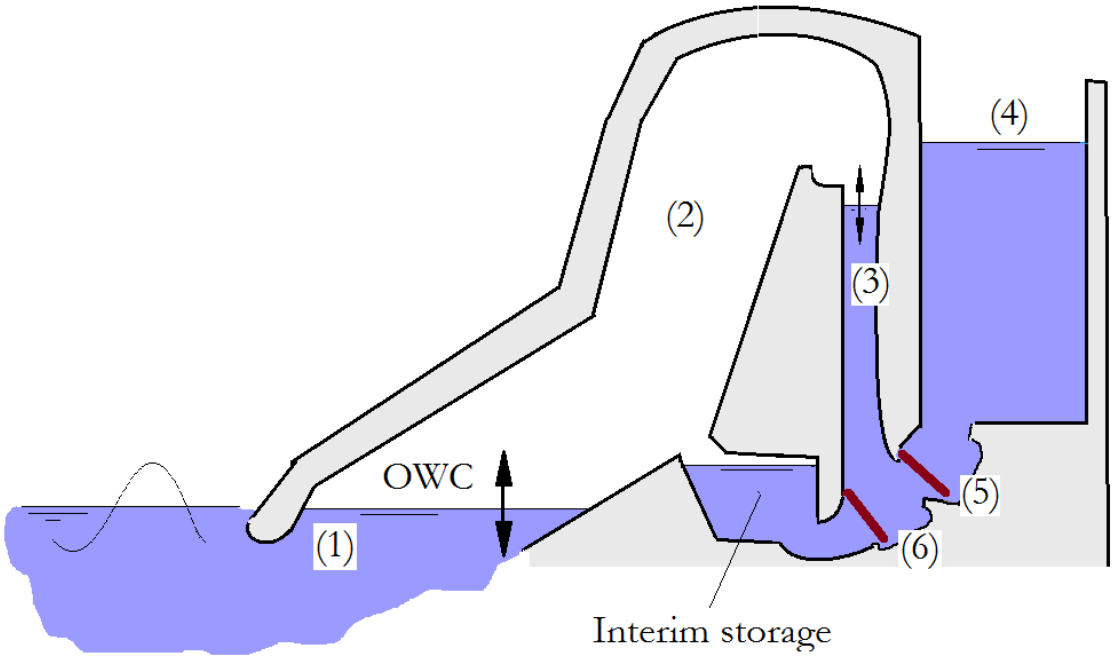

Figure 2.2: Cross-section of the Hydraulic Pumping OWC

After the crest of the wave has passed the air pressure will decrease. Thus there is a backwards pressure on the aperture (5), induced by the different height of the columns which would consequently lead to a backflow of the water. This is prevented by a simple flap, closing the aperture (5) automatically and sufficient fast when backflow occurs. Further decrease of the OWC generates an underpressure in the whole chamber. This underpressure leads to suction on the discharged rear water column that results in turn in the opening of the second flap (6). Thus whilst the OWC lowers up to the deepest point of the trough, the rear water column will rise again. The water which is sucked into the rear column is drawn, either directly through connection channel from the surrounding sea, or, as indicated in the figure, from an interim storage which contains already partially uplifted

water, filled by the wave crest. One has to bear in mind that water can not be sucked up to arbitrary heights; absolute limit is below 10 m (limited by the density of water and the atmospheric pressure).

The surface areas of the oscillating water column and the rear water column are essential for the conversion ratio and thus the discharged height. The height of the rear water column as well as its surface area are related to the amount of damping acting on the air mass and thus in turn on the waves. To extract maximum power it is necessary to achieve the appropriate damping. However, once designed for the prevailing wave conditions the properties of the water column can not be adjusted. To resolve this issue the rear water column inside one chamber is divided into several single columns along the chamber, each with own flaps. A simple controlling mechanism can arrest each flap and thus the working surface area of each single rear column can be switched of. Hence the overall moving surface area inside one chamber can appropriately be adjusted to the incident wave height.

Several of the described chambers will be placed along a shoreline and the hydrostatic storage, which is the water column behind each chamber, is interconnected between all of them. At some point of this interconnected hydrostatic storage channel there will be a low head hydraulic turbine discharging the stored water back to the sea and generating electricity. Due to the interconnection of a lot of chambers and the buffering of the hydrostatic storage columns a well smoothed power output is given. It is generally also conceivable to use just at one place a hydrostatic storage pond, instead of a storage column per device, and interconnect the apertures (5) at the lower end of the rear water columns just by a common pressure pipe.

So far just the basic idea of the principle of a Hydraulic Pumping OWC was explained. There are a lot of uncertainties concerning the performance of the device, about the feasibility of a controlling matching most of the wave climates, about the losses in the moving columns, about a stable constant discharge height over many discharge loops, just to mention some. Those concerns may lead to a loss of efficiency but generally it seems to be possible to cope with them. And, due to the great simplicity of the described concept it may still, even if not that efficient, be economical.

This concept is due to its principle clearly destined for onshore installation. On the one hand this reduces capital and maintenance costs on the other hand this also reduced the incoming wave energy significantly. Furthermore, like for all onshore OWC devices, appropriate coastlines are required. Voith Hydro Wavegen Ltd has already acquired a lot of

experience with their OWC called Limpet, sited on the island Islay in Scotland. They came to the conclusion that onshore wave energy harvesting may be a good point to start from and to gather experience but they clearly estimate the future of wave power to be offshore [5]. The purpose of this work though is, as implied in the very beginning, to give a contribution to sustainable great scale electricity generation from water waves. As the concept of Hydraulic Pumping OWC does not seem to have the capability therefore it came finally to a third concept of wave energy harvesting, the one which will be investigated within the work at hand.

Nevertheless the here described device could be used in niche applications like implementation in breakwater or harbour walls. Thus it may be worth to investigate and try to improve this concept at some point in the future as well.

3 Background – And how the Concept Arose

Invented existing concepts which are related to the third final concept of wave energy conversion, the WaveGyro, will be explained in this chapter. It will be elucidated how parts of the final concept came together and were influenced by preceding work. The necessary background to be able to relate the basic principles of the WaveGyro will be given.

3.1 Triplate WEC and the Ampere Wave Device

The concept of the WaveGyro was initially inspired by other concepts of wave energy devices as e.g. the Ampere Wave device. The Ampere Wave device is an invention by Chris Budd, in turn based on the Triplate Wave Energy Converter (WEC), which will thus be briefly described first. The Triplate idea was developed by Dr. Francis Farley [6] and his team in the late 70s. The conception is, to use the oscillating irrotational motion of water waves to induce a pitch motion on a vertical submerged plate from which then power can be extracted. Hydraulic rams were thought to extract power from the pivoting plate which is the very right one in Figure 3.1. This entails the need to transfer a reactive force away from the moving plate. Thus there are two more plates, rigidly placed a half wavelength $(\lambda/2)$ apart. Due to this displacement a resonant standing wave is created between them, providing the exact counteracting force for the power extraction without any net movement. The pivoting plate is positioned a quarter of a wavelength $(\lambda/4)$ in front of the two rigid plates, facing the incident waves. This distance is thought to produce, due to reflection, a standing wave between pivoting and the first rigid plate, and thus a maximum horizontal motion of the leading plate.

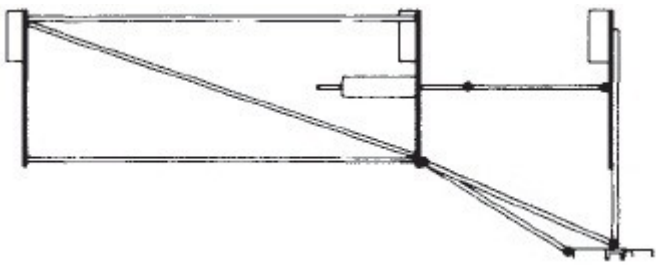

Figure 3.1: Schematic of the Triplate WEC with the pivoting plate on the right [7]

Beside the ease and lightness of the structure this working principle offers a quite high efficiency. Experiments as well as simulations indicated efficiencies up to 80% for the de-

sign wave length and still high values for wavelength above. For shorter wave length the efficiency, though, drops quite fast. Due to the light structure and the cancelling of wave forces due to reflection, the loads on device and mooring line seem to be comparable low, even for heavy wave conditions [7].

This idea was picked up by Chris Budd [8],[9] and developed to a further concept, the Ampere Wave Device. As main difference the number of plates is thereby reduced to two and the distance between them is variable, to have the possible to adjust to an optimum power extraction even for changing wavelength. Therefore, two vertical submerged plates are floating almost independently just connected by a cable. Adjusting their distance to be half a wavelength $(\lambda/2)$ apart they are considered to move always contrawise. This can be imagined by considering one plate in the wave crest, moving with the wave oscillation in direction of wave propagation whilst the other plate, a half wavelength further and thus in the trough moves with the here backwards oriented oscillation motion, in opposite direction. This leads to a relative 'together' motion of the walls and a half period later the motion is clearly reversed to an 'apart' motion. The cable connecting them transfers a force between the plates and restricts their apart motion. Force and motion can then be used to drive a, by the inventor so far not specifically defined, power take of unit. The 'together' motion of the plates will then bring them, without power extraction, back to the initial position, ready for the next power stroke.

Chris Budd built a 1:20 scale model of his device and estimated by simulations and experiments capture ratios of up to impressive 115%. And furthermore he predicted quite low electricity costs between 2.4 - 3.5 p/kWh [8] which would already be in very economical range. Both estimates seem to be fairly optimistic and it is not that obvious how these values actually came together. If for example the transformation of the experimental performance to a full scale device was done accordance with the correct scaling theory.

Beside that, for the author of the work at hand arose several concerns about the feasibility of a full scale implementation of the Ampere Wave Device, operating in the harsh sea environment. Main concern is hereby the long cable as only part used to keep the device together. A common wave spectrum has significant (useful) wavelength between about 50 to 200 m, thus the distance of the plates has to be adjusted up to 100 m (half the wavelength) which seems, from the engineering point of view, to be a rather long range to cover with a cable. This concern of the long distance is clearly also relevant for the Triplate device. For stormy conditions the free floating plates of Chris Budd's device are thought to

be pulled completely together, however it is probably not farfetched to imagine issues with cluttering and tangling. Furthermore the cable (if steel or synthetic fibre) will have to resist fairly high fatigue stress loadings. During the idle back motion the cable will due to his weight slack; followed, due to an incident wave, by an abrupt applied tension. What leads probably also to inconstant power output and power picks. Also controlling of the wall distance and the motion as well as the appropriate damping by the cable, necessary for maximum power extraction, may work well in theory but can be conceived to be quite difficult to accomplish practically.

Nevertheless the general concept of both the Ampere Wave Device as well as the Triplate Wave Energy Converter attracted with their potentially high capture ratios combined with still light structures and less moving parts. Both devices are thought to be 'terminators' in terms of ideally no waves will pass through the device; incident wave energy is either captured or reflected.

The idea of using a vertical plate to capture the kinetic energy of the wave's particle oscillation up to ample depths was picked up when the concept of the WaveGyro device initially evolved. The concept was simplified to just one vertical plate pitching, slack moored, in the water waves. Utilization of just one plate entails that no power generating force or moment can be transferred away from it. Thus an internal power latching is required which provides by any manner a counteracting reaction against the induced pitching motion of the plate. There are different methods to realise such a power latching, one of them which is used in the concept of the WaveGyro is a fast spinning gyroscope. However there have been investigations in devices which using inertia masses placed inside a pitching structure to provide reacting forces. The academic work for SEAREV and the PS Frog device represent the leading present theory related to reaction based wave energy converter. Thus those both will now be briefly explained before following on with the WaveGyro concept.

3.2 PS Frog Device

The concept of the PS Frog device was initially developed in the Lancaster University which investigated in wave energy since the mid-1970s. The initial design of the Frog was thought to work as point-absorber buoy in heave motion, using a resonant mass-spring-damper system for the power take-off [10]. Variations lead to the PS Frog device which still used the reaction of an internal mass. Where PS stands for pitching and surging (or ambiguous for postscript), and Frog was just an appealing name and in addition the acronym

of French's reactionless oceanic generator [11]. It followed with an improved hull the PS Frog Mk 5 which is indicated in Figure 3.2.

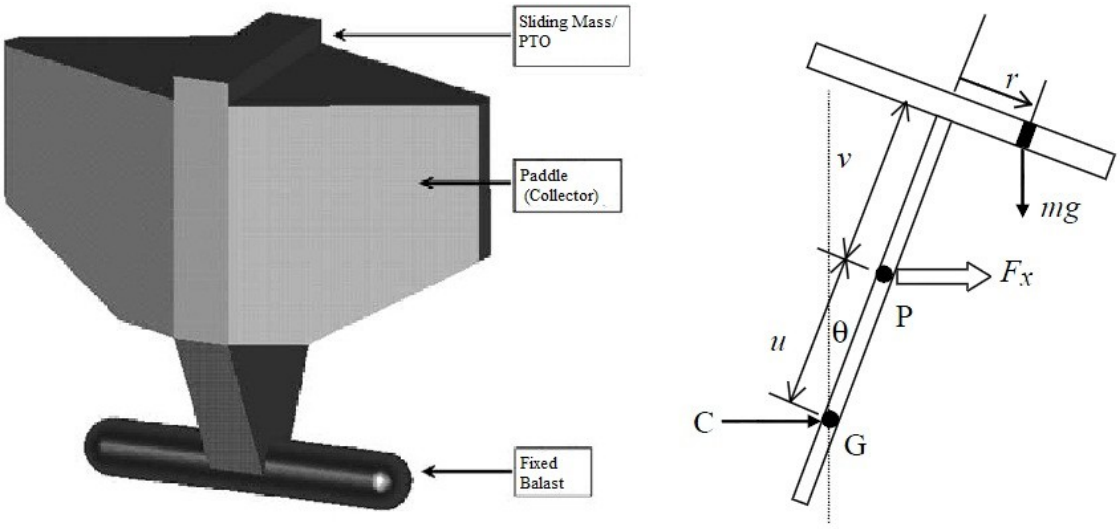

Figure 3.2: External view (left) and schematic internal view (right) of the PS FROG Mk 5 [12] (reprinted with the kind permission of A. P. McCabe)

The displayed device, described by McCabe et al. [12] consists of a large paddle which is also the buoyancy, and a fixed ballast at the bottom end. The ballast at the lower end serves as reacting inertia against the wave force (indicated as Fx in the schematic, Figure 3.1 (right side)). The 'paddle' was initially just a flat plate. Optimization lead first to a rhomboid shaped paddle which was further improved to the shown form named KRATER 2. A heavy mass is placed inside, at the very top of the device, and can slide translational, in same direction as the wave propagation. Its damping is controlled to oscillate at maximum amplitude, respectively in resonance. A hydraulic system damps the movement off the sliding mass and serves as power take-off (PTO). Hydraulically captured energy will be transformed through a generator and then be electrically transmitted to the main land. Besides controlling by hydraulic damping, is the movement of ballast (e.g. water) inside the hull intended as a resonance tuning system, matched to the appropriate wave frequency.

Widden and French developed the theory describing the motion and power capture of such a pitching wave energy converter which acts against an internal mass [13]. Generally a good capture ratio where calculated and experimentally tested. Without going into deeper explanations it was found that the shape of the hull has a crucial contribution to the performance as well as the positioning of the sliding mass [12] [13]. Due to the principle of the concept of a sealed-in mechanism a long lifetime with low maintenance is predicted for such a device.

Table 3.1: General dimensions of the full-scale PS Frog Mk 5 device [12]

Maximum beam (width)	36 m
Overall draught (height)	ca. 22 m
Maximum length	16 m
Displacement mass	ca. 4600 ton
Slider mass	150 ton

The sizing and mass of the device are given by McCable as stated in Table 3.1. Those figures are just for one proposed design of the PS Frog. As mentioned there are a lot of varieties of the concept, and for the depict one are some possible improvements indicated which may allow to reduce the sliding mass [13]. Nevertheless, the concept of an internal reacting mass will require a heavy mass. Just to give a figuratively impression of the stated 150 ton slider mass: it falls roughly in the range of the mass of two typical diesel locomotives. It may not be a general issue to manufacture and maintain bearings and guides for such an inertia mass, but it can be imagined to be costly. Further just the high mass itself is related to cost as well as it leads to an increased wave load in rough sea conditions.

3.3 SEAREV Device

In France was a wave energy converter, similar to the PS Frog developed, called SEAREV (French: *Système Électrique Autonome de Récupération d'Énergie des Vagues*, which stands for: autonomous power system for recovery of energy from waves). Unlike the PS Frog which can be considered as submerged device, the SEAREV is more a floating device as indicated in Figure 3.3 (left side).

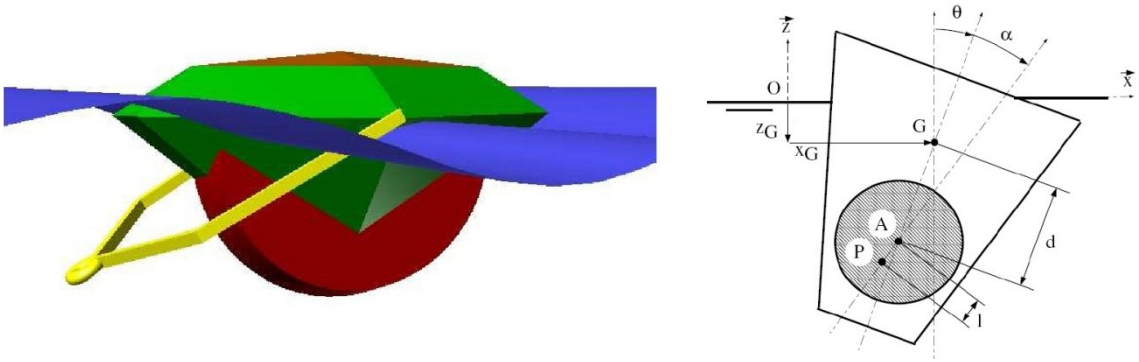

Figure 3.3: External view (left) and schematic internal view (right) of the SEAREV device [14] (reprinted with the kind permission of Alain H. Clément)

The right side of the figure gives an inside in the working principle. A heavy wheel with horizontal axis is used as reacting mass. The center of gravity (P) has an offset to the center

of rotation (A), thus the wheel acts like a pendulum. Pitching of the device, induced by waves, lead to a relative rotational motion between hull and wheel. This motion is used by a hydraulic power take-off to capture energy which in a further step is transformed to electricity. Babarit et al. [14] formed the theory describing the whole device, including the mechanical model the hydrodynamics of the wave interaction and the nonlinear internal power take-off (PTO). Utilizing this theory allowed to optimize external shape as well as the internal PTO. Despite mentioned advantages of the wheel as rotational latching mechanism were generally quite similar conclusions drawn like for the PS Frog device.

Table 3.2: Typical dimensions of SEAREV device [14]

Width	15 m
Draught (depth)	14 m
Length	25 m
Displacement mass	1000 T
Pendulum mass	400 T

For a typical SEAREV device as shown in Figure 3.3 the dimensions are stated in Table 3.2. Again the mass and especially the moving pendulum mass are quite large. As for the PS Frog device it followed concepts based on the SEAREV idea like e.g. the so-called "Rocking Buoy" [15] which essentially uses a different shape, a simplified ordinary cylindrical hull.

3.4 ISWEC Device

The ISWEC (Inertial Sea Wave Energy Converter) is a concept investigated at the University of Edinburgh. As the name indicates it also based on an inertial reacting system and thus uses the advantage of a completely closed hull. Instead of a heavy reacting mass a gyroscope is used to provide a reacting moment. Such a concept already appeared in one variant of the Salter Duck, one of the first (1974) and perhaps best known wave energy concepts. In one proposed variant of the Duck, Salter [16] proposed the use of four fast spinning gyros placed inside the nodding hull. The precession motion, due to momentum conservation, was intended to be used to run hydraulic ring-cam pumps as intermediate step towards the generation of electricity. However he abandoned this gyro based concept and proceeded towards a PTO using a huge shaft to conduct the torque moment away from the device.

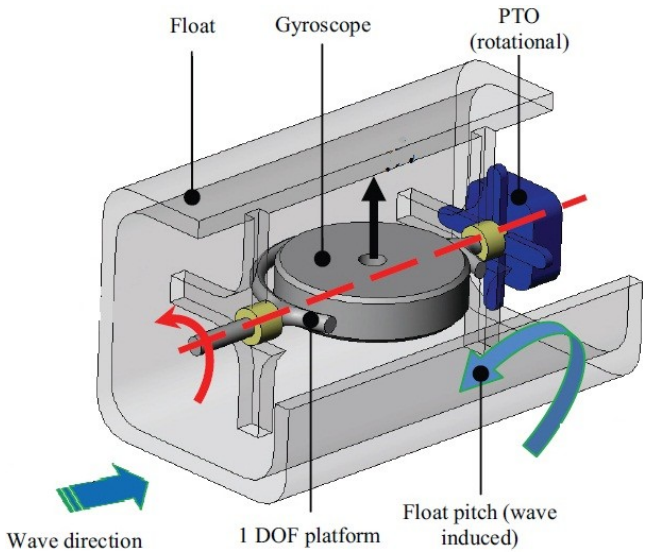

Figure 3.4: Simplified one degree of freedom ISWEC device [17] (reprinted with the kind permission of Giovanni Bracco)

The ISWEC design picked the gyro-concept in 2006 up again. A linearised model of a simplified device was extrapolated and an outline for the execution of wave tank test was made [17]. A schematic view, given in Figure 3.4 indicates the vertical spinning gyro suspended on a one degree of freedom (DOF) platform or gimbal. Incoming waves induce a pitch motion of the floating structure, resulting in a torque, acting on the gimbal. Due to the, already by Newton discovered principle of momentum conversation follows a precession motion of the gyro. The precession motion is, as indicated with the red arrow, around an axis orthogonal to the axis of the spinning gyro (vertical) and the axis of the acting torque (lateral). A PTO unit, in the shown case a linear rotational one, utilizes the precession to extract energy and acts as a damping mechanism.

In difference to internal reacting mass which can act in all 6 DOF, translational and rotational, provides a gyroscope maximally in 2 DOF, rotationally reacting moments. In other words, a gyro can not directly be used to act against a translational motion like surge or heave. The great advantage, however, is that the rate of reaction of the gyro is given by its spin rate and the moment of inertia of its flywheel. The moment of inertia depends of the mass distribution in the flywheel. Thus the reaction moment can be tuned by those factors, without the need of an extreme heavy moving mass.

Another quite early concept of harvesting wave energy by means of gyroscopic effects was patented by Sachs et al. [18] in 1982. A double gimbal gyroscope is based on a float, rolling and pitching in response to the waves. 'Transferring members' between the gimbals transmit, in a not closer specified way, the precession torque from the inner gimbal to the

outer one. After the aggregation of both precession torques, a generator matched on the outer gimbal axis converts the torque into electricity. The working principle of the generator is also not closer specified.

Lately the concept of harvesting wave energy by gyroscopes placed on marine vessels was pursued by Townsend at the University of Southampton [19]. Several experimental systems have been developed and most recently (March 2011) trials in the Solent, a sea strait close to Southampton were carried out. The gyroscopic device was placed on a small boat moving in the waves. Results of this test are not yet available. Ram damper were used to represent the intended linear hydraulic PTO.

Kanki et al. [20] developed as well a gyroscopic based wave energy converter in the last years. Wave power is first captured by a pitching floating structure. The precession of a gyroscope, placed on this structure, is, by dint of a generator, directly converted into electricity. A prototype of their concept with a size of 45 kW has been tested. It is not that clear how exactly the precession motion and moment are transformed into electricity.

4 General Working Principle of the WaveGyro

Having explained the motivations and steps towards the concept of the present work, the WaveGyro, and having given a review of related concepts, its principle of operation will be elucidated now. First the general idea will be explained, followed by the description of the individual parts as well as their interconnection and thus the behaviour and characteristics of the complete device. The explanations will be underpinned by figures and drafts which may be quite useful to comprehend the in words described behaviour.

As mentioned, the general idea of the device is to reduce mechanical complex parts exposed to the sea environment. Hence an internal reaction based concept follows, where all mechanical moving parts (bearings, gears, generator, etc.) are inside of just one completely sealed hull. The almost completely submerged device is thought to pitch, induced by water waves. A vertical spinning gyro is placed inside the hull to provide a reaction without the need of heavy mass. A fast spinning gyroscope tries to maintain its axis of rotation, and can thus exert a quite large momentum, acting against the change of this axis. As for described concepts, the precession motion of the gyro-axis will be used to extract energy. The torque moment of the precession motion will be fairly high, but its frequency still as low as the incident waves are, and its motion is an oscillating one. For the desired generation of electricity, however, a constant, fast and rotational motion with moderate torque is most appropriate. Thus a transformation step is required. Mentioned concepts which use a reacting gyro realize this intermediate step be the use of hydraulic rams or pumps. For the WaveGyro the use of hydraulic systems, as one more complex and expensive system, will be avoided. The idea instead is, to use the fast spinning gyro to 'kill two birds with one stone', the described reacting moment and also for the transformation of the slow precession motion directly into the fast spinning motion of the gyroscope. This means to use a subtle gearing system, which permits the utilization of the precession moment and motion to spin the gyro further up. The electric generator is then directly matched on the axis of the gyro, probably even incorporated in it, using the gyro flywheel multifunctional also as armature (rotor of the generator). This multipurpose use of components as well as the avoidance of additional systems, as the hydraulic would be, can dramatically reduce costs. On the other hand it presents an enhanced challenge on the initial engineering design and the implementation of all functions. Next a more detailed explanation of the device's shape, the plate, will be given before picking up the gyro concept again.

4.1 The Plate

Side, top and front views of the rigid plate are shown in Figure 4.1. The buoyancy of the plate is balanced, to keep it almost completely submerged in the water. Intended is an off-shore placement, in deep water. Deep water on the one hand to capture a larger portion of the power available, on the other hand to have a cyclic oscillating wave motion. The waves, as illustrated in the figure, propagating from the left to the right (x) leading, due to their oscillating irrotational motion to a pitching of the plate. Because the internal cyclic wave motion decreased logarithmically with depth the induced vertical forces and movements on the plate is maximal at its top and almost zero at its lower edge. This is just the case if the height of the plate is dimensioned appropriate compared with the mean wave height. The almost zero motion at the bottom end is crucial to ensure maximum pitch and minimum surge motion, since only the pitch motion can be 'captured' by the gyro and converted into electricity.

Even if the surge motion of the water wave is almost zero at the depth of the plate's lower end, it does not necessarily imply the same for the plate. That is, because there is no reacting force. A ballast mass, as used in the PS Frog device (chapter 3.2; p.21), can provide a inertial force and thus provide stability against surge. Sufficient surface area of the plate, even at the lower end, can lead to enough resistance avoiding a relative motion against the water particles, reducing the surging as well. Hence, as indicated in the front view (Figure 4.1) the plate is initially considered to have a constant width down to it's under edge. Nonetheless all heavy system components, from gyro about the generator to the transformer, will be placed in the lower end of the device. Extra ballast will, however, be avoided as good as possible. Appropriate mooring could also restrain the surge motion, but would lead to significantly higher demands on the design and connection of the mooring, which is aimed to be kept simple and cheap.

To have a low mass but still a submerged plate required generally a sufficient low displace volume. Thus the plate is thought to be slender, except at the bottom end, more space is required there to place the large, vertical spinning gyroscope. In shaping this bulge for more space cylindrical, unnecessary resistance against pitching can be evaded.

The issue in using a single gyro is, that its precession torque which acts against the device, leads to a net moment on the device in roll direction (this will get clear when later on the equation of motions are explained). Integration of a second gyro, with a roation in opposite direction to the first and thus leading to the second contrawise precession torque

can avoid this issue. However it is maybe sufficient to provide enough hydrodynamic resistance (added mass) against a roll motion of whole device. This could easily be done by extending the so far flat plate with orthogonal vertical 'rudders' in the plane of wave propagation (x-y-plane). In Figure 4.1 is one possibility shown by heaving such a rudder on each side of the plate. Extra buoyancy, placed on the top of the plate, may be another method to guaranty roll stability due to hydrostatic stiffness.

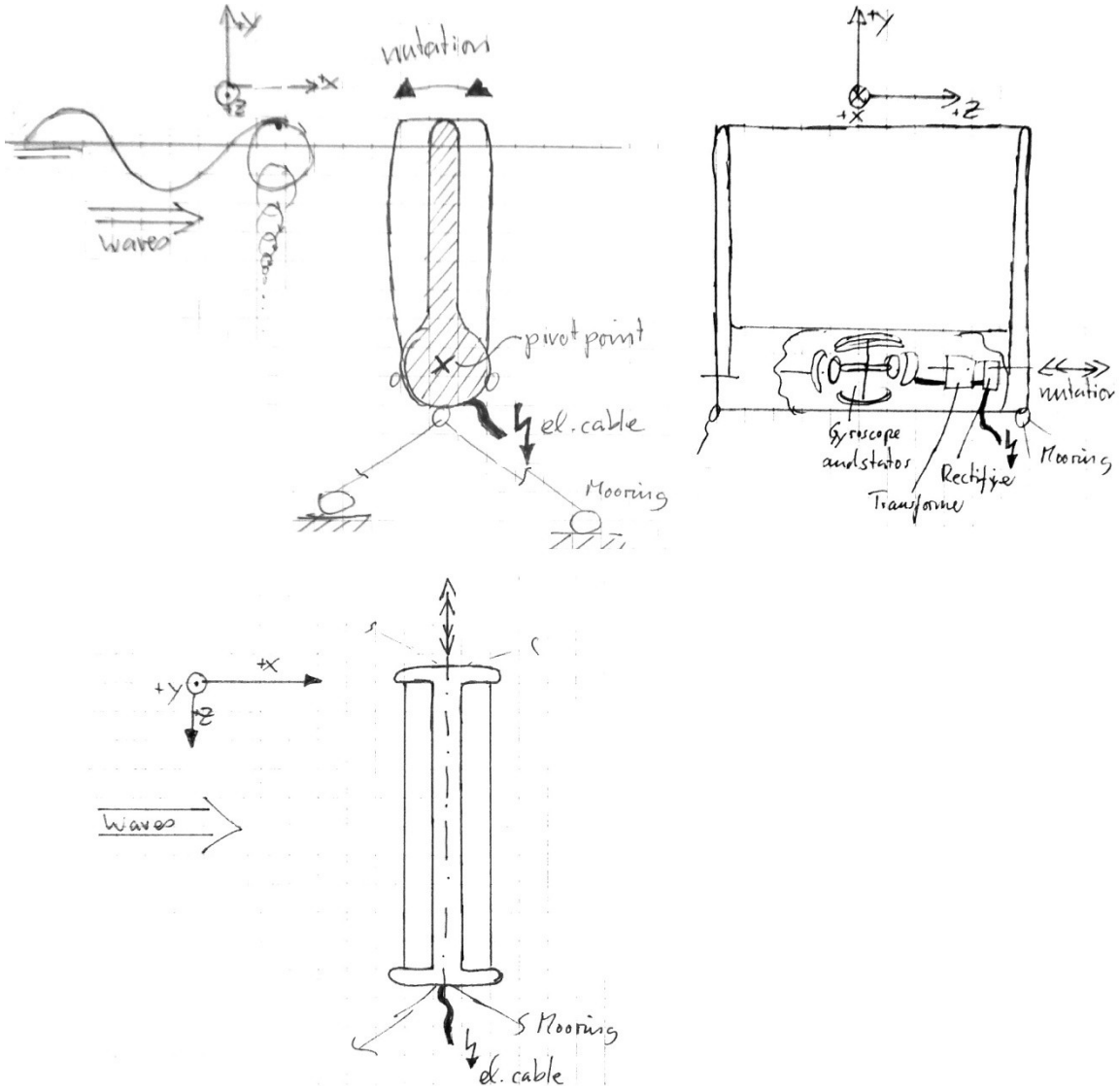

Figure 4.1: Initial draft of the three views of the wave energy device

If a proper variation of the hull is sufficient to prevent rolling motion, or if there is in the end no way around the use of two gyroscopes has to be investigated. Generally may the flat plate not be the best solution, more complex shapes, as shown by the study of the PS Frog device may lead to increased performance. Only further investigation can answer this uncertainty.

4.2 The Gyroscope

The fundamental equation describing the behaviour of the gyroscope, respectively any rotating system, is the principle of angular moment:

$$M = \dot{L} = I\,\dot{\omega} \tag{4.1}$$

Discovered by Newton it gives the relation of applied torque M to the rate of change of the angular moment $\dot{L}$. Or respectively the rate of change of the rotation speed ω, because I, the moment of inertia is a constant. So far this equation describes the motion about one axis of a body. If three axes are considered, to cover all rotational DOF, the equation has to be written vectorial form. The moment of inertia I, however is just constant related to the body (gyro) fixed coordinates. The applied moment, though, is considered in an inertial reference system. Thus the derivation of the angular momentum has to be expanded, due to Euler as it will be explained later in detail, and leads to an extra term describing the precession:

$$\vec{M}_z = \vec{\dot{\varphi}}_x \times \vec{L}\,. \tag{4.2}$$

Here is $\vec{\dot{\varphi}}_x$ the angular velocity vector of the body, i.e. the precession velocity of the gyroscope. I follows from the cross product that a torque applied perpendicular to the axis of rotation, in other words perpendicular to $\vec{L}$, leads to a rotation $\vec{\dot{\varphi}}_x$ which is orthogonal to both, the applied moment and the gyro's spin axis.

WaveGyro is designated to have a gyroscope with a vertical spinning axis, y, and an angular velocity in positive direction, according to the right hand rule (compare the definition of the coordinate frame Figure 4.1). The gyro is suspended in a gimbal restraining its rotation about the pitch axis, z, and thus a wave induced pitch motion of the device will apply a torque on the gimbal and respectively on the gyro. Because the device is considered to pivot around its lower end, an incident wave crest will lead to a negative torque about the pitch axis, z. It follows a rotational precession of the gyro and gimbal perpendicular to both, hence about the x-axis which is the direction of wave propagation. An incident wave crest leads, for conditions given, in a negative precession motion, and a wave trough in a positive precession about the x-axis (right hand rule).

How this oscillating precession motion and its moment can be used to produce an accelerating torque on the spin axis of the gyroscope will be explained next. The fundamental principle which will be used was an invention of Mishler [21] in 1973, inter alia called the 'Powerball'. The Powerball is a palm sized exercising tool to train arm muscles. A view of the original patent drawings is given in Figure 4.2, since then, over the intervening years, a lot of variants with names like e.g. 'GyroTwister', 'Gyro Exerciser' or 'Dynabee' evolved.

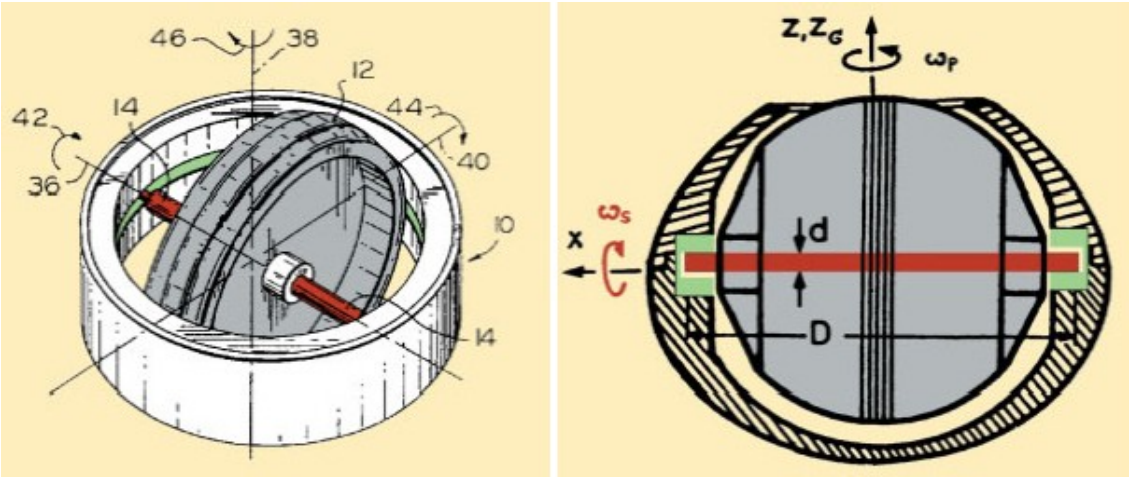

Figure 4.2: Powerball or Gyroscope Device (Patent drawing of Archie L. Mishler; 1973)[21] (reprinted with the kind permission of Christian Ucke)

The ends of the flywheel axis (red) are embedded in a u-shaped groove or guiding rail (green). The opening width of the groove has enough allowance for clearance for the revolving axles. Initially the flywheel (grey) is accelerated to a sufficient spin rate. Then by tilting the whole Powerball with the wrist, both ends of the flywheel axis (the axles) are pressed on the groove. This is due to the stability, respectively the moment of inertia of the rotating mass. Whilst the axle on one side is pressed on the upper edge of the guiding rail, is the axle on the other end pressed on the lower edge, i.e. on the opposite groove edge, as it is shown on the right side of Figure 4.2. Due to the explained precession, performs the gyro and its axis a rotation in the groove, indicated with the vector z. If the wobbling is carried out in a proper way, both effects together, the precession motion and the pressing of the axles on the groove, will lead to a rolling friction constraint. Thus, the rolling friction can transfer an accelerating or retarding torque on the spin axis. And with a bit skill and enough initial spin rate, one is able to speed the flywheel up to fairly high velocities even above 10,000 rpm [22]. The best and fastest acceleration can be achieved if a conical wobbling (nutational like) wrist motion is performed, and this in resonance. Resonance implies here that there is a relation between the spin rate of the gyro and the optimum 'wobbling'

frequency, which is given by the ratio of the diameters of groove and axles [23]. If the Powerball is driven in resonance and in a pure wobbling mode, the precession motion will always be in the same direction with 90° phase shift to the wobbling motion. On that condition, the axles will always roll one the same groove edge, but opposed to each other.

The WaveGyro device will clearly not perform such a wobbling motion. Ideally more just a pure pitch motion about one axis, induced by waves. This in turn will lead to a constantly changing precession direction, what is actually even desired. Otherwise, for constant precession in one direction, it would be impossible to connect an electrical generator to the flywheel. In the purposed wave energy converter a more sophisticated approach than acceleration though rolling friction has to be used. Thus, instead of a plain smooth groove, a toothed one will be used and cogwheels will be mounted on both ends of the flywheel axis. Obviously a cogwheel can not cog in both sides of a groove at the same time, thus there has to be an offset between the two edges of the toothed groove. In other words one of the toothed rims has to have a smaller diameter then the other one (see Figure 4.3). It follows that for each end of the axis there are two cogwheels required, one running in the outer rim the other one in the inner rim. The cogwheels have to be connected to the axis via an overrunning clutch, allowing always one of the two cogwheels of one side to crawl completely free.

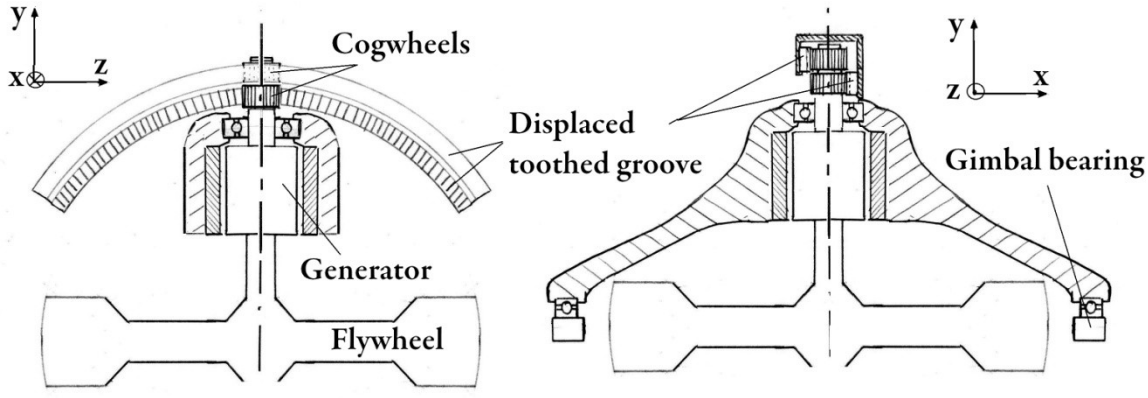

Figure 4.3: Half-section of the gyroscope and generator

Back to the wave force originated precession motion. If the gyro performs now a precession which leads to a faster crawling of the cogwheels then the rotation speed of the flywheel axis would be, than one of the sprag clutches grasps. This causes a restraint between the both rotational speeds and thus to an acceleration of the flywheel. The accelerating moment is thereby provided by the toothed rim which acts against the precession motion and moment. The sprag clutch of the other cogwheel (of the same axle) stays clearly

open. This is due to its opposite rotational direction when crawling on the opposed groove edge, i.e. the other rim.

Due to the high spin rate of the gyroscope the cogwheels have to be sufficiently small to achieve the described working principle. However they can not be design arbitrary small, mechanical issues will arise otherwise. The use of planetary gears could be a solution and would in addition give the possibility to control and match the spin rate at which the sprag clutch catches (by controlling the rotation speed of the planet-carrier). It is even cogitable that therefore the sprag clutch could be left out completely. It may also be reasonable to use just a groove on one side of the axis. Those are all points which have to be investigated further but shall not be of further concern for the time being.

4.3 The Generator

It has to be mentioned that the gyroscope will in fact not be spun up to faster velocities by the described principle; rather will a generator withdraw constantly power, and thus provide a counteracting moment and keep hence the gyro at an equilibrium speed. In controlling this equilibrium speed it may be possible to adjust the reaction moment of the whole device and thus match a maximized power capture for each wave frequency. But now to the generator, due to the precession motion of the gyro axis it is not possible to easily connect a generator. The generator has to follow completely or at least part of it, this precession motion.

The rotor of the generator clearly acts exactly like a flywheel. Probably it is crucial to have the centre of gravity of the whole rotating mass at the pivot of the gimbal, symmetrically distributed to either side of the flywheel axis. It follows that the generator either has to be symmetrically split up into two smaller generators (as indicated in Figure 4.3), one on either side of the flywheel, or that the rotor of one generator is designed multifunctional, appropriate to provide the electrical requirements as well as the flywheel requirements. In both cases the generator has to follow the oscillating gimbal motion.

There is a further possible layout to avoid this undesired motion of the generator, which would slightly complicate the electrical connection and the controlling. This variant is considered to have a stationary (relative to the whole device) stator, and just the inner part of the generator, the rotor, follows, incorporated in the flywheel, the precession motion. In other words the rotor tilts laterally in respect to the stator, and thus is moving partially in and out of the stator windings. The inner shape of the stator and the outer shape of the

rotor, respectively flywheel, have to be spherical to allow this relative movement. This would lead, however, to a quite uncommon rotor and stator design where the windings have to follow the spherical shape. The drift motion, which changes the orientation of the elsewise symmetrically aligned magnetic field lines could lead to odd unbalanced electromagnetic forces and thus to heavy oscillations and vibrations in the whole system. To asses this issue, further investigation into the electrical design of generators is needed.

It is generally mainly an economical question which of the concept for the implementation of the generator will be the most appropriate one. A design which is not using available off-the-shelf technology is generally more costly.

4.4 Power Transmission and Mooring

The generator will run with inconstant speed and thus the produced AC voltage will have a varying frequency. Thus, as well as most reasonable for power transmission either way, the generated voltage will be transform, up to a higher uniform voltage and then rectify it to DC voltage. DC voltage makes it possible to connect several devices and thus allows designing of whole wave energy farms.

Each device has to be fixated by suitable moorings. This can be done by common chain and steel cable moorings, or by newly more and more emerging fibre cables. The different buoyancy of them and thus different slacking behaviour gives quite different mooring conditions. It can further be questioned if it is more appropriate to moor each device separately or to interconnect them first; both have advantages as well as disadvantages. However, mooring system and also the power transmission is beyond the scope of the present work.

5 Gyroscope Kinetics

Heaving explained the working principle of the WaveGyro, the basic equations of motion of the gyroscope shall now be derived. For the present this will be done under certain assumptions and simplification, as it will be explained. The interaction of the waves, and thus the combined equation of motion of the whole device and the gyroscopes will be treated in the subsequent chapter. Here the fundamental equations of motion, following the momentum theorem of Newton and Euler shall be described first. Two different approaches will be shown, one using simplifications from the onset and then another, more general approach.

5.1 Simplified Approach

The following derivation of the equation of motion will be based on of Nick Townsend's paper: "Gyrostabiliser Vehicular Technology" [24].

This approach starts with initial simplification. The assumptions used are, that the angular pitch velocity and acceleration (here $\dot{\theta}_z$ and $\ddot{\theta}_z$) are much smaller then the spin velocity of the gyroscope, hence their influence can be neglected. Then in the following section, a more general derivation of the gyroscope kinetics will be shown, pointing out the influences of these simplifications which are used here.

As it was mentioned in chapter 4.2 "The Gyroscope", the issue for deriving the equation of motion are the relative motion of the gyroscope in respect to the device as well as the relative motion of the device itself. To cope with this relative motions, three coordinate frames, as shown in Figure 5.1, are introduced, one inertial frame (X_i, Y_i, Z_i) and two accelerated, non-inertial frames (x_d, y_d, z_d) and (x_g, y_g, z_g). The subscripts d, and g are standing for 'device' and respectively 'gimbal'. The non-inertial frame (x_d, y_d, z_d) is body fixed to the whole device with its origin at the centre of gravity. The third coordinate frame (x_g, y_g, z_g) is fixed to the gimbal, or respectively gyroscope but not spinning about its axis. In other words the y_g points in direction of the flywheel axis while x_g points in the direction of the gimbal axis and hence z_g, perpendicular to both, stays in the plane of the precession motion. The origin is again considered to be at the centre of gravity of the gyroscope. In a first step simplification is done by defining both origins to coincide and further more, both origins are at the pivot point of the device's pitch motion.

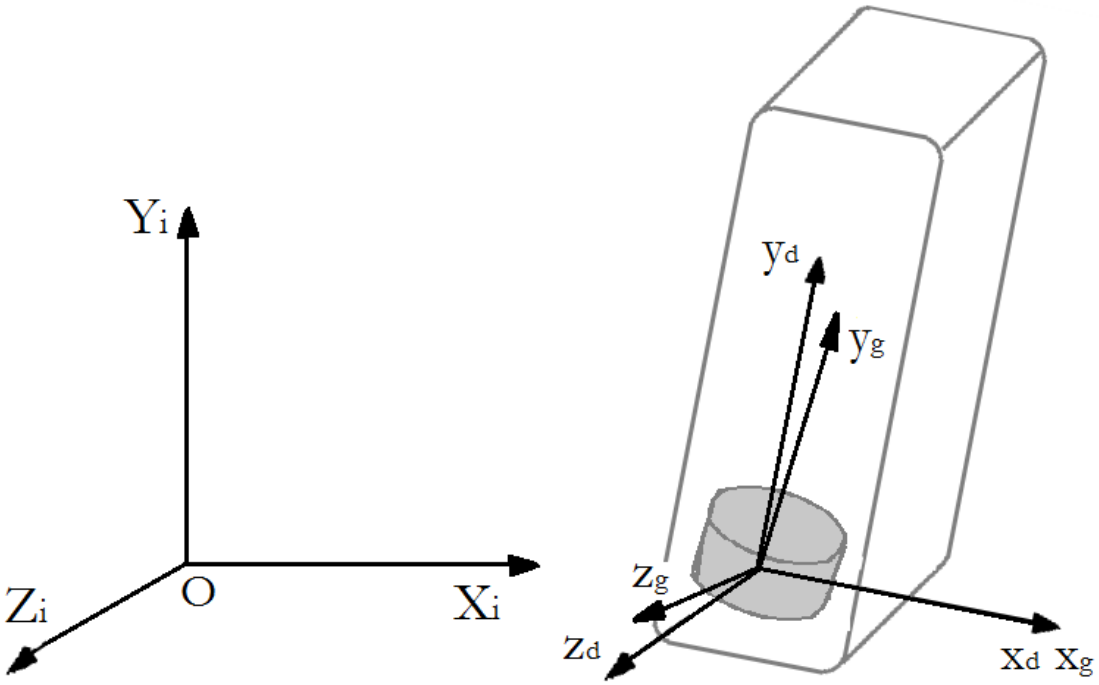

Figure 5.1: Definition of the three coordinate frames

The moment of inertia **I** of any body is determined by the distribution of its mass m:

$$\mathbf{I} = \int \vec{r}^2 \, dm \, . \tag{5.1}$$

The distribution here is given by the distance $\vec{r}$ in respect to an arbitrary reference point (which is usually on the axis of rotation). In general, $\vec{r}$ is a vector in three dimensions and thus the moment of inertia a tensor:

$$\mathbf{I} = \begin{bmatrix} I_x & I_{xy} & I_{xz} \\ I_{yx} & I_y & I_{yz} \\ I_{zx} & I_{zy} & I_z \end{bmatrix} . \tag{5.2}$$

The components on the diagonal, I_x, I_y and I_z are the principal moments of inertia, while the other components are called the products of inertia. For each body there is a reference system for which those product of inertia vanish, the so-called principal axis. For the symmetric gyroscope, respectively flywheel, the principal axes are (x_g, y_g, z_g) and thus for the flywheel's moment of inertia about this axis system:

$$\mathbf{I_f} = \begin{bmatrix} I_{fx} & 0 & 0 \\ 0 & I_{fy} & 0 \\ 0 & 0 & I_{fz} \end{bmatrix}. \tag{5.3}$$

Here I_{fx} and I_{fz} are equal, due to the rotation-symmetry of the flywheel.

The angular momentum $\vec{L}_g$ with respect to the gimbal frame (x_d, y_d, z_d) is then just:

$$\vec{L}_g = \mathbf{I_f}\, \dot{\vec{\varphi}}\,, \tag{5.4}$$

where $\dot{\vec{\varphi}}$ describes the angular velocity of the gyroscope with the components $\left(\dot{\varphi}_x, \dot{\varphi}_y, \dot{\varphi}_z\right)^{\mathrm{T}}$ about the gimbal-frame axis. An upright spinning gyroscope is considered, thus $\dot{\varphi}_y$ expresses the 'spin rate' and $\dot{\varphi}_x$ the 'velocity of precession' (compare Figure 4.1 and Figure 5.1). However, the gimbal gives a mechanical restriction which does not allow any rotation about the z-axis, and it follows that $\dot{\varphi}_z = 0$. Use of the simplification was made in this step, which is, that the angular velocity $\dot{\vec{\varphi}}$ in equation (5.4) is actually not in respect to an inertial frame.

The angular velocity $\dot{\vec{\varphi}}$ is expressed in the gimbal fixed coordinate frame (x_g, y_g, z_g). To deduce the angular momentum $\vec{L}_d$ in the device fixed coordinate system (x_d, y_d, z_d), the rotation between them has to be considered. That is, by the definition of these coordinate frames, however, just given by φ_x, the 'precession displacement' about their coincident x-axes. A rotation matrix, $\mathbf{A_{gd}}$ describing this rotation can be formed by the use of quaternion representation, or by Euler angels [24]. Because the precession angle is far beneath 90°, issue with gimbal lock will not occur, and thus the latter method, Euler's rotation matrix used is (compare Figure 5.2):

$$\mathbf{A_{gd}} = \begin{bmatrix} 1 & 0 & 0 \\ 0 & \cos(\varphi_x) & -\sin(\varphi_x) \\ 0 & \sin(\varphi_x) & \cos(\varphi_x) \end{bmatrix}. \tag{5.5}$$

Hence the angular momentum with respect to the device coordinate frame is expressed as:

$$\vec{L}_d = \mathbf{A_{gd}}\, \vec{L}_g = \mathbf{A_{gd}}\, \mathbf{I_f}\, \dot{\vec{\varphi}}\,. \tag{5.6}$$

The principle of angular momentum is, according to Newton (as already stated in equation (4.1)), that a resultant moment equals the rate of change of angular momentum:

$$\vec{M} = \frac{d}{dt}\vec{L}\,. \tag{5.7}$$

The resultant moment $\vec{M}$ is described in the same coordinate frame as $\vec{L}$ is, hence for the intended purpose in the device's frame. The time derivation in (5.7) is however in respect to the inertial coordinate frame. To combine equations (5.6) and (5.7), this time derivation in equation (5.7) with respect to the inertial coordinate frame, must be considered. Whereas the angular momentum $\vec{L}_d$ in equation (5.6) is defined with respect to a moving coordinate frame. The relation of the time derivation between a moving, and thus time dependent, and a rigid coordinate frame, is however given by [25]:

$$\frac{d}{dt}\vec{L}_d = \frac{d^*}{dt}\vec{L}_d + \dot{\vec{\theta}} \times \vec{L}_d\,, \tag{5.8}$$

where $\frac{d^*}{dt}$ denotes the time differentiation in the moving system, here the device frame. And $\dot{\vec{\theta}}$ is the angular velocity of the moving system. In other words, the vector $\left(\theta_x, \theta_y, \theta_z\right)^{\mathrm{T}}$ denotes the rotation of the device's body fixed coordinates (x_d, y_d, z_d) relative to the inertial system (X_i, Y_i, Z_i). Instead of the cross product in the last term of the equation (5.8), a skew-symmetric expression with the matrix:

$$\mathbf{\Theta^x} = \begin{bmatrix} 0 & -\dot{\theta}_z & \dot{\theta}_y \\ \dot{\theta}_z & 0 & -\dot{\theta}_x \\ -\dot{\theta}_y & \dot{\theta}_x & 0 \end{bmatrix} \tag{5.9}$$

may be preferable. This then leads to:

$$\frac{d}{dt}\vec{L}_d = \frac{d^*}{dt}\vec{L}_d + \mathbf{\Theta^x}\,\vec{L}_d\,. \tag{5.10}$$

Upon substituting for $\vec{L}_d$ the expression derived in equation (5.6) yields:

$$\frac{d}{dt}\vec{L}_d = \frac{d^*}{dt}\left(\mathbf{A_{gd}}\,\mathbf{I_f}\,\dot{\vec{\varphi}}\right) + \mathbf{\Theta^x}\left(\mathbf{A_{gd}}\,\mathbf{I_f}\,\dot{\vec{\varphi}}\right). \tag{5.11}$$

Since in the first term of the right hand side $\vec{\varphi}$ as well as $\mathbf{A_{gd}}$ are time dependent the product rule for matrix differentiation [26] has to be used, that is:

$$\frac{d^*}{dt}\left(\mathbf{A_{gd}}\,\mathbf{I_f}\,\dot{\vec{\varphi}}\right) = \frac{d^*}{dt}\left(\mathbf{A_{gd}}\right)\mathbf{I_f}\,\dot{\vec{\varphi}} + \mathbf{A_{gd}}\,\mathbf{I_f}\frac{d^*}{dt}\left(\dot{\vec{\varphi}}\right). \tag{5.12}$$

Consequently equation (5.11) may be rewritten as:

$$\dot{\vec{L}}_d = \left(\mathbf{A_{gd}}\,\mathbf{I_f}\right)\ddot{\vec{\varphi}} + \left(\dot{\mathbf{A}}_{\mathbf{gd}}\,\mathbf{I_f} + \boldsymbol{\Theta}^{\mathbf{x}}\,\mathbf{A_{gd}}\,\mathbf{I_f}\right)\dot{\vec{\varphi}}. \tag{5.13}$$

Where now the dot-writing is used for the time differentiation instead of $\frac{d^*}{dt}$. Expanding the matrices and vectors with the given definitions leads to:

$$\dot{\vec{L}}_{d,1} = \begin{bmatrix} I_{fx}\,\ddot{\varphi}_x + I_{fy}\,\dot{\varphi}_y\,\dot{\theta}_y\,sin(\varphi_x) - I_{fy}\,\dot{\varphi}_y\,\dot{\theta}_z\,cos(\varphi_x) \\ I_{fy}\,\ddot{\varphi}_y\;cos(\varphi_x) - I_{fy}\,\dot{\varphi}_x\,\dot{\varphi}_y\;sin(\varphi_x) + I_{fy}\,\dot{\varphi}_y\,\dot{\theta}_x\;sin(\varphi_x) + I_{fx}\,\dot{\varphi}_x\,\dot{\theta}_z \\ I_{fy}\,\ddot{\varphi}_y\;sin(\varphi_x) + I_{fy}\,\dot{\varphi}_x\,\dot{\varphi}_y\;cos(\varphi_x) + I_{fy}\,\dot{\varphi}_y\,\dot{\theta}_x\;cos(\varphi_x) - I_{fx}\,\dot{\varphi}_x\,\dot{\theta}_y \end{bmatrix}. \tag{5.14}$$

So far the derivations were done general. However, in equation (5.14) and henceforth the index '1' is used to point out that the motions and moments of the first gyroscope are described. This is necessary because now a second gyroscope will be implemented, identified with the index '2'. In chapter 4.2 it was stated that one concept of the WaveGyro intends to use two counterwise spinning gyroscopes to balance lateral (roll) moments. Following this concept, it has to be considered that for this second gyro, beside the counterwise rotation $\dot{\varphi}_{y2} = -\dot{\varphi}_{y1}$, also the precession angle is (at least for the ideal controlled condition) exactly reversed, $\varphi_{x2} = -\varphi_{x1}$. Bearing further in mind that cosine is an even and sine an odd function, it follows that the second gyroscope satisfies:

$$\dot{\vec{L}}_{d,2} = \begin{bmatrix} -I_{fx}\,\ddot{\varphi}_x + I_{fy}\,\dot{\varphi}_y\,\dot{\theta}_y\,sin(\varphi_x) + I_{fy}\,\dot{\varphi}_y\,\dot{\theta}_z\,cos(\varphi_x) \\ -I_{fy}\,\ddot{\varphi}_y\;cos(\varphi_x) - I_{fy}\,\dot{\varphi}_x\,\dot{\varphi}_y\;sin(\varphi_x) + I_{fy}\,\dot{\varphi}_y\,\dot{\theta}_x\;sin(\varphi_x) - I_{fx}\,\dot{\varphi}_x\,\dot{\theta}_z \\ +I_{fy}\,\ddot{\varphi}_y\;sin(\varphi_x) + I_{fy}\,\dot{\varphi}_x\,\dot{\varphi}_y\;cos(\varphi_x) - I_{fy}\,\dot{\varphi}_y\,\dot{\theta}_x\;cos(\varphi_x) + I_{fx}\,\dot{\varphi}_x\,\dot{\theta}_y \end{bmatrix}. \tag{5.15}$$

Both gyroscopes are placed in the same device and thus the resulting moments can be added. It follows for the two gyro system that the combined reaction moment acting in the device frame is:

$$\vec{M}_D = \dot{\vec{L}}_{d,1} + \dot{\vec{L}}_{d,2} = \begin{bmatrix} 2\, I_{fy}\, \dot{\varphi}_y\, \dot{\theta}_y\, sin(\varphi_x) \\ -2\, I_{fy}\, \dot{\varphi}_y\, \dot{\theta}_x\ \ sin(\varphi_x) \\ 2\, I_{fy}\, \ddot{\varphi}_y\ sin(\varphi_x) + 2\, I_{fy}\, \dot{\varphi}_x\, \dot{\varphi}_y\ cos(\varphi_x) \end{bmatrix}. \tag{5.16}$$

As a first step pure pitch motions is considered, that is $\dot{\theta}_x = \dot{\theta}_y = 0$, and furthermore a constant spin rate of the gyroscopes, that implies $\ddot{\varphi}_y = 0$. Hence the free precession motion of the gyroscopes under an applied pitch moment satisfies:

$$\vec{M}_{pitch} = \vec{M}_D = \begin{bmatrix} 0 \\ 0 \\ 2\, I_{fy}\, \dot{\varphi}_x\, \dot{\varphi}_y\ cos(\varphi_x) \end{bmatrix}. \tag{5.17}$$

Now advertence to the power take of moment will be given, which is a consequence of the spin-up mechanism, as it was explained in section 4.2. This moment gives a reaction against the precession motion of the gyroscopes, which is about the x_d-axis in the device's frame. As it was explained the two gyroscopes are operating in a mirrored way, thus the both power take-off moments are acting in opposite directions. Hence, if they are just added together, as it was done in equation (5.17), they cancel entirely (i.e. no net roll moment will act on the device as a whole). Considering however the power take-off moments for the sake of power capture, their direction is not important. It follows that just their modulus is significant. In other words, due to the exactly mirrored condition it is appropriate to take just the double of the power take-off moment of the first gyroscope to describe the entire system composed of two gyroscopes.

Starting again with the 'first' gyroscope, equation (5.14), and the stated assumption that $\dot{\theta}_x = \dot{\theta}_y = 0$, and $\ddot{\varphi}_y = 0$ gives:

$$\dot{\vec{L}}_{d,1} = \vec{M}_{d,1} = \begin{bmatrix} I_{fx}\, \ddot{\varphi}_x - I_{fy}\, \dot{\varphi}_y\, \dot{\theta}_z\, cos(\varphi_x) \\ -I_{fy}\, \dot{\varphi}_x\, \dot{\varphi}_y\ sin(\varphi_x) + I_{fx}\, \dot{\varphi}_x\, \dot{\theta}_z \\ I_{fy}\, \dot{\varphi}_x\, \dot{\varphi}_y\ cos(\varphi_x) \end{bmatrix}. \tag{5.18}$$

The third entry of this vector gives again the reaction moment due to an applied pitch moment M_D, but here just for one gyroscope. The second entry denotes the moment about the y-axis which has to be taken by the gimbal and the first entry gives the power take-off moment, M_p of one gyroscope.

$$M_p = I_{fx}\,\ddot{\varphi}_x - I_{fy}\,\dot{\varphi}_y\,\dot{\theta}_z\,cos(\varphi_x)\ . \tag{5.19}$$

Heaving derived this relation for the power take of moment as well as the gyroscopic response due to pitch motion it is possible to derive the whole kinetics of the WaveGyro including the hydrodynamics of the waves. Before treating this in chapter 6 in depth, a more holistic approach for the derivation of the gyroscope kinetics will be given next.

5.2 Holistic Approach

The as yet done derivation of the moment acting in the device frame was subject to simplification. That was, the angular pitch velocity $\dot{\theta}_z$ of the whole device, is small compared to the spin velocity of the gyroscope. For completeness and insight, the full derivation of the moment shall be given now. The coordinate frames used are the same as in the previous derivation.

Going back to Newton, the angular momentum is given by:

$$\vec{L} = \mathbf{I}\,\vec{\omega}\,, \tag{5.20}$$

where, in general, the moment of inertia, $\mathbf{I}$ as well as the angular velocity, $\vec{\omega}$ are time dependent. The moment of inertia of any body, described in its own, body fixed coordinates, is however constant. Furthermore, if the coordinates are chosen appropriate (along the axis/plane of symmetry and through the CG) one can get rid of the products of inertia (see explanation given to equation (5.3)). Due to this advantageous properties the angular momentum shall be described in the flywheel fixed coordinates (x_f, y_f, z_f), denoted by $\mathbf{I_f}$. This requires for equation (5.20) that also the complete angular velocity $\vec{\omega}$ is described in this coordinates. Here complete indicates that $\vec{\omega}$ has to be in respect to an inertial frame. In other words $\vec{\omega}$ is the angular velocity of the flywheel frame (x_f, y_f, z_f) in respect to the inertial frame (X_i, Y_i, Z_i), denoted by $\vec{\omega}_{fi}$. To derive this angular velocity, the coordinate

frames in between, hence the device frame (x_d, y_d, z_d) and the gimbal frame (x_g, y_g, z_g), and their relative motions have to be considered.

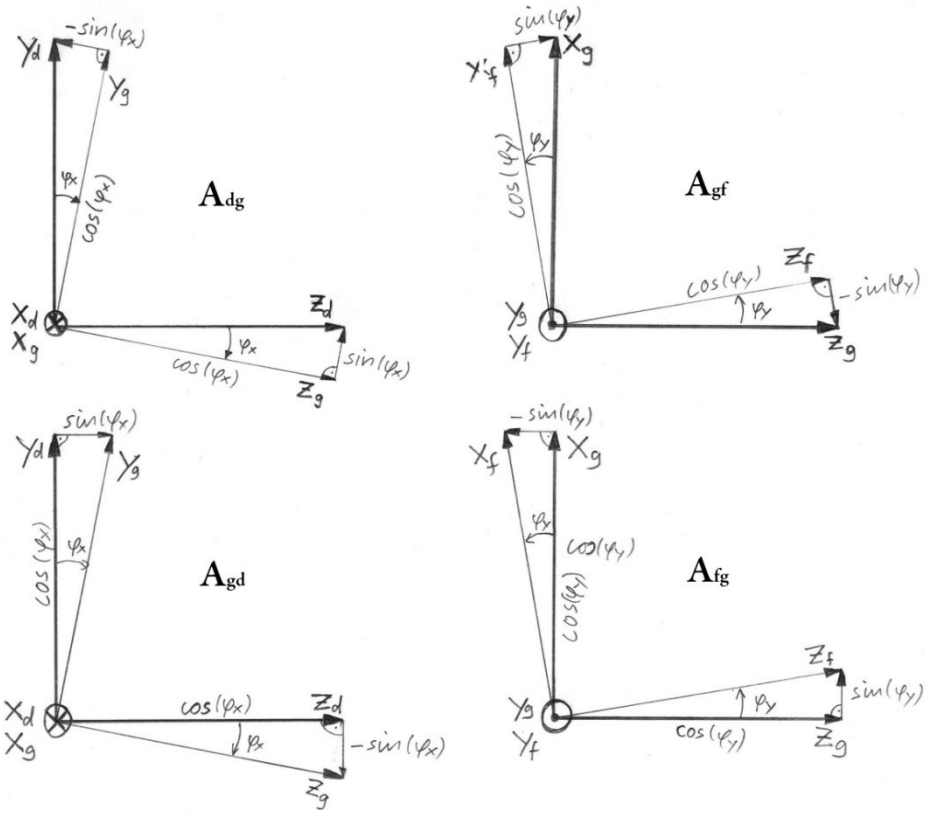

Figure 5.2: Rotations between coordinate systems

Starting from the outer frame, first the angular velocity $\vec{\omega}_{di}$ of the device frame in respect to the inertial frame is described (hence subscript 'di'; this indexing will be used analogues henceforth). It is important to notice that $\vec{\omega}_{di}$ is the rotation descried in its own coordinates, the coordinates of the device. Considering pure pitch motion that is:

$$\vec{\omega}_{di} = \begin{bmatrix} 0 \\ 0 \\ \dot{\theta}_z \end{bmatrix}. \tag{5.21}$$

In the next step the motion of the gimbal is considered. The angular velocity of the gimbal frame $\vec{\omega}_{gi}$ is composed of its own velocity in respect to the devices frame, $\vec{\omega}_{gd}$, plus the inertial motion of the device frame $\vec{\omega}_{di}$. The angular velocity shall again be expressed in its own coordinate frame, hence here in the gimbal frame. This requires a transformation of $\vec{\omega}_{di}$, which is yet described in device frame coordinates, into the coordinates of the gimbal. The rotation between those coordinates is given by the precession angle φ_x.

Mathematically this transformation from the device to the gimbal frame is expressed with the rotation matrix $\mathbf{A_{dg}}$, built up with this angle.

Hence the inertial velocity of the gimbal frame is:

$$\vec{\omega}_{gi} = \vec{\omega}_{gd} + \mathbf{A_{dg}}\,\vec{\omega}_{di}\,, \tag{5.22}$$

with $\vec{\omega}_{gd}$ as the precession velocity, which is about the x-axis of the gimbal and hence:

$$\vec{\omega}_{gd} = \begin{bmatrix} \dot{\varphi}_x \\ 0 \\ 0 \end{bmatrix}. \tag{5.23}$$

To comprehend how $\mathbf{A_{dg}}$ is composed it may help to familiarise oneself with the illustration of the coordinate frame rotation, given in Figure 5.2. From that, it follows:

$$\mathbf{A_{dg}} = \begin{bmatrix} 1 & 0 & 0 \\ 0 & \cos(\varphi_x) & \sin(\varphi_x) \\ 0 & -\sin(\varphi_x) & \cos(\varphi_x) \end{bmatrix}. \tag{5.24}$$

(Compare with the rotation matrix for the opposed transformation, given in equation (5.5))

Now the flywheel itself is considered. Again, the angular velocity of the flywheel is composed of its own velocity in respect to the gimbal, that is its spin velocity $\vec{\omega}_{fg}$, and the inertial motion of the gimbal coordinates $\vec{\omega}_{gi}$. As before, it is necessary to transform $\vec{\omega}_{gi}$ into the coordinates of the flywheel, done by the rotation matrix $\mathbf{A_{gf}}$.

Hence the complete (in respect to an inertial frame) angular velocity of the flywheel is:

$$\vec{\omega}_{fi} = \vec{\omega}_{fg} + \mathbf{A_{gf}}\,\vec{\omega}_{gi}\,. \tag{5.25}$$

Where the spin velocity $\vec{\omega}_{fg}$ is in respect to the gimbal frame, and because the flywheel is spinning about the y-axis of the gimbal it is defined as:

$$\vec{\omega}_{fg} = \begin{bmatrix} 0 \\ \dot{\varphi}_y \\ 0 \end{bmatrix}. \tag{5.26}$$

And the rotation matrix used is (compare Figure 5.2):

$$\mathbf{A_{gf}} = \begin{bmatrix} \cos(\varphi_y) & 0 & -\sin(\varphi_y) \\ 0 & 1 & 0 \\ \sin(\varphi_y) & 0 & \cos(\varphi_y) \end{bmatrix}. \tag{5.27}$$

Insertion of equation (5.22) into equation (5.25) gives for the absolute inertial angular velocity of the flywheel, as described in its own axis:

$$\vec{\omega}_{fi} = \vec{\omega}_{fg} + \mathbf{A_{gf}} \left(\vec{\omega}_{gd} + \mathbf{A_{dg}}\, \vec{\omega}_{di}\right). \tag{5.28}$$

Hence the angular momentum of the flywheel respectively gyroscope can, according to equation (5.20), be expressed as:

$$\vec{L}_f = \mathbf{I_f}\, \vec{\omega}_{fi}\,. \tag{5.29}$$

An applied resultant moment leads to a change of the angular momentum with respect to time. In other words the differentiation with respect to time of the angular momentum equals the applied moment (as stated in equation (5.7)). One has to notice that the resultant moment, calculated in this way, is described in the same coordinate frame as the angular momentum, i.e. here in the flywheel frame. As mentioned earlier, a time differentiation in a moving coordinate frame requires consideration of the change of the frame itself in respect to time. With some mathematics it is deducible, as it was already done by Euler, that the time variation of the angular momentum in a moving frame is described (as in equation (5.8)) by:

$$\frac{d}{dt}\vec{L} = \frac{d^*}{dt}\vec{L} + \vec{\omega} \times \vec{L}\,, \tag{5.30}$$

with $\frac{d^*}{dt}$ denoting the time derivative in respect to the moving system. (Note that this is respectively applicable for any vector differentiation in a non-inertial frame). Hence the applied flywheel moment, using equation (5.29) in (5.30), is:

$$\vec{M}_f = \frac{d}{dt}\vec{L}_f = \frac{d^*}{dt}\vec{L}_f + \vec{\omega}_{fi} \times \vec{L}_f = \mathbf{I_f}\, \dot{\vec{\omega}}_{fi} + \vec{\omega}_{fi} \times \left(\mathbf{I_f}\, \vec{\omega}_{fi}\right). \tag{5.31}$$

Inserting herein equation (5.28), while keeping the product differentiation rule in mind, yields:

$$\vec{M}_f = \mathbf{I_f}\left[\dot{\vec{\omega}}_{fg} + \dot{\mathbf{A}}_{\mathbf{gf}}\left(\vec{\omega}_{gd} + \mathbf{A_{dg}}\,\vec{\omega}_{di}\right) + \mathbf{A_{gf}}\left(\dot{\vec{\omega}}_{gd} + \dot{\mathbf{A}}_{\mathbf{dg}}\,\vec{\omega}_{di} + \mathbf{A_{dg}}\,\dot{\vec{\omega}}_{di}\right)\right] + \left[\vec{\omega}_{fg} + \mathbf{A_{gf}}\left(\vec{\omega}_{gd} + \mathbf{A_{dg}}\,\vec{\omega}_{di}\right)\right] \times \left[\mathbf{I_f}\left(\vec{\omega}_{fg} + \mathbf{A_{gf}}\left(\vec{\omega}_{gd} + \mathbf{A_{dg}}\,\vec{\omega}_{di}\right)\right)\right].$$

(5.32)

This resultant moment is however still described in the flywheel frame. For engineering purposes and the layout of the device the moment in the gimbal and even more in the device frame is of interest. Therefore, the moment needs to be transformed back into the gimbal frame, done by a rotation matrix given by:

$$\mathbf{A_{fg}} = \begin{bmatrix} \cos(\varphi_y) & 0 & \sin(\varphi_y) \\ 0 & 1 & 0 \\ -\sin(\varphi_y) & 0 & \cos(\varphi_y) \end{bmatrix}. \tag{5.33}$$

The here considered rotation is between the same frames as for which $\mathbf{A_{gf}}$ was derived, just backwards. It thus follows directly that $\mathbf{A_{fg}}$ is the transpose of $\mathbf{A_{gf}}$ (see also Figure 5.2). Furthermore, due to the orthogonality (i.e. a determinant of ± 1) of rotation matrices it follows that these matrices are each other's inverse. That is:

$$\mathbf{A_{fg}} = \mathbf{A_{gf}}^{\mathbf{T}} = \mathbf{A_{gf}}^{-\mathbf{1}}. \tag{5.34}$$

It follows subsequently for the moment about the gimbal frame:

$$\vec{M}_g = \mathbf{A_{fg}}\,\vec{M}_f = \mathbf{A_{gf}}^{-\mathbf{1}}\,\vec{M}_f. \tag{5.35}$$

One can argue in the same way for $\mathbf{A_{gd}}$, the rotation matrix for back rotation from the gimbal to the device frame. Hence the moment from the flywheel, described in the device's frame is determined by:

$$\vec{M}_d = \mathbf{A_{gd}}\,\vec{M}_g = \mathbf{A_{dg}}^{-\mathbf{1}}\,\vec{M}_g = \mathbf{A_{dg}}^{-\mathbf{1}}\,\mathbf{A_{gf}}^{-\mathbf{1}}\,\vec{M}_f. \tag{5.36}$$

And inserting the flywheel moment from equation (5.32) yields subsequently:

$$\vec{M}_d = \mathbf{A_{dg}}^{-1}\,\mathbf{A_{gf}}^{-1}\left\{\mathbf{I_f}\left[\dot{\vec{\omega}}_{fg} + \dot{\mathbf{A}}_{\mathbf{gf}}\left(\vec{\omega}_{gd} + \mathbf{A_{dg}}\,\vec{\omega}_{di}\right) + \mathbf{A_{gf}}\left(\dot{\vec{\omega}}_{gd} + \dot{\mathbf{A}}_{\mathbf{dg}}\,\vec{\omega}_{di} + \mathbf{A_{dg}}\,\dot{\vec{\omega}}_{di}\right)\right]\right.$$
$$\left. + \left[\vec{\omega}_{fg} + \mathbf{A_{gf}}\left(\vec{\omega}_{gd} + \mathbf{A_{dg}}\,\vec{\omega}_{di}\right)\right] \times \left[\mathbf{I_f}\left(\vec{\omega}_{fg} + \mathbf{A_{gf}}\left(\vec{\omega}_{gd} + \mathbf{A_{dg}}\,\vec{\omega}_{di}\right)\right)\right]\right\}.$$

(5.37)

All the matrices and vectors in this expression are known and given. It is hence possible to calculate $\vec{M}_d$. The reader can readily appreciate that these calculations will lead to huge expressions which are not easy to follow. The step by step derivation of $\vec{M}_d$ is therefore given in Appendix A. Considering now, as done earlier, again two gyroscopes, with opposing spin velocity and opposing precession velocity ($\dot{\varphi}_y = -\dot{\varphi}_{y2}$, $\dot{\varphi}_x = -\dot{\varphi}_{x2}$) allows calculating the combined moment, $\vec{M}_D = \vec{M}_{d,1} + \vec{M}_{d,2}$. The expression for the combined moment is, due to the opposing components in $\vec{M}_{d,1}$ and $\vec{M}_{d,2}$ fairly reduced. By taking the flywheel's spin rate as constant, $\ddot{\varphi}_y = 0$, and using the furthermore the symmetry of the flywheel, $I_{fz} = I_{fx}$ a further reduction can be archived, leading to a combined moment as follows (compare Appendix A):

$$\vec{M}_D = \begin{bmatrix} 0 \\ 0 \\ 4\left(I_{fy} - I_{fx}\right)\dot{\varphi}_x\dot{\theta}_z \sin(\varphi_x)\cos(\varphi_x) + 2\ddot{\theta}_z\left(I_{fy}\sin^2(\varphi_x) + I_{fx}\cos^2(\varphi_x)\right) + 2I_{fy}\dot{\varphi}_x\dot{\varphi}_y\cos(\varphi_x) \end{bmatrix}.$$

(5.38)

As it can bee seen immediately, all components of the rotation matrix $\mathbf{A_{gf}}$, respectively $\mathbf{A_{gf}^{-1}}$, are vanished. From a physical point of view this is quite logical, because the flywheel is actually rotationally symmetric about its spin axis.

Generally it is not that straight forward to comprehend this resultant moment in a physical sense though. Hence a bit of 'fiddling' with this equation shall help to gain more inside.

Case (1): In a first case the flywheel is considered as to be not spinning, that is $\dot{\varphi}_y = 0$, and the gimbal to be fixed, that is $\varphi_x = 0$. Using this condition in equation (5.38) gives for the moment about the pitch axis:

$$M_{D_{z1}} = 2\,I_{fx}\ddot{\theta}_z\,. \tag{5.39}$$

Calling back the introduction that $I_{fx} = I_{fz}$, this is clearly just the basic moment of a body which is accelerated about one axis, here the z-axis (hence just the angular representation of '$F = ma$'). The factor 2 is just due to the reason that two gyroscopes are destined.

Case (2): In a second case the gimbal is still considered to be fixed, $\varphi_x = 0$, but the flywheel is now rotating with a constant rate. This condition gives for the pitch moment:

$$M_{D_{z2}} = 2\, I_{fx}\ddot{\theta}_z\,. \tag{5.40}$$

That is also quite reasonable, because the basic, pure gyroscopic moment is acting perpendicular to the momentum of inertia (y-axis) and perpendicular to its rate of change (z-axis). The gyroscopic moment acts thus just about the x-axis against the interlocking of the gimbal. There is no contribution to the moment about the z-axis, the considered pitch moment. The only remaining term is hence the same as for case 1, for which the flywheel was not rotating.

Case (3): The third case considers the vice-versa condition, so to speak the flywheel does not spin about is main axis, $\dot{\varphi}_y = 0$, but it is free to rotate about its gimbal axis. The pitch moment, following equation (5.38), is then:

$$\begin{aligned} M_{D_{z3}} = {} & 4\big(I_{fy} - I_{fx}\big)\dot{\varphi}_x\dot{\theta}_z \sin(\varphi_x)\cos(\varphi_x) \\ & + 2\ddot{\theta}_z\big(I_{fy}\sin^2(\varphi_x) + I_{fx}\cos^2(\varphi_x)\big)\,. \end{aligned} \tag{5.41}$$

The reason for this slightly more complex result, compared with (5.40), is, that here the spin axis is not the axis of symmetry. If however a spherical gyroscope is considered, that is in addition to $I_{fz} = I_{fx}$ also the symmetry $I_{fy} = I_{fx}$, this moment reduces to:

$$M_{D_{z3}} = 2I_{fx}\ddot{\theta}_z\,. \tag{5.42}$$

This can be argued with the same reasoning as done for equation (5.40). In other words, the difference to the moment in equation (5.41) is due to the change of the moment of inertia about the device's z-axis. That is: for $\varphi_x = 0$ remains I_{fx} and for $\varphi_x = 90°$ remains I_{fy} and for any angle in between a composition of both, just as expressed with (5.41). When using a ring-mass approximation for the flywheel it can be shown that $I_{fx} = \frac{1}{2}I_{fy}$.

Where 'ring-mass' just implies that the mass of the flywheel is evenly spread on ring which has everywhere the same distance from the spin axis.

Heaving comprehended the components of the combined pitch moment (equation (5.38)) it may be worth to retract the simplification necessary to end up with the same result as derived in the previous section (see equation (5.17)). The initial simplification used in the previous approach (p. 35) was, that the angular pitch velocity of the device, $\dot{\theta}_z$ is much smaller then the spin rate, $\dot{\varphi}_y$ of the flywheel. This is justified by considering that the pitch is just an oscillation about a few degrees with the quite low wave frequency, while the gyroscopes are destined to spin with several thousand rpm. The precession velocity $\dot{\varphi}_x$ is in resonance with $\dot{\theta}_z$ (as it will get clear later) and hence in the same order of magnitude, thus as well small compared to $\dot{\varphi}_y$. Furthermore, given that $\dot{\theta}_z$ is an harmonic oscillation with the wave frequency it can be argued that its differentiation $\ddot{\theta}_z$ is in the same order of magnitude like the product $\dot{\varphi}_x \dot{\theta}_z$. Deductive reasoning is to neglect all those components in the combined pitch moment (equation (5.38)) which do not include the flywheel's spin rate $\dot{\varphi}_y$. Doing this yields:

$$\vec{M}_D = \begin{bmatrix} 0 \\ 0 \\ 2\, I_{fy}\, \dot{\varphi}_x\, \dot{\varphi}_y\, cos(\varphi_x) \end{bmatrix}, \tag{5.43}$$

which is exactly what was already derived earlier in equation (5.17) and thus validates the earlier shown simplified approach.

It may also be important to see the difference in the power take of moment M_p between the two different approaches. Using the same conditions and assumptions as in the previous section, equation (5.18) and (5.19), but using now the holistic gyroscopic moment as given in equation (5.37) yields for the power take-off moment:

$$M_p = I_{fx}\, \ddot{\varphi}_x - I_{fy}\, \dot{\varphi}_y\, \dot{\theta}_z\, cos(\varphi_x) + \left(I_{fx} - I_{fy}\right) \dot{\theta}_z{}^2\, sin(\varphi_x)\, cos(\varphi_x)\,. \tag{5.44}$$

The last term in this equation is, as the first in equation (5.38), due to the flywheel's axis of symmetry which alternates about its vertical position. Arguing that $I_{fx} - I_{fy}$ is approximately $-0.5\, I_{fy}$ (ring-mass assumption, see explanation to equation (5.42)) and that $sin(\varphi_x)\, cos(\varphi_x) \leq 0.5$ gives that the last term is from minor influence. Furthermore it can be assumed that $\dot{\theta}_z{}^2$ is comparable small, hence the last term is neglected and the equa-

tion reduces to the one already deduced with the simplified approach, which was (see equation (5.19)):

$$M_p = I_{fx}\,\ddot{\varphi}_x - I_{fy}\,\dot{\varphi}_y\,\dot{\theta}_z\,cos(\varphi_x)\ . \tag{5.45}$$

It can bee readily seen that for the case of vanishing power take-off moment, $M_p = 0$, any pitch, $\dot{\theta}_z$ leads directly to an acceleration of the gyroscopes about their roll axis, $\ddot{\varphi}_x$, the so-called precession.

6 Optimum Power Capture

This chapter deals with the combination of wave hydrodynamics and gyroscope kinetics. Analytic formulas will be deduced which relate the dimensions and operational parameters of the WaveGyro to the efficiency of wave power capture. It gives hence the basic considerations which are required for optimum power capture. Two different approaches will be used to deduce these relations, starting with the superposition principle.

6.1 Superposition Principle

To derive the operation conditions and dimensions of the WaveGyro device, it is necessary to deduce the acting forces and moments and the related motions. This then permits maximum wave power capture. The basic approach used to deduce these desired values follows Widden et al. [13] in the paper: "Analysis of a pitching-and-surging wave-energy converter that reacts against an internal mass, when operating in regular waves", (2008). The WaveGyro is a quite complex system with several independent degrees of freedom, simplifications and assumptions are thus required to facilitate an analytical analysis.

The assumptions made are:

- Linear wave theory is sufficient and accurate enough.
- The angular displacement (i.e. the pitch angle) of the whole device is assumed to be sufficiently small to justify use of linear analysis. In other words the individual forces acting on the hull are all taken to act in a constant direction (i.e. horizontal), not varying with the inclination of the device. That expresses just that the cosine of the time varying pitch angle is taken as if to be unity.
- The precession motion of the gyroscope is controlled to oscillate with the same frequency as the incident waves.
- Self alignment of the submerged structure into the propagation direction of the waves occurs.
- Due to the symmetry about the x-y-plane the motion of the device are treated to be two dimensional, thus only pitch, surge and heave are relevant. Furthermore, heave is neglected because the horizontal cross-section (water plane area) of device is comparable small, leading to a natural oscillation frequency in the heave mode well bellow the wave frequency.

- The natural frequency in the pitch mode is 'tuned' to be close to the wave frequency. This is not generally the case for any pitching structure and needs hence to be included as a special condition for the dimensioning of the device as it will be treated later. This so-called resonance condition is essential to get a maximum oscillation amplitude and thus maximum power capture. Because the incident wave frequency can vary during the operation of the device it is reasonable to adjust the mass (or restoration buoyancy) of the whole device to achieve always this resonance condition.
- In practice the device is fixed with a slack mooring intended to cope with the second order wave drift forces. For the power capture analysis pure linear theory will be used and thus second order effects are not taken into account. Hence mooring forces or constraints are not considered.
- The added mass and hence the centre of gravity, CG, as well as the centre of wave pressure, P, are dependent on the wave frequency. The same is also the case for the damping B, and the added moment of inertia, A_{66}. For simplicity it is initially just one main wave frequency considered.

The following variable definitions and abbreviations in conjunction with the free-body diagram of Figure 6.1 are used in the subsequent analysis presented:

- Overall mass of the device, including the added mass in surge and the gyroscopes masses is: M_x
- Centre of gravity of the mass M_x (thus just for surge) is: CG
- Centre of wave pressure, the point at which the total wave pressure force is thought to be acting without leading to any moment, is: P
- The device's overall moment of inertia, including the added moment of inertia, is: I_P
- Restoration coefficient in pitch direction is: C_P
- Radiation damping in surge is: B

6.1.1 Balance of Forces and Moments

A free-body-diagram of the WaveGyro, presented in Figure 6.1, indicates all the essential forces and moments that need to be considered. The wave excitation force F_{exc}, which is essentially a pressure force, is considered as a combined force acting at one point, the centre of wave pressure, P. The wave excitation force is due to the dynamic pressure of the incident and diffracted water waves. The point P is also taken as the theoretical 'pivot

point', because this reduces the equation of moments. That is because P is the point chosen such that the wave pressure has no acting moment about it. The pitch angle and surge motion are denoted by θ_z and x. Where x is defined as the surge motion of point P. The position of the gyroscopes is defined in terms of their precession angle φ_x. Hence there are three degrees of freedom, namely surge and pitch of the structure and the precession angle of the gyroscopes.

With the use of the previously derived gyroscopic reaction moment two differential equations describing the structures motion can be formed. That is the dynamic equilibrium of acting forces and acting moments respectively.

The acting forces are treated first. Obviously there is no hydrostatic stiffness in surge, hence the reaction force against the wave excitation is here formed by an inertia term plus a damping term. The damping force is in-phase with the velocity of the device and is dependent upon the surge radiation damping, B. For the inertia term, M_x is used as the combined mass, consisting of the device's real mass, m_D and the 'added mass' in surge direction A_{11}.

The distance between the centre of gravity, CG, and the centre of wave pressure, P, is denoted by s. For the inertial force, the relative acceleration between the two points (CG and P) needs to be taken into accounted. Due to the linearization assumption this relative acceleration is simply taken into accounted by the subtraction of the term $s\ddot{\theta}_z$. In other words, because the pitch angle is assumed to be small, the cosine of it is, as approximation, taken to be unity, that is $\cos(\theta_z) \approx 1$.

The gyroscopes are capable to provide a reaction moment but they do not contribute in any way to the balance of forces (as explained in chapter 5). The gyroscope's mass is though already accounted for in the device's real mass m_D.

The for the force balance in surge, i.e. x-direction can be expressed as a resultant force which equals an inertia or acceleration force (d'Alembert's principle):

$$\sum F_x = 0: \qquad F_{res} = F_{inertia} \tag{6.1}$$

That is:

$$F_{exc} - B\,\dot{x} = M_x\left(\ddot{x} + s\,\ddot{\theta}_z\right). \tag{6.2}$$

As mentioned the balance of moments is considered about the point P. Again, because the CG has an offset from the pivot point P an inertia term (the inertia force component of equation (6.2)) with the leaver s provides a moment. Because the inertia moment is the forcing moment it is written on the left hand side of equation (6.3). Reaction against this inertia moment is given by the device's angular moment of inertia, I_P, its hydrostatic stiffness against pitch, C_P, and last but not least the gyroscopic reaction moment. Those are all pure moments and hence they can readily be added regardless their origin location. Heaving given this explanation one can already appreciation that the inertia moment on the left hand side, and thus the mass, leaver and acceleration, should be large to get large gyroscopic reaction moments and in turn a good power capture.

It follows for the balance of moments about point P, that:

$$\sum M_P = 0: \quad M_x\left(\ddot{x} + s\,\ddot{\theta}_z\right) s = -I_P\,\ddot{\theta}_z - C_P\theta_z + 2I_{fy}\,\dot{\varphi}_x\,\dot{\varphi}_y\,cos(\varphi_x)\,. \tag{6.3}$$

For comprehension one may take a look back to Figure 6.1.

There is no contribution of damping in the balance of moments. This is justified by Newman [27] (p. 304 eq. 174), he states a direct proportionality between the damping and the square of the exciting force/moment in the same direction. This relation is valid for bodies, which are symmetric about the x-plane, which is the case for the WaveGyro. This relation gives readily that the damping about the mode of motion in which the excitation on the structure goes to zero vanishes completely. Calling back that point P was defined as the point where the excitation moment vanishes, justifies hence that there will be no contribution of radiation damping in the balance of moments about exactly this points. That is actually what makes this point so important and why it was chosen as the reference point for the force and moment balances.

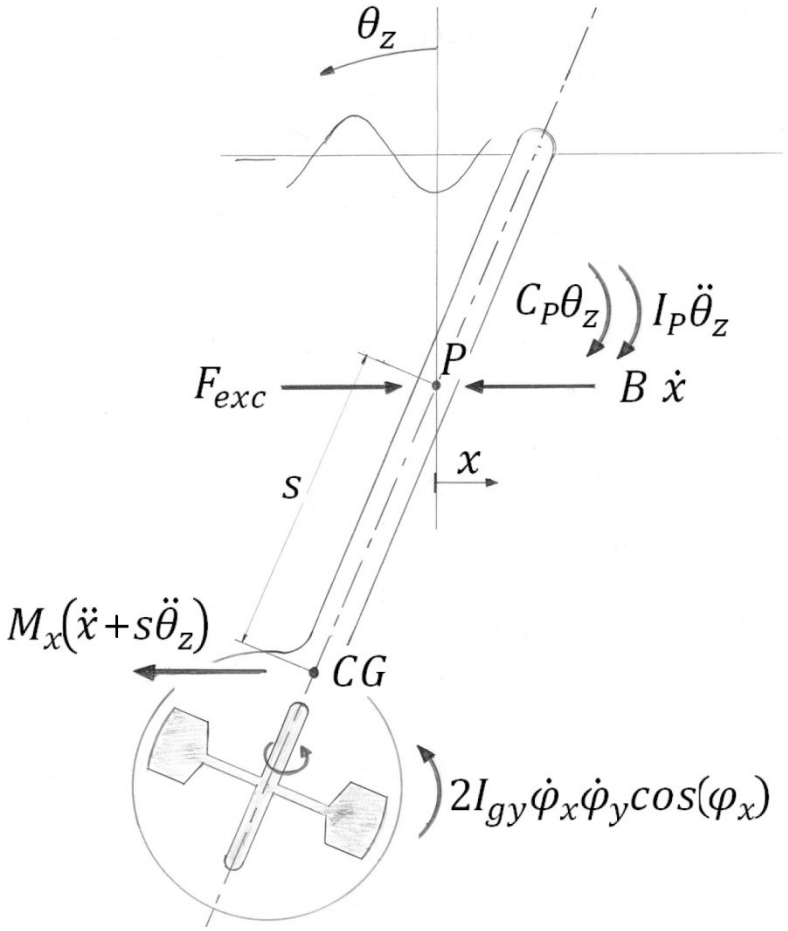

Figure 6.1: Free-body diagram of the WaveGyro

The stiffness against pitch, given by the coefficient C_P, is purely related to the hydrostatic behaviour and hence completely independent from the wave frequency. It will be shown in section 6.6.1 how this coefficient can be deduced. All other components in the both balance equations (6.2) and (6.3) however are highly related to the wave frequency, including the position of P and CG. For the later one this is because the position of CG is dependent on the added mass in surge.

6.1.2 Phase-amplitude Expression

All motion related variables (the 3 DoF) are assumed to vary harmonically with the same frequency, ω, as the waves. This assumption is based on the fact that a reasonable level of power capture consistent with an operation at resonance. It follows that that these variables can be expressed in two components one in-phase and one out-of-phase with the excitation force F_{exc}. Assuming the force is to be described as a real function with cosine time dependency it may be expressed in the form:

$$F_{exc} = F_1 \cos(\omega t)\,. \tag{6.4}$$

The displacement in surge may be written as:

$$x = X_1 \cos(\omega t) + X_2 \sin(\omega t)\,, \tag{6.5}$$

taking into account phase shift with respect to the excitation force. Here X_1 and X_2 are the oscillation amplitudes in-phase and out-of-phase with the excitation force. Differentiation with respect to time gives the oscillation velocity:

$$\dot{x} = \omega X_2 \cos(\omega\, t) - \omega X_1 \sin(\omega t)\,, \tag{6.6}$$

and acceleration:

$$\ddot{x} = -\omega^2\, X_1 \cos(\omega\, t) - \omega^2\, X_2 \sin(\omega t)\,. \tag{6.7}$$

The process is treated in the same manner for the pitch degree of freedom namely:

$$\theta_z = \Theta_1 \cos(\omega\, t) + \Theta_2 \sin(\omega\, t)\,, \tag{6.8}$$

$$\dot{\theta}_z = \omega\, \Theta_2 \cos(\omega\, t) - \omega\, \Theta_1 \sin(\omega\, t) \tag{6.9}$$

and

$$\ddot{\theta}_z = -\omega^2\, \Theta_1 \cos(\omega\, t) - \omega^2 \Theta_2 \sin(\omega\, t)\,. \tag{6.10}$$

Initially the gyroscopic precession angle is considered to oscillate harmonically with the incident wave frequency. In the case of zero power take-off there is no moment acting against the precession motion and it will hence be either way harmonically oscillating with wave frequency. However, if a power take-off moment is applied it needs to be controlled to maintain a harmonic precession. Hence, as above for the pitch angle, the precession angle is expressed in its phase amplitudes:

$$\varphi_x = \Phi_1 \cos(\omega t) + \Phi_2 \sin(\omega t)\,, \tag{6.11}$$

$$\dot{\varphi}_x = \omega \Phi_2 \cos(\omega t) - \omega \Phi_1 \sin(\omega t) \tag{6.12}$$

and

$$\ddot{\varphi}_x = -\omega^2 \Phi_1 \cos(\omega t) - \omega^2 \Phi_2 \sin(\omega t)\,. \tag{6.13}$$

The influence of the precession angle is more complicated than pitch and surge, as its influence is readily seen to be non-linear upon inspection of equation (6.3). This nonlinearity makes identification of an analytic solution impossible. To make the formulation solvable the precession angle, φ_x is initially considered to be small. Hence $cos(\varphi_x)$ is close to unity. Rather then using this feasible simplification one may consider how far a given amplitude of φ_x, that is $\cos(\varphi_x)$ varies over a wave period. This is treated later in section 6.1.6.

The power take of moment is assumed to be controlled to oscillate in a harmonically. It thus may also be expressed in term of in-phase and out-of-phase components:

$$M_p = M_{p1} \cos(\omega\, t) + M_{p2} \sin(\omega\, t)\,. \tag{6.14}$$

The force balance (6.2) and the moment balance (6.3) may be split into their two phase components (using equation (6.4) to (6.13) as required). This split into phase components can by justified by the argument that both equations have to be valid for all times. It follows that these equation have to be valid for both phase components separately because they are exactly out-of-phase. That is, the terms in-phase with the wave excitation (i.e. the cosine terms) in the force balance lead to:

$$F_1 - \omega\, B\, X_2 = -\omega^2 M_x (X_1 + s\, \Theta_1)\,. \tag{6.15}$$

Similarly the out-of-phase force components (i.e. the sine terms), yield:

$$\omega\, B\, X_1 = -\omega^2 M_x (\, X_2 + s\, \Theta_2)\,. \tag{6.16}$$

From the moment balance equation it follows for the in-phase moment equation:

$$-\omega^2 M_x (X_1 + s\, \Theta_1)\, s = \omega^2 I_P \Theta_1 - C_P\, \Theta_1 + 2\omega\, I_{fy} \dot{\varphi}_y \Phi_2\, cos(\varphi_x)\,. \tag{6.17}$$

And similarly it follows from the components out-of-phase with the wave excitation:

$$-\omega^2 M_x (X_2 + s\, \Theta_2)\, s = \omega^2 I_P \Theta_2 - C_P\, \Theta_2 - 2\omega\, I_{fy}\, \dot{\varphi}_y\, \Phi_1\, cos(\varphi_x)\,. \tag{6.18}$$

For maximum energy capture, the device should have a natural pitch frequency close to wave excitation frequency. That is given by the pure pitch relation, that is:

$$I_P\ddot{\theta}_z + C_P\theta_z = -\omega^2 I_P\theta_z + C_P\theta_z = 0\,. \tag{6.19}$$

Where the hydrostatic stiffness, C_P and the angular moment of inertia, I_P are both influenced by the design as e.g. the geometric form the hull. To achieve this resonance condition and thus maximum power capture it is hence essential to design these both parameters appropriate. Bearing in mind that the wave frequency is non-constant it may even by necessary to envisage some kind of adjustment for the both parameters. How this condition can be tackled is treated in detail in section 6.6. For the time being, it is assumed that the resonance condition (equation (6.19)) is satisfied for all wave frequencies.

Including the resonance condition (6.19) into the moment balance equations (6.17), (6.18) permits complete elimination of the hydrostatic stiffness and the angular moment of inertia terms (see also Falnes p.52 eq. (3.42)).

6.1.3 Absorbed Power

Maximum wave power capture implies maximum power absorption by the device. The absorbed power is due to the resultant force, F_{res} and the velocity of the same point, i.e. here the point P. Due to the linearization assumption, this resultant force is supposed to be purely horizontal. Analogical the displacement x is taken to be purely horizontal and hence also the velocity $\dot{x}$. From basic physics it follows for the absorbed power (compare equation (6.1) and (6.2)) that:

$$P_{abs} = F_{res}\,\dot{x} = F_{exc}\,\dot{x} - B\dot{x}^2\,. \tag{6.20}$$

To appreciate the influence of the different phase-amplitudes it is worth to write the absorbed power in its phase components. Therefore the resultant force shall, with the use of equation (6.1), (6.2) and (6.15), first be expressed in its in-phase component:

$$F_{res1} = F_1 - \omega\, B\, X_2\,, \tag{6.21}$$

and its out-of-phase component:

$$F_{res2} = \omega\, B\, X_1\,, \tag{6.22}$$

which follows from equation (6.1), (6.2) and (6.16).

The instantaneous absorbed power may then also be written in terms of phase-amplitudes:

$$\begin{aligned} P_{abs} = F_{res}\,\dot{x} \\ &= \{(F_1 - \omega B X_2)\cos(\omega t) + (\omega B X_1)\sin(\omega t)\} \\ &\cdot \{\omega\, X_2 \cos(\omega t) - \omega\, X_1 \sin(\omega t)\}\,. \end{aligned} \tag{6.23}$$

For a power capture analysis it is however the mean power absorbed which is more a matter of interest. Therefore it is reasonable to split the multiplication in equation (6.23) into its time dependent mixed cosine and sine modes. That is for the cos²-amplitude of the absorbed power:

$$P_{abs}^{cos^2} = (F_1 - \omega B X_2)\omega X_2\,, \tag{6.24}$$

and for the sin²-amplitude of the absorbed power:

$$P_{abs}^{sin^2} = -\omega^2 B {X_1}^2\,. \tag{6.25}$$

Due to the mixed terms in the multiplication there is also a sin-cos-amplitude:

$$P_{abs}^{sin\,cos} = -(F_1 - \omega\, B\, X_2)\omega\, X_1 + (\omega^2\, B\, X_1 X_2) = -\omega X_1 F_1\,. \tag{6.26}$$

The time average, effective or mean power can be found by integration over one period. Because the whole instantaneous absorbed power is a sum of its three modes presented, the integration can be done in parts. The effective value of cos^2 as well as of sin^2 is $1/2$. It follows for the mean absorbed power in the cos²-mode:

$$\bar{P}_{abs}^{cos^2} = \frac{1}{2}(F_1 - \omega B X_2)\omega X_2\,, \tag{6.27}$$

and for the sin²-mode:

$$\bar{P}_{abs}^{sin^2} = -\frac{1}{2}\omega^2 B {X_1}^2\,. \tag{6.28}$$

The mixed sin-cos-mode of the power absorption is however just an oscillation about zero and thus pure power latching. Hence there is no mean power absorption in this mode:

$$\bar{P}_{abs}^{sin\,cos} = 0\,. \tag{6.29}$$

From the negative sign in equation (6.28) it follows directly that any displacement of the device X_1 which is in-phase with the excitation force leads to power losses. In this case the power is lost by radiation damping that is the generation of non-evanescent radiation waves. Maximum power capture can hence just be yield when the out-of-phase displacement $X_1 = 0$. The only reaming contribution to the mean power absorption is from $\bar{P}_{abs}^{cos^2}$ with an oscillation displacement X_2 which is out-of-phase with the wave excitation. This fact is in accordance with the general physical behaviour of any forced oscillating system for which resonance, i.e. fastest swing up, is always obtained for the exact out-of-phase condition between force and displacement.

6.1.4 Maximum Power Conditions

The condition $X_1 = 0$ is just one, necessary for maximum power capture. To find further condition the reaming contribution to the absorbed power, equation (6.27) has to be investigated further. Taking a look at this equation one may appreciate that the only parameter which may be controlled by regulation of the power take-off unit is the displacement amplitude X_2. The other values influencing the power absorption are either determined by the sea stated (wave characteristics) or by the design of the device. Furthermore one sees that the dependency between absorbed power $\bar{P}_{abs}^{cos^2}$ and displacement X_2 is from quadratic nature. There is no power absorption for the case of zero oscillation $X_2 = 0$. And for oscillation amplitude large enough to lead to a damping which equals the wave excitation, $X_2 = \frac{F_1}{\omega B}$ there is also no absorption of any power. Hence, there has to be a certain amplitude X_2 in between these extreme cases which allows maximum power capture. This optimum amplitude can readily be found by setting the derivative of the mean power absorbed to zero:

$$\frac{d}{dX_2} P_{mean} = 0 = \frac{1}{2}(\omega F_1 - 2\,\omega^2 B X_2)\,. \tag{6.30}$$

Rearranging leads to the optimum amplitude, that is:

$$X_{2opt} = \frac{F_1}{2\omega B}\,. \tag{6.31}$$

This is, as it was also derived by Widden [13], half the amplitude as for the zero-power capture condition, when the whole excitation goes into damping. Widden mentioned in his paper, that the power take-off unit can be thought of as to bring this reduction of the amplitude about.

Having obtained $X_1 = 0$ as one required condition for maximum power capture (see explanation to equation (6.28)), it follows from equation (6.16) as further conditions for the out-of-phase pitch amplitude that:

$$\Theta_2 = -\frac{X_2}{s}. \tag{6.32}$$

It needs to be pointed out that this condition implies that Θ_2 is negative. This fact is not further surprising when remembering the right hand coordinate system used for the analysis and the related positive direction for the pitch angle (compare Figure 6.1). It follows subsequently from equation (6.18) that $\Phi_1 = 0$. The condition for Θ_2 is a design issue whilst the condition for Φ_1 requires appropriate control and operation of the power take-off moment. Using furthermore the just deduced optimum amplitude condition, equation (6.31), in equation (6.15) allows derivation of the in-phase pitch amplitude:

$$\Theta_1 = -\frac{F_1}{2\, s\, \omega^2 M_x}, \tag{6.33}$$

which, by the use of equation (6.17), may also be written as:

$$\Theta_1 = -\frac{2\omega\, I_{fy} \dot{\varphi}_y \Phi_2\, cos(\varphi_x)}{s^2 \omega^2 M_x}. \tag{6.34}$$

Whilst for Θ_2 there is a direct relation with X_2 and hence the power capture condition, there is no such relation for Θ_1. Bearing in mind that viscous damping, which was hitherto neglected, can implicate power losses, leads to the appraisal that Θ_1 should not be unnecessarily large. Taking a glance back to equation (6.33) and (6.34) one sees that just M_x can influence Θ_1 without affecting Θ_2 or X_2. That is, a huge mass M_x will lead to a small in-phase pitch amplitude Θ_1. A huge M_x can be thought of as heavy ballast at the lower end of the device which has, due to its inertia, almost the same effect as if the device would be pivot-mounted on its lower edge. For reasons given in the introductory chapters, technical hinges are avoided anyway. A huge ballast mass is however also related with expenses

and it is hence necessary to find a reasonable trade-off between a feasible M_x and an acceptable Θ_1. The fact, that the mass M_x is including the added mass in surge gives that it may also be increased by pure consideration of the structures geometry. Once again: This is not of main priority, because Θ_1 is not directly affecting the maximum power capture.

The maximum power capture may now be found by substitution of the optimum amplitude condition (equation (6.31)) into the mean absorbed power (equation (6.27)). That is:

$$P_{max} = \frac{1}{2}\left(F_1 - \omega B \frac{F_1}{2\,\omega\,B}\right)\omega \frac{F_1}{2\,\omega\,B} = \frac{{F_1}^2}{8\,B}. \tag{6.35}$$

This is in accordance with derivations done by Widden [13] and Falnes [28].

Would one like to avoid expression of the maximum power with the generally not known damping coefficient B one may, starting from the same equations, deduce that:

$$P_{max} = \frac{1}{4} F_1 X_2 \omega\,. \tag{6.36}$$

6.1.5 Conclusion for Control

The differential equation for the power take of moment can be included into the balance of moments. For this, equation (5.19) (respectively (5.45)) need first to be rewritten in the following form:

$$I_{fy}\,\dot{\varphi}_y\,cos(\varphi_x) = \frac{\left(I_{fx}\,\ddot{\varphi}_x - M_p\right)}{\dot{\theta}_z}\,, \tag{6.37}$$

where one has to bear in mind that M_p is the power take-off moment of one gyroscope. Integrating this equation into the gyroscopic reaction component (last term) of the balance of moments (equation (6.3)) yields:

$$M_x\left(\ddot{x} + s\,\ddot{\theta}_z\right) s = -I_P\,\ddot{\theta}_z - C_P\theta_z + 2\left(I_{fx}\,\ddot{\varphi}_x - M_p\right)\frac{\dot{\varphi}_x}{\dot{\theta}_z}. \tag{6.38}$$

In the previous section it was shown that Θ_1 and even more Φ_1 should be as close to zero as possible. By the use of equation (6.6) and (6.9) it follows for the fraction $\frac{\dot{\varphi}_x}{\dot{\theta}_z} = \frac{\Phi_2}{\Theta_2}$. Phase amplitude writing gives then the in-phase moment balance (i.e. cosine terms) to:

$$-\omega^2 M_x(X_1 + s\,\Theta_1)\,s = \omega^2 I_P \Theta_1 - C_P \Theta_1 - 2\left(\omega^2 I_{fx} \Phi_1 + M_{p1}\right)\frac{\Phi_2}{\Theta_2}. \tag{6.39}$$

Simplification is possible by using $\Phi_1 = 0$ and the resonance condition, see equation (6.19). Including further the force balance according to equation (6.15) yields:

$$(F_1 - \omega B X_2)\,s = -2\,M_{p1}\frac{\Phi_2}{\Theta_2}. \tag{6.40}$$

Using subsequently the optimum amplitude condition (6.31) gives:

$$\frac{1}{2}F_1\,s = -2\,M_{p1}\frac{\Phi_2}{\Theta_2}, \tag{6.41}$$

which may be rewritten in terms of the in-phase power take of moment:

$$M_{p1} = -\frac{sF_1\Theta_2}{4\,\Phi_2}. \tag{6.42}$$

The negative sign is due to the fact that Θ_2 has a negative amplitude (as explained in the previous section). The deduced formula not just allows estimation of the required moment for retardation of the gyroscopic precession, but also estimation of the related loads which are induced in the gyroscopes suspension. It shall be mentioned as advantage that this formula does not include anymore the $cos(\varphi_x)$-term, and thus the related issues with its time dependency.

Inserting equation (6.32) in (6.36) and comparing with equation (6.35) and (6.42) yields:

$$M_{p1}\Phi_2\omega = \frac{{F_1}^2}{8\,B}. \tag{6.43}$$

This allows to estimate M_{p1} without knowledge of the pitch amplitude Θ_2. Similarly as it follows from equation (6.28) that $X_1 = 0$, one can show that M_{p2} should be as small as possible for optimum power capture.

6.1.6 Conclusion for Design Parameter

As mentioned the optimum amplitude condition has to be regulated by the power take-off unit, i.e. the operation of the gyroscopes. Hence to achieve the deduced maximum power

capture (according to equation (6.35)) there are constraints on the gyroscope design and operation. The constraints can be found by further evaluation of the kinematic behaviour of device and gyroscopes. Inserting the balance of forces (6.15) and the resonance condition (6.19), in the balance of moments (6.17) gives:

$$(F_1 - \omega B X_2)\, s = 2\omega\, I_{fy} \dot{\varphi}_y \Phi_2\, cos(\varphi_x)\,. \tag{6.44}$$

Elimination of X_2 by the use of the optimum amplitude condition (6.31) leads subsequently to:

$$\frac{1}{2} F_1\, s = 2\omega\, I_{fy} \dot{\varphi}_y \Phi_2\, cos(\varphi_x)\,, \tag{6.45}$$

which may, for a more technical aspects, be rewritten as:

$$\frac{F_1\, s}{4\, \omega\, \Phi_2\, cos(\varphi_x)} = I_{fy} \dot{\varphi}_y\,. \tag{6.46}$$

This relation allows appreciation of required dimensions which are essential from an engineering point of view. Technical and economical it is of interest to keep the right hand side of this equation, namely the moment of inertia I_{fy} and the spin rate $\dot{\varphi}_y$, as small as possible. The moment of inertia is related with mass and diameter of the flywheels and influences thus directly, and through acting forces also indirectly, the costs. Similarly requires a high spin rate very precise manufacturing and fairly advanced technology for gears, bearings, control and drive which again influences the costs. It may be worth to examine the left hand side of equation (6.46) a bit more in detail, to identify how these both parameters can be kept small, though still in accordance with the maximum power condition.

The excitation force, F_1, is clearly desired to be as large as possible to yield maximum power capture (see equation (6.35) and (6.36)). The same is actually true for the distance s between P and CG. Elimination of X_2 in equation (6.36) by using the relation (6.32) yields:

$$P_{max} = \frac{1}{4} \omega F_1 s\, (-\Theta_2\,), \tag{6.47}$$

while bearing in mind that Θ_2 is negative. This equation seems to indicate that the pitch amplitude Θ_2 should be increased as much as possible. This is however due to an issue with the linearization and superposition used. As one may readily comprehend the lineari-

zation and superposition assumption are only applicable for small oscillations, Θ_2, in pitch. The argument that a large Θ_2 leads to a large power capture by the using a formula based on these assumptions is hence contradictory and can thus not be used. Based on practical tests, Widden [13] points out that there is however either way a limit for the maximum pitch amplitude.

Back to equation (6.47) one can thus argue that the distance s needs to be reasonable large to allow good power capture. Hence a small s also drops out as an option to reduce the product $I_{fy}\dot{\varphi}_y$ according to equation (6.46). Because the wave frequency ω is based on the sea state the only remaining term, which influence can reduce this product is $\Phi_2\, cos(\varphi_x)$. Because this term is part of the denominator of equation (6.46), it is desired to be as large as possible to decrease the demands on I_{fy} and $\dot{\varphi}_y$. The issue is that φ_x as given in (6.11) undergoes a time dependent oscillation. Because $\Phi_1 = 0$ this oscillation is:

$$\varphi_x = \Phi_2 \sin(\omega t)\,, \tag{6.48}$$

which gives for the product which has to be maximized:

$$\Phi_2\, cos(\varphi_x) = \Phi_2\, cos(\Phi_2\, sin(\omega t))\,. \tag{6.49}$$

This is analytically not anymore resolvable. It is assumed that replacement of this product by its time average is an appropriate approach to get rid of the time dependency. The time average, $\Phi_2{}'$ is gained by integration over one period:

$$\Phi_2' = \frac{\Phi_2}{2\pi}\int_0^{2\pi} cos(\Phi_2 \sin(\tau))\, d\tau \approx \Phi_2\, cos(\varphi_x)\,, \tag{6.50}$$

with $\tau = \omega t$ as the so-called periodic time. Because it is impossible to solve this integral analytically, a numeric solution is presented in Figure 6.2, indicating that the maximum power capture with a minimum engineering effort is yield at a precession amplitude of $\Phi_2 \approx 75°$. The graph shows also solutions for $\Phi_2 > 90°$, this is however physically not possible. If $\Phi_2 \to 90°$ the time-average-approach is not suitable anymore, due to the fact that for this case there are times for witch equation (6.49) goes to zero and hence (6.46) to infinity. Technically this means nothing more than, that the gyroscope stops its precession when reaching $90°$.

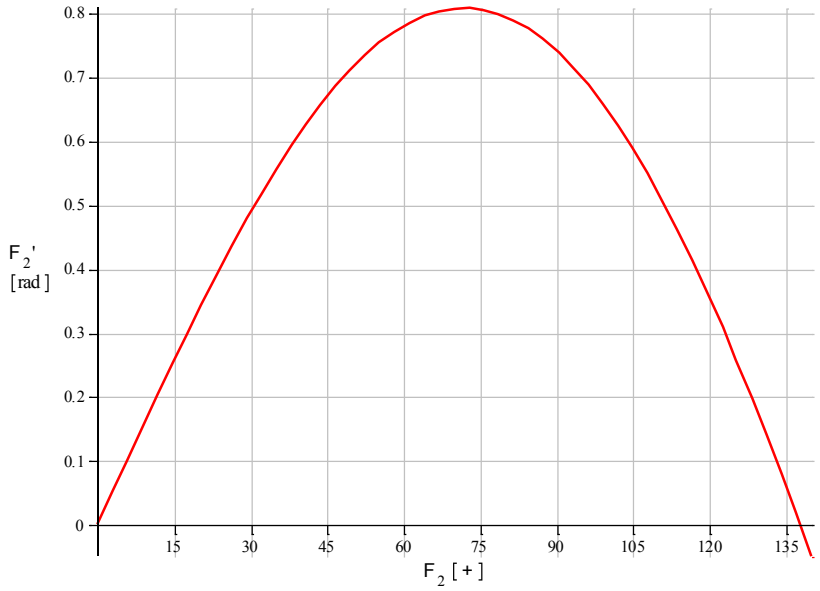

Figure 6.2: Time averaged precession oscillation amplitude

All values which, according to equation (6.32), influence the demands on the moment of inertia, I_{fy} and the spin velocity, $\dot{\varphi}_y$ have been inspected and there is no more leeway for design optimisation reaming. Knowing the excitation force for a given sea state would hence allow to make first estimation for the essential I_{fy} and $\dot{\varphi}_y$.

A careful reader might have recognized that the differentiation in equation (6.30) was based on the condition that the wave excitation force F_1 is independent of the displacement amplitude X_2. Reason therefore is, the, in wave hydrodynamics, commonly used superposition assumption. That is the superposition of a force acting on a rigid structure (excitation) with the kinetics of the same structure when moving without wave excitation (radiation). This is e.g. used and explained by Hudspeth [29]. Considering this superposition assumption of a rigid and a moving mode one may wonder if there is actually really independency between these both modes. Imagined the wave excitation force is generated due to the disturbance of the circular water particle motion by the structure, than it seems that the excitation should decrease with increasing motion of the structure. That is, because any motion of the structure leads to less disturbance of the wave's natural oscillation motion. In other words, a structure moving exactly with the same displacement as given by the wave's natural particle motion should not experience any excitation force. Hence there is the argument that the used superposition is quite inaccurate for large oscillation amplitudes. Large amplitudes are however essential for reasonable wave power capture. Whilst in ship science this issue is of minor importance because offshore structures are typically designed to be subject to as less motion as possible, and hence to move out of resonance. Therefore,

and due to its simplicity, the superposition of excitation and radiation is so commonly used. The inaccuracy of the superposition for the WaveGyro can be appreciated when looking at equation (6.31) and (6.35). Both the oscillation displacement and the captured power would go to infinity for a damping going to zero. Whilst physically the damping can go towards zero, infinite power capture from waves is clearly absurd. For a physical mass-spring system, which are excited with a constant displacement amplitude (see e.g. Spyrides [30]) the infinite power capture according to equation (6.35) does, at least theoretically, make sense.

Nevertheless, the next chapter will trade the wave excitation given by the superposition assumption, which then allows first estimates for the important parameters I_{fy} and $\dot{\varphi}_y$. Afterwards, in the section 6.3, the presumed dependency of wave excitation and displacement will be covered.

6.2 Use of Pure Froude-Krylov Force

In this chapter it shall be shown how the wave excitation force can be yield, which is actually acting on a rigid structure. That is the excitation force, which is needed in the power analysis according to the superposition approach, given in the previous chapter.

6.2.1 Hydrodynamic Pressure Force

The wave excitation force is the hydrodynamic wave pressure force, which is acting at point P. It can be deduced from the incident and diffraction wave velocity potential, Φ_I and Φ_D. The diffraction potential is generally not known and depends in a large extend on the not yet determined property and shape of the considered structure. As a first step the diffraction potential is hence just considered by a factor f_D which multiplies the incident velocity potential. That is, the overall potential is described as:

$$\Phi = \Phi_I + \Phi_D = f_D \Phi_I \,. \tag{6.51}$$

The wave force acting on any structure is due to the dynamic wave pressure on its surface, which is:

$$p_{FK} = -\rho \frac{\partial \Phi}{\partial t} = -\rho \, f_D \frac{\partial \Phi_I}{\partial t} \,. \tag{6.52}$$

The subscript FK stands for Froude-Krylov, although the diffraction potential is here included by the empiric factor f_D. Here ρ is the density of the seawater and the real part of Φ_I, the incident velocity potential, is with linear wave theory described as:

$$\Phi_I = \frac{H}{2}\frac{g}{\omega}\frac{\cosh\big(k(y+d)\big)}{\cosh(kd)}\sin(kx-\omega\, t)\,. \tag{6.53}$$

Here is H the wave height and hence $H/2$ the wave amplitude, g the gravity constant, d the water depth and k the wavenumber. Where the wavenumber is just a different expression of the wave length, that is $k = \frac{2\pi}{\lambda}$. Using the double angle formula for hyperbolic functions allows expanding the velocity potential as follows:

$$\Phi_I = \frac{H}{2}\frac{g}{\omega}\frac{\cosh(ky)\cosh(kd)+\sinh(ky)\sinh(kd)}{\cosh(kd)}\sin(kx-\omega\, t)\,. \tag{6.54}$$

And because the WaveGyro is designed to operate in deep water, the deep water assumption, that is $\tanh(kd) \approx 1$, can be used to reduce the potential to:

$$\Phi_I = \frac{H}{2}\frac{g}{\omega}(\cosh(ky)+\sinh(ky))\sin(kx-\omega\, t)\,. \tag{6.55}$$

Calling back that hyperbolic functions are composed of exponential functions, this can also be written as:

$$\Phi_I = \frac{H}{2}\frac{g}{\omega}\mathrm{e}^{ky}\sin(kx-\omega\, t)\,. \tag{6.56}$$

This incident velocity potential leads, according to equation (6.52), to a dynamic pressure, which, for a device placed at $x = 0$ is:

$$p_{FK} = \rho\, f_D \frac{H}{2}\, g\, \mathrm{e}^{ky}\cos(\omega t)\,. \tag{6.57}$$

Here the extent of thickness (in wave propagation direction) of the device is neglected. Further the devices's cross-section is considered to be just a rectangular plate. Then it follows for the hydrodynamic force, which acts on the wave facing area dA of device's hull:

$$dF_{FK} = p_{FK}\, dA = p_{FK}\, l_z\, dy\,, \tag{6.58}$$

with l_z as the beam length or width of the device. The whole force is then by integration from the draught, l_y of the device up to the free surface:

$$F_{FK} = \int_{-l_y}^{0} p_{FK}\ l_z\, dy = \rho\, f_D \frac{H}{2}\, g\, l_z \cos(\omega t) \int_{-l_y}^{0} \mathrm{e}^{ky}\, dy \tag{6.59}$$

That is:

$$F_{FK} = \rho\, f_D \frac{H}{2}\, g\, l_z \frac{1}{k} \left(1 - \mathrm{e}^{-kl_y}\right) \cos(\omega t) \tag{6.60}$$

And hence the amplitude of the force (compare equation (6.4)):

$$F_{FK1} = \rho\, f_D \frac{H}{2}\, g\, l_z\, \frac{1}{k} \left(1 - \mathrm{e}^{-kl_y}\right) \tag{6.61}$$

6.2.2 Centre of Wave Pressure, *P*

The position of point P, the centre of wave pressure is significant and hence need to be known (see Figure 6.1 and equation (6.46)). The centre of wave pressure is by definition the point on which the centralised force F_{Fk} does not lead to a torque. In other words, the moment induced by the wave pressure above point P has to be equal and opposite to the moment induced by the wave pressure beneath this point. Defining l_P as the positive depth about which P is beneath the still water level, this can mathematically be expressed as:

$$\int_{-l_y}^{0} dF_{Fk}(y + l_P) = 0\,. \tag{6.62}$$

Inserting equation (6.58) and (6.57) yields:

$$\int_{-l_y}^{0} \rho\, f_D \frac{H}{2} g l_z\, \mathrm{e}^{ky} \cos(\omega t)\, (y + l_P)\, dy = 0\,, \tag{6.63}$$

which can be reduced to the integral:

$$\int_{-l_y}^{0} \mathrm{e}^{ky}(y + l_P)\, dy = 0\,. \tag{6.64}$$

Carrying out the integration gives:

$$\left(\frac{ky-1}{k^2} + \frac{l_P}{k}\right) e^{ky}\Big|_{-l_y}^{0} = \left(-\frac{1}{k^2} + \frac{l_P}{k}\right) - \left(\frac{-kl_y - 1}{k^2} + \frac{l_P}{k}\right) e^{-kl_y} = 0\,. \tag{6.65}$$

This can be rewritten as:

$$-\frac{1}{k} + l_P + \left(l_y - l_P + \frac{1}{k}\right) e^{-kl_y} = 0\,. \tag{6.66}$$

Hence:

$$l_P = \frac{\frac{1}{k}(e^{-kl_y} - 1) + l_y e^{-kl_y}}{e^{-kl_y} - 1} = \frac{1}{k} + l_y \frac{e^{-kl_y}}{e^{-kl_y} - 1} = \frac{1}{k} - l_y \frac{1}{e^{kl_y} - 1}\,. \tag{6.67}$$

Introducing l_{Py} as the distance from point P to the lower end of the device, it follows:

$$\begin{aligned} l_{Py} = l_y - l_P &= l_y - \frac{1}{k} + l_y \frac{1}{e^{kl_y} - 1} = -\frac{1}{k} + l_y \frac{e^{kl_y}}{e^{kl_y} - 1} \\ &= l_y \frac{1}{1 - e^{-kl_y}} - \frac{1}{k}\,. \end{aligned} \tag{6.68}$$

It may be worth to express these both formulas in a generalized unit-less way. Therefore the relative distances $l_P^* = \frac{l_P}{l_y}$ and $l_{Py}^* = \frac{l_{Py}}{l_y}$ and the relative wavenumber $k^* = kl_y$ are introduced. This allows writing equation (6.67) as:

$$l_P^* = \frac{1}{k^*} - \frac{1}{e^{k^*} - 1} \tag{6.69}$$

and equation (6.68) as:

$$l_{Py}^* = 1 - l_P^* = \frac{1}{1 - e^{-k^*}} - \frac{1}{k^*}\,. \tag{6.70}$$

The both relative distances which define the position of P are now functions of just one remaining variable. Both are visualized in Figure 6.3.

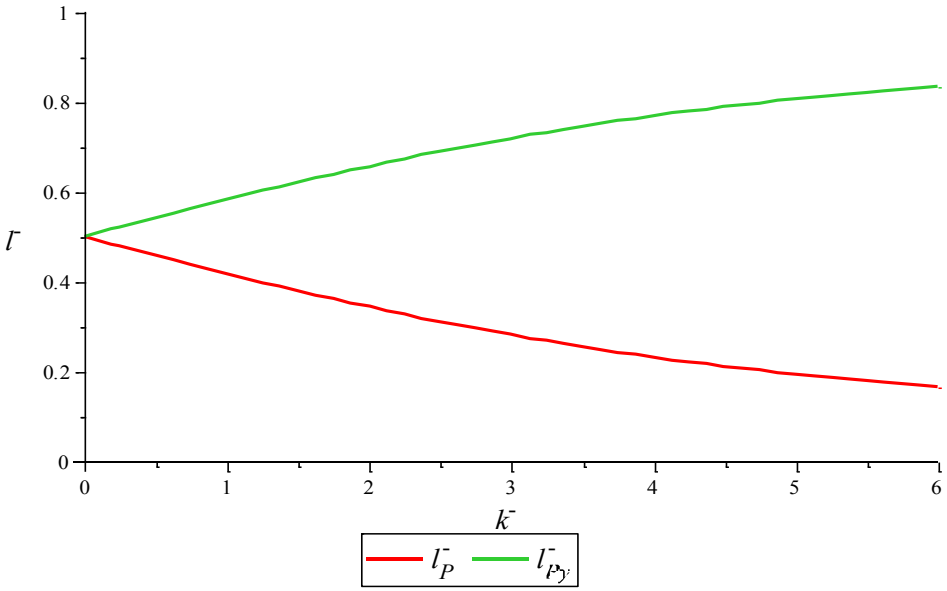

Figure 6.3: Relative distances l_P^* and l_{Py}^* versus relative wavenumber k^*

A characteristic which attracts immediately attention is, that $l_P^* < \frac{1}{2}$ for all k^*. This means the dynamic wave pressure force acting on the lower half of a rigid rectangular plate can never be greater then the force acting on the upper half. This is due to the fact that the velocity potential always decreases with depth. The distance l_P^* goes towards the boundary value of $\frac{1}{2}$ for $k^* \to 0$, that is, the wave length to device draught ratio $\frac{\lambda}{l_y} \to \infty$. This indicates very long wavelength. On the opposite, when the wavelength gets extremely short $\frac{\lambda}{l_y} \to 0$, the point P will be quite close to the free surface, $l_P^* \to 0$. That is however not further relevant because the force, and hence the power capture, for very short wavelength is negligible (for a finite draught l_y, see equation (6.61)). A ready-for-use WaveGyro will have a specific draught and will operate in sea conditions with certain prevailing wavelength. This will limit the actual range of l_P^*. Exemplarily a draught of 20m may be chosen and range of wavelength from maximal 50 to 250m for which reasonable power capture is possible. Then the range of k^* spans from 0.5 to 2.5 and comparison with Figure 6.1 indicates that l_P for this case varies for just a bit more then 10% of the whole draught l_y. One can further appreciate that linearising l_P^* in this range would be more then accurate enough.

6.2.3 First Estimate

To make estimates for the essential design and operation parameters, the distance s between the two points P and CG needs to be known (see section 6.1.6). First, due to its small variations, a fixed value for l_P^* shall be chosen. Taking the main wavelength to be 160m, what will be justified later, a good value for l_P^* is 40%. Hence the distance from point P to the lower edge, l_{Py}^*, will be 60% of l_y. It was derived in section 6.1.4 that a low centre of gravity is essential. Thus feasibility of a design with a CG just 10% above the lower edge is assumed. From which then follows that the length s is roughly 50% of the whole draught, l_y of the device.

In a second step the dimensions of the device are chosen. The draught l_y is taken to be 20m. The width l_z is more a question of economy then of power capture and is chosen to be 20m, which lies between the beam width used for the PS Frog Mk 5 and the one used for the SEAREV device (see Table 3.1 and 3.2Typical dimensions of SEAREV device). The best precession amplitude was derived with equation (6.50) to be about 75°, that is in radians $\Phi_2 \approx 1.3$. It follows subsequently from the graph in Figure 6.2 that $\Phi_2' \approx 0.8$. A summary of the just mentioned sizes and dimensions is:

$$l_y = 20m; \quad l_z = 20m; \quad s = 0.5 \cdot l_y = 10m; \quad \Phi_2 \approx 1.3; \quad \Phi_2' \approx 0.8\,. \tag{6.71}$$

And typical wave properties for the northeast Atlantic around Great Britain are [13]:

$$T = 10s; \quad H = 2.2m\,. \tag{6.72}$$

It follows for the wave frequency:

$$\omega = \frac{2\pi}{T} = \frac{2\pi}{10s} = 0.628\frac{rad}{s}. \tag{6.73}$$

Using further the deep water assumption in the dispersion relation:

$$\omega^2 = gk\,, \tag{6.74}$$

allows to deduce the wavenumber:

$$k = \frac{\omega^2}{g} = \frac{4\pi^2}{T^2 g} \approx 0.04\frac{1}{m}, \tag{6.75}$$

which then gives for the wavelength:

$$\lambda = \frac{2\pi}{k} \approx 160\, m\ . \tag{6.76}$$

The seawater density is $\rho = 1025 \frac{kg}{m^3}$, choosing further a diffraction potential of 40%, that is $f_D = 1.4$, it follows, according to equation (6.61), for the amplitude of the wave excitation force:

$$F_{Fk1} = \rho g f_D \frac{H}{2} l_z \frac{1}{k} \left(1 - \mathrm{e}^{-k l_y}\right) \approx 4300\ \mathrm{kN}\,. \tag{6.77}$$

Consequently it follows from equation (6.46) for the technical important angular momentum which needs to be provided:

$$I_{fy}\, \dot{\varphi}_y = \frac{F_1\, s}{4\, \omega\, \Phi_2\, cos(\varphi_x)} = \frac{F_1\, s}{4\, \omega\, \Phi_2{}'} = \frac{4300\mathrm{kN} \cdot 10m}{4 \cdot \frac{2\pi}{10s} \cdot 0.8} \approx 21{,}400 \frac{t\, m^2}{s}. \tag{6.78}$$

Clearly, if it is possible to operate the gyroscopes at very high spin rates, their mass and dimension can be reduced significantly. There is not a specific upper limit for the spin rate although technical effort and costs for manufacturing as well as expenses for operation will rise rapidly with an increased spin rate. Beacon Power, a US company produces and operates flywheels for grid energy storage which run at speeds up to 16,000 rpm [31]. However, they are just used as mechanical energy storage; hence there is no precession and thus also no lateral load in the bearings. From an engineering point of view this may be for such high spin rates an important difference. There are also existing gyroscopic devices made to reduce the roll motion of ships and yachts. Some of those gyroscopes are controlled actively, i.e. a moment is applied about the precession axis, leading to high lateral loads in the bearings. The later case is more similar to the conditions intended for the WaveGyro. The company Seakeeper is producing such active roll reduction systems, and one of their models has a rated speed of 10,000 rpm [32]. Supposed this is also feasible for the flywheels used in the WaveGyro then it follows for the angular moment:

$$I_{fy} = \frac{1}{\dot{\varphi}_y} 21{,}400 \frac{t\, m^2}{s} = \frac{1}{10{,}000 \frac{2\pi}{60s}} 21{,}400 \frac{t\, m^2}{s} \approx 20.4\, t\, m^2\,. \tag{6.79}$$

Here the spin rate is inserted in radians, which is in accordance with the definition of the angular momentum. To get a perception of the flywheel mass needed it may further be assumed that the required flywheel can be produced with a large radius $r_f = 3m$. Using then a ring-mass approximation yields for the mass of one flywheel:

$$m_f = \frac{I_{fy}}{r_f^2} = \frac{20.4\ t\ m^2}{(3m)^2} \approx 2.3\ t\ . \tag{6.80}$$

One need to bear in mind that the here calculated mass m_f is the mass of one of the two flywheels. The following table shows some other possible configurations:

Table 6.1: Required flywheel ring-mass in tonnes for different radii and spin rates:

$r_f \downarrow \quad \dot{\varphi}_y \rightarrow$	5,000rpm	10,000rpm	15,000rpm
1m	40.8	20.4	13.6
2m	10.2	5.1	3.4
3m	4.5	2.3	1.5
4m	2.6	1.3	0.85

A large radius could require that the gyroscopes are placed in the top of the device because there may not be enough space in the lower end. The consequence would however be, that the position of the centre of gravity rises, which is not desired. The gyroscopes require on the other hand also free space, synonymic to buoyancy which is, for the same reason, not wanted on the lower end. A trade-off has to be found and most probably it is not possible to get around an extra ballast mass at the lower end of the structure.

6.3 Relative Motion Principle

It was mentioned in the previous sections that issues 'like infinite' power capture arise if the superposition principle of excitation and radiation is used for the power analysis. By using this superposition one supposes that the excitation force acting on a structure is independent of the structure's displacement. This is accurate for small oscillation amplitudes. For large displacement, as needed for reasonable power capture, this is however not the case. To cope with the dependency of force and displacement the relative motion principle shall be introduced in this chapter. Subsequently a power analysis similar to the one already done will be carried out, but now based on this relative motion principle.

Journée et al. introduced in the book 'Offshore Hydrodynamics' [33] the relative motion principle on a heaving vertical cylinder. He used as displacement in the equation of motion

the relative displacement between the undisturbed water particles at the lower end of the cylinder and the displacement of cylinder itself (respectively for velocity and acceleration). The undisturbed water particles displacement is just the reduced wave elevation given by the velocity potential at the depth of interest. For a pitching device the situation is slightly different, first due to the reason that the undisturbed water particle displacement is clearly not constant along the draught, and second the displacement of the device is due to the pitch motion also not constant. Therefore the relative motion principle will here be introduced be considering the wave pressure force as an oscillating stiffness in surge. This can be thought as if the in surge oscillating water acts as a spring on the device, leading to its pitch motion.

The dynamic pressure force acting at a stripe of thickness dy of a submerged plate is:

$$dF_{exc} = \rho g l_z \frac{H}{2} \mathrm{e}^{ky} \cos(\omega t) \,. \tag{6.81}$$

(Compare equation (6.57) and (6.58) without diffraction contribution).

The water density is here ρ, the wave height H, the gravity constant g, the width of the plate l_z, the draught l_y and the wave number is k. As the integral shows, this force changes along the draught just as the water particle displacement does. If the force shall be expressed as stiffness times a deflexion one may find an equivalent water particle displacement leading to the same force. Therefore the water particle displacement has to be deduced. The horizontal water particle velocity is equal to the rate of change of the velocity potential with the distance x. Using the velocity potential (6.56), as used for the force and the dispersion relation for deep water (6.74), one readily yields:

$$\dot{x}_w = \frac{d\Phi_I}{dx} = \frac{gk}{\omega} \frac{H}{2} \mathrm{e}^{ky} \cos(kx - \omega\, t) = \omega \frac{H}{2} \mathrm{e}^{ky} \cos(kx - \omega\, t) \,. \tag{6.82}$$

The oscillation displacement of a water particle at the mean position $x = 0$ is then gained by integration with respect to time:

$$x_w = \int \dot{x}_w dt = \frac{H}{2} \mathrm{e}^{ky} \sin(\omega t) \,. \tag{6.83}$$

It has to be noticed that the displacement amplitude is out-of-phase to the force. The amplitude may be summarized in X_{w2} times the factor e^{ky}, which accounts for the change of

amplitude with water depth (where the '2' in the subscript is due to the out-of-phase condition). Hence the maximum amplitude of the water particle displacement is quite clearly just the half of the wave height:

$$X_{w2} = \frac{H}{2}. \tag{6.84}$$

To express the force in terms of the displacement, their ratio may be formed. Due to the out-of-phase condition, this ratio is expressed in terms of their amplitudes:

$$\frac{dF_1}{X_{w2}\mathrm{e}^{ky}} = \frac{\rho g l_z \frac{H}{2}\mathrm{e}^{ky}}{\frac{H}{2}\mathrm{e}^{ky}} = \rho g l_z = C_w^*\,, \tag{6.85}$$

where C_w^* can be seen as a stiffness constant (the superscript '*' is used to point put that it is per dy). Using this relation, the maximum excitation force which would act on a stationary plate (i.e. breakwater) may be written as:

$$dF_{max1} = C_w^* X_{w2}\mathrm{e}^{ky}\,. \tag{6.86}$$

Thinking about the stationary plate one may here grasp $X_{w2}\,\mathrm{e}^{ky}$ as the 'disturbance' of the water particle motion. Here comes the relative motion principle into play. Because if now a device is considered which is moving with an oscillation amplitude X_{D2}, the 'disturbance' of the water particle motion can be thought as to be reduced to $(X_{w2}\mathrm{e}^{ky} - X_{D2})$. Where X_{D2} is in-phase with the water particle displacement. The amplitude of the relative excitation force, acting on a moving device is thus expressed as:

$$dF_{rel1} = C_w^*(X_{w2}\mathrm{e}^{ky} - X_{D2})\,. \tag{6.87}$$

Considering exemplarily a body (e.g. a canvas) moving everywhere with exactly the same motion as the waves, $X_{D2} = X_{w2}\mathrm{e}^{ky}$, there will be no acting force.

As done in equation (6.20), the captured power may now be written as the resultant force on point P times its velocity:

$$dP_c = dF_{res}\,\dot{x} = dF_{rel}\,\dot{x}_D - B^*\dot{x}_D{}^2 = dF_{rel1}\cos(\omega t)\,\dot{x}_D - B^*\dot{x}_D{}^2\,. \tag{6.88}$$

The resultant force is here however composed of the relative excitation force and the damping. The relative excitation force is yet expressed as a differential force acting on dy. Thus the captured power is also in a differential expression and the damping coefficient B^* is per unit draught, and has hence the unit: $kg\ m^{-1}s^{-1}$. The velocity $\dot{x}_D$ is clearly the velocity of the device (at the point P). This velocity does not have to be in-phase with the wave particle velocity and thus needs to be expressed in-phase amplitudes. The device's displacement expressed as:

$$x_D = X_{D1}\cos(\omega t) + X_{D2}\sin(\omega t)\,, \tag{6.89}$$

where it becomes apparent that displacement X_{D2} is in-phase with the horizontal displacement of the water particles. It follows for the velocity, by differentiation that:

$$\dot{x}_D = \omega X_{D2}\cos(\omega t) - \omega X_{D1}\sin(\omega t)\,. \tag{6.90}$$

Inserting the equation for the relative force (6.87), the displacement (6.89) and the velocity (6.90) into the power capture (6.88) gives:

$$\begin{aligned} dP_c = {} & C_w^*(X_{w2}\mathrm{e}^{ky} - X_{D2})\cos(\omega t)\,(\omega X_{D2}\cos(\omega t) - \omega X_{D1}\sin(\omega t)) \\ & - B^*(-\omega X_{D1}\sin(\omega t) + \omega X_{D2}\cos(\omega t))^2 \\ = {} & \omega C_w^*(X_{w2}\mathrm{e}^{ky} - X_{D2})(X_{D2}\cos^2(\omega t) - X_{D1}\sin(\omega t)\cos(\omega t)) \\ & - \omega^2 B^*(X_{D1}^2\sin^2(\omega t) - 2X_{D1}X_{D2}\sin(\omega t)\cos(\omega t) + X_{D2}^2\cos^2(\omega t))\,. \end{aligned} \tag{6.91}$$

To comprehend this power capture equation it shall now be split into its mixed cosine and sine modes, similarly as it was done in an earlier section from equation (6.24) to (6.26). That is for the cos²-amplitude of the captured power:

$$dP_c^{\cos^2} = \omega C_w^*(X_{w2}X_{D2}\mathrm{e}^{ky}) - (\omega C_w^* + \omega^2 B^*)X_{D2}^2\,, \tag{6.92}$$

for the sin²-amplitude:

$$dP_c^{\sin^2} = -\omega^2 B^* X_{D1}^2 \tag{6.93}$$

and for the mixed term amplitude:

$$dP_c^{sincos} = -\omega C_w^*(X_{w2}\mathrm{e}^{ky} - X_{D2})X_{D1} + 2\omega^2 B^* X_{D1}X_{D2}\,. \tag{6.94}$$

In the power analysis which followed the superposition approach it was argued that the time average of the sin-cos-component of the capture power is zero. The same reasoning may be used here, hence the last equation, (6.94) is of no further interest. The time average of the sin²-component will be negative due to the negative sign in equation (6.93). Similarly as earlier for equation (6.28), it follows that the in-phase amplitude X_{D1} should be as close to zero as possible if maximum power capture shall be yield. The reaming equation (6.92), the power capture which is in cos²-mode is the most significant. Before drawing conclusions for optimum power capture from it, this power mode has to be integrated over the draught of the device. Thus the full power, captured in the cos²-mode, by a device with the draught l_y, is:

$$\begin{aligned} P_c^{\cos^2} &= \int_{-l_y}^{0} dP_c^{\cos^2}\, dy \\ &= \omega C_w^*(X_{w2}X_{D2}) \int_{-l_y}^{0} \mathrm{e}^{ky} dy - (\omega C_w^* + \omega^2 B^*) X_{D2}^2 \int_{-l_y}^{0} dy \\ &= \omega C_w^*(X_{w2}X_{D2}) \frac{\left(1-\mathrm{e}^{-kl_y}\right)}{k} - (\omega C_w^* + \omega^2 B^*) X_{D2}^2 l_y\,. \end{aligned} \tag{6.95}$$

In terms of X_{D2} this is a negative quadratic equation and thus has a certain displacement amplitude X_{D2} for witch it will become maximum. This amplitude may be found by setting the derivation to zero, that is:

$$\frac{dP_c^{\cos^2}}{dX_{D2}} = \omega C_w^*(X_{w2}) \frac{\left(1-\mathrm{e}^{-kl_y}\right)}{k} - 2(\omega C_w^* + \omega^2 B^*) X_{D2} l_y = 0, \tag{6.96}$$

which then yields for the optimum out-of-phase amplitude:

$$X_{D2opt} = \frac{X_{w2}}{2} \frac{C_w^*}{C_w^* + \omega B^*} \frac{\left(1-\mathrm{e}^{-kl_y}\right)}{l_y k}. \tag{6.97}$$

This optimum amplitude can be perceived as to be composed of three components. That is the main component, $\frac{X_{w2}}{2}$, which is just half the maximum amplitude of the water particle motion. The second factor, $\frac{C_w^*}{C_w^*+\omega B^*}$ is a reduction coefficient which can be thought of as to account for the radiation damping. For the ideal condition of zero damping, this factor vanishes. The third factor, $\frac{\left(1-\mathrm{e}^{-kl_y}\right)}{l_y k}$, accounts for the draught of the device. The wa-

ter particle oscillation x_w goes to zero when the depth goes to infinity whereas the oscillation of the device x_D is taken to stay constant for along the depth. For this condition it follows that any displacement x_D of a device with infinite draught will just lead to power losses. In other words the factor $\frac{\left(1-\mathrm{e}^{-kl_y}\right)}{l_y k}$ reduces to 1 for a draught l_y going to zero. It may be pointed out that, with the use of the relative motion principle, the earlier issue of infinite amplitude (see equation (6.31), for a damping going to zero) does not arise any more. But a careful reader may also have noticed that x_D is actually the horizontal displacement at exactly the point P whereas the displacement at any other point along the plate requires actually consideration of the pitch angle θ_z. This influence will be treated later in the subsequent section.

For the time being, the derived optimum amplitude shall be used to deduce the maximum power which can be captured. That is inserting equation (6.97) in (6.95) and using the factor $\frac{1}{2}$ to account for the effective value, i.e. mean value, of $\cos^2(\omega t)$:

$$\begin{aligned} P_{max} &= \frac{1}{2}\Bigg\{\omega C_w^* X_{w2}\left[\frac{X_{w2}}{2}\frac{C_w^*}{C_w^*+\omega B^*}\frac{\left(1-\mathrm{e}^{-kl_y}\right)}{l_y k}\right]\frac{\left(1-\mathrm{e}^{-kl_y}\right)}{k} \\ &\quad -(\omega C_w^*+\omega^2 B^*)\left[\frac{X_{w2}}{2}\frac{C_w^*}{C_w^*+\omega B^*}\frac{\left(1-\mathrm{e}^{-kl_y}\right)}{l_y k}\right]^2 l_y\Bigg\} \\ &= \frac{1}{2}\omega X_{w2}^2\Bigg\{\frac{1}{2}\frac{{C_w^*}^2}{C_w^*+\omega B^*}\frac{\left(1-\mathrm{e}^{-kl_y}\right)^2}{l_y k^2} \\ &\quad -(C_w^*+\omega B^*)\frac{1}{4}\frac{{C_w^*}^2}{(C_w^*+\omega B^*)^2}\frac{\left(1-\mathrm{e}^{-kl_y}\right)^2}{l_y^2 k^2} l_y\Bigg\}. \end{aligned} \tag{6.98}$$

This can be further simplified to:

$$P_{max} = \frac{1}{8} C_w^* \frac{\omega}{k} X_{w2}^2 \left(\frac{C_w^*}{C_w^*+\omega B^*}\right)\frac{\left(1-\mathrm{e}^{-kl_y}\right)^2}{l_y k}, \tag{6.99}$$

where $\left(\frac{C_w^*}{C_w^*+\omega B^*}\right)$ is again the factor accounting for the radiation losses and $\frac{\left(1-\mathrm{e}^{-kl_y}\right)^2}{l_y k}$ is a factor accounting for the finite draught of the device. The dispersion equation for deep water gives the identity $\frac{\omega}{k} = \frac{g}{\omega}$. Using that and inserting further equation (6.84) and (6.85) yields:

$$P_{max} = l_z \frac{\rho g^2}{32\omega} H^2 \left(\frac{C_w^*}{C_w^* + \omega B^*} \right) \frac{\left(1 - \mathrm{e}^{-kl_y}\right)^2}{l_y k} . \tag{6.100}$$

As for the amplitude, the issue with infinite increase, for a damping which goes to zero, does not arise anymore.

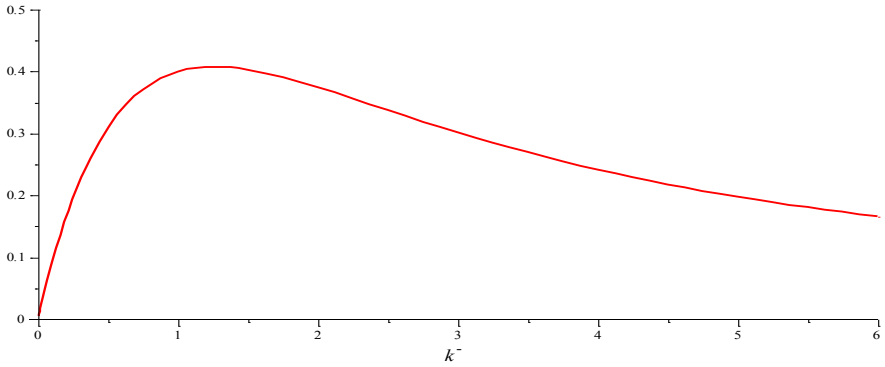

Figure 6.4: Reduction factor accounting for the draught

It may be worth to compare the power available in a given sea stated with the maximum power which can be captured according to equation (6.100). The power transported by waves of frequency ω and wave height H may readily by looked-up in any pertinent literature, as e.g. in [34]. The power transported and hence available in a wave of crest width l_z is:

$$P_{ave} = l_z \frac{\rho g^2}{16\omega} H^2 . \tag{6.101}$$

Comparison gives that the maximum power which theoretically can be captured is just half the power available.

6.3.1 Conclusion for design parameter

The same approach as used in section 6.1.6 will here be used to derive the optimum design parameters according to the relative motion principle. Equation (6.44), that is:

$$(F_1 - \omega B X_{D2}) s = 2\omega \, I_{fy} \dot{\varphi}_y \Phi_2 \, cos(\varphi_x) , \tag{6.102}$$

gives that the hydrodynamic force F_1 is required therefore. This force is according to the relative motion principle found by integration of equation (6.87). That is:

$$F_1 = F_{rel1} = \int_{-l_y}^{0} dF_{rel1}dy = C_w^* \int_{-l_y}^{0} (X_{w2}\mathrm{e}^{ky} - X_{D2})dy$$
$$= C_w^* l_y \left(X_{w2} \frac{(1-\mathrm{e}^{ky})}{kl_y} - X_{D2} \right). \tag{6.103}$$

It follows for the left hand side of equation (6.102):

$$(F_1 - \omega B X_{D2})s = \left(C_w^* l_y \left(X_{w2} \frac{(1-\mathrm{e}^{ky})}{kl_y} - X_{D2} \right) - \omega B X_{D2} \right) s$$
$$= l_y \left(C_w^* X_{w2} \frac{(1-\mathrm{e}^{ky})}{kl_y} - \left(C_w^* + \omega \frac{B}{l_y} \right) X_{D2} \right) s\,. \tag{6.104}$$

The damping coefficient can be expressed as: $B = B^* l_y$ and X_{D2} can be replaced by the optimum amplitude, X_{D2opt} according to equation (6.97). This yields:

$$(F_1 - \omega B X_{D2})s = l_y \left(C_w^* X_{w2} \frac{(1-\mathrm{e}^{ky})}{kl_y} - \left(C_w^* + \omega \frac{B}{l_y} \right) X_{D2} \right) s$$
$$= l_y \left(C_w^* X_{w2} \frac{(1-\mathrm{e}^{ky})}{kl_y} \right.$$
$$\left. - (C_w^* + \omega B^*) \frac{X_{w2}}{2} \frac{C_w^*}{C_w^* + \omega B^*} \frac{\left(1-\mathrm{e}^{-kl_y}\right)}{kl_y} \right) s$$
$$= l_y C_w^* X_{w2} \left(\frac{(1-\mathrm{e}^{ky})}{kl_y} - \frac{1}{2} \frac{\left(1-\mathrm{e}^{-kl_y}\right)}{l_y k} \right) s$$
$$= \left(C_w^* l_y \frac{X_{w2}}{2} \frac{(1-\mathrm{e}^{ky})}{kl_y} \right) s\,. \tag{6.105}$$

Rearranging equation (6.102) and inserting the last result gives for the essential design parameter:

$$I_{fy}\dot{\varphi}_y = \frac{\left(C_w^* X_{w2} \frac{(1-\mathrm{e}^{ky})}{k} \right) s}{4\omega \Phi_2 \cos(\varphi_x)}\,. \tag{6.106}$$

One may use the definition of X_{w2} and C_w^* (equation (6.84) and (6.85)) to compare this result with equation (6.77) and (6.78). Doing so, one sees that they are essentially the same except for the diffraction factor f_D, what clearly has to be the case, because diffraction was not considered in the latter approach.

6.4 Inclusion of Pitch

The hitherto applied relative motion principle did not account for pitch motion. Actually the relative displacement of any point of the device, except P, will however be influenced by pitch motion. To account for this influence the relative force as given in equation (6.87) is expanded as follows:

$$dF_{rel1} = C_w^* \left(X_{w2} \mathrm{e}^{ky} - X_{D2} + \Theta_2 \left(l_p + y \right) \right). \tag{6.107}$$

Where Θ_2 is the pitch amplitude in-phase with X_{w2} and $\left(l_p + y \right)$ the distance between any point and point P. Hence their product is, due to the linearization, an additional relative displacement. Considering the distance $\left(l_p + y \right)$, one has to bear in mind that y is negative below the still water level. Bearing further in mind that the positive pitch motion is defined to be anticlockwise (compare Figure 6.1) it follows that its surge influence has to be added positive. Hence there is no negative sign like for X_{D2}.

Following the approach done for equation (6.91), but using the force as just given, yields for the captured power:

$$\begin{aligned} dP_c = C_w^* \left(X_{w2} \mathrm{e}^{ky} - X_{D2} + \Theta_2 \left(l_p + y \right) \right) \cos(\omega t) \left[\omega X_{D2} \cos(\omega t) \right. \\ \left. - \omega X_{D1} \sin(\omega t) \right] - B^* (\omega X_{D2} \cos(\omega t) - \omega X_{D1} \sin(\omega t))^2 . \end{aligned} \tag{6.108}$$

That is $\sin^2$-component of the power capture is given by:

$$dP_c^{\sin^2} = -\omega^2 B^* X_{D1}^2, \tag{6.109}$$

which is again negative indicating that X_{D1} should be zero. It was already mentioned that the mixed term sin-cos-component vanishes in time average either way. Hence the reaming power capture is in the $\cos^2$-mode, which is:

$$dP_c^{\cos^2} = \omega C_w^* \left(X_{w2} \mathrm{e}^{ky} - X_{D2} + \Theta_2 \left(l_p + y \right) \right) X_{D2} - \omega^2 B^* X_{D2}^2$$
$$= \omega \left\{ C_w^* \left(X_{w2} \mathrm{e}^{ky} + \Theta_2 \left(l_p + y \right) \right) X_{D2} - \left(C_w^* + \omega B^* \right) X_{D2}^2 \right\}. \quad (6.110)$$

Integration over the draught leads to:

$$P_c^{\cos^2} = \omega \left\{ C_w^* \left(X_{w2} \int_{-l_y}^{0} \mathrm{e}^{ky} dy + \Theta_2 \int_{-l_y}^{0} \left(l_p + y \right) dy \right) X_{D2} - \left(C_w^* + \omega B^* \right) X_{D2}^2 \int_{-l_y}^{0} dy \right\}$$
$$= \omega \left\{ C_w^* \left(X_{w2} \frac{\left(1 - \mathrm{e}^{-kl_y} \right)}{k} + \Theta_2 l_y \left(l_p - \frac{1}{2} l_y \right) \right) X_{D2} - \left(C_w^* + \omega B^* \right) X_{D2}^2 l_y \right\}.$$

(6.111)

To gain the optimum displacement amplitude the derivate of this needs to be set equal to zero. That is:

$$\frac{dP_c^{\cos^2}}{dX_{D2}} = \omega C_w^* l_y \left\{ \left(X_{w2} \frac{\left(1 - \mathrm{e}^{-kl_y} \right)}{l_y k} + \Theta_2 \left(l_p - \frac{1}{2} l_y \right) \right) - 2 \frac{\left(C_w^* + \omega B^* \right)}{C_w^*} X_{D2} \right\} = 0. \quad (6.112)$$

It follows for the optimum amplitude:

$$X_{D2opt} = \frac{C_w^*}{2\left(C_w^* + \omega B^* \right)} \left(X_{w2} \frac{\left(1 - \mathrm{e}^{-kl_y} \right)}{l_y k} + \Theta_2 \left(l_p - \frac{1}{2} l_y \right) \right). \quad (6.113)$$

Including this optimum amplitude condition into the power capture, equation (6.111), whilst considering that the effective value of $\cos^2$ is $\frac{1}{2}$ gives for the maximum power that can be captured:

$$P_c = \frac{1}{2} \omega \left\{ C_w^* \left(X_{w2} \frac{\left(1 - \mathrm{e}^{-kl_y} \right)}{k} + \Theta_2 l_y \left(l_p - \frac{1}{2} l_y \right) \right) \frac{C_w^*}{2\left(C_w^* + \omega B^* \right)} \left(X_{w2} \frac{\left(1 - \mathrm{e}^{-kl_y} \right)}{l_y k} + \Theta_2 \left(l_p - \frac{1}{2} l_y \right) \right) \right.$$
$$\left. - \left(C_w^* + \omega B^* \right) \left(\frac{C_w^*}{2\left(C_w^* + \omega B^* \right)} \right)^2 \left(X_{w2} \frac{\left(1 - \mathrm{e}^{-kl_y} \right)}{l_y k} + \Theta_2 \left(l_p - \frac{1}{2} l_y \right) \right)^2 l_y \right\}.$$

(6.114)

This can be simplified to:

$$P_c = \frac{1}{2}\omega l_y \frac{C_w^{*\,2}}{(C_w^* + \omega B^*)}\left\{\left(X_{w2}\frac{\left(1-\mathrm{e}^{-kl_y}\right)}{l_y k} + \Theta_2\left(l_p - \frac{1}{2}l_y\right)\right)^2 - \frac{1}{4}\left(X_{w2}\frac{\left(1-\mathrm{e}^{-kl_y}\right)}{l_y k} + \Theta_2\left(l_p - \frac{1}{2}l_y\right)\right)^2\right\} = \frac{1}{8}\omega l_y \frac{C_w^{*\,2}}{(C_w^* + \omega B^*)}\left(X_{w2}\frac{\left(1-\mathrm{e}^{-kl_y}\right)}{l_y k} + \Theta_2\left(l_p - \frac{1}{2}l_y\right)\right)^2. \tag{6.115}$$

In section 6.2.2 (see Figure 6.3) it was shown that l_p is always smaller then $\frac{1}{2}l_y$. Considering hence that $\left(l_p - \frac{1}{2}l_y\right)$ is negative gives:

$$P_c = \frac{1}{8}\omega l_y \frac{C_w^{*\,2}}{(C_w^* + \omega B^*)}\left(X_{w2}\frac{\left(1-\mathrm{e}^{-kl_y}\right)}{l_y k} - \Theta_2\left(\frac{1}{2}l_y - l_p\right)\right)^2 \tag{6.116}$$

Bearing in mind that Θ_2 will as well be negative, indicates that the last lat term in the brackets should be as large as possible. The logical conclusion would be that the achievable power capture can be unlimited. Hence, there has to be a catch when drawing this conclusion.

Radiation damping in pitch motion was, due to Newman [27] (p. 304 eq. 174) (see section 6.1.1) considered to be zero, hence there is from a theoretical point of view no factor which could limit the pitch amplitude. Nevertheless one may experimentally include losses due to pitch damping. Taking the additional velocity related to pitch, $\omega\Theta_2\left(l_p + y\right)$ times the damping coefficient, B^* times the leaver $\left(l_p + y\right)$, yields, after integration along the draught, a damping moment. Damping moment times angular pitch velocity, $\omega\Theta_2$ is the power loss related with this damping. This power loss is proportional to Θ_2^2 and may hence be compared with the last term of the (expanded) binomial in equation (6.116). One gets a combined proportionality factor, with which Θ_2^2 is contributing to the power capture. For the case that this factor is negative (damping losses are negative) there would be an optimum Θ_2 after which further increase would decrease the power capture. However, carrying out the steps explained, one can show that Θ_2^2 goes just for the case of comparable large

damping negative into the power capture equation. Thus, beside the actual question if there is radiation damping at all for pitch about P, this gives either way not the answer to the dispute in equation (6.116).

Going back to the issue in equation (6.116) of unlimited power capture for unlimited Θ_2 one may however call back that surge and pitch motion are actually related. This relation was deduced form the force and moment balance. In equation (6.32) this dependency was given as:

$$\Theta_2 = -\frac{X_2}{s}, \tag{6.117}$$

which is for the here used approach still valid. If this relation shall be used, this needs to be done before any differentiation with respect to X_2 is carried out. By using this relation in equation (6.114) and setting subsequently its differentiation to zero it can be shown that the optimum amplitude emerge to be:

$$X_{D2opt} = \frac{X_{w2}}{2} \frac{C_w^*}{C_w^* \left(1 - \frac{l_y/2 - l_p}{s}\right) + \omega B^*} \frac{\left(1 - \mathrm{e}^{-kl_y}\right)}{l_y k}. \tag{6.118}$$

(This derivation procedure was already done twice and is thus here not given step by step)

Substitution of Θ_2 and X_{D2opt} according to equation (6.117) and (6.118) into the power capture, equation (6.114) yields for the maximum power:

$$P_{max} = \frac{1}{8} C_w^* \frac{\omega}{k} X_{w2}^2 \frac{C_w^*}{C_w^* \left(1 - \frac{l_y/2 - l_p}{s}\right) + \omega B^*} \frac{\left(1 - \mathrm{e}^{-kl_y}\right)^2}{l_y k}, \tag{6.119}$$

where again the factor $\frac{1}{2}$ for the effective value of cos^2 was considered.

This result may be compared with equation (6.99), the maximum power according to the relative motion principle without pitch. The only additional component in the latter equation is: $\frac{l_y/2 - l_p}{s}$. Bearing in mind that $l_p \leq l_y/2$ is always valid (see Figure 6.3), a reduced denominator is the consequence and hence an increased power capture. This can be thought of as to compensate the reduction related with finite draught, that was: $\frac{\left(1 - \mathrm{e}^{-kl_y}\right)^2}{l_y k}$, as indicated in Figure 6.4. In a more descriptive way one could say that a plate which has a

surge and pitch motion aligns better to e^{ky}, the decreases of the water particle displacement with depth. And this improved alignment could be thought of as to compensate for the 'finite draught reduction' which is actually also due to e^{ky}.

Nevertheless, also the latter equation for the power capture (equation (6.119)) goes to infinity for the case of $B^* = 0$ and $\frac{l_y/2-l_p}{s} = 1$. This would require a quite small s, the distance between centre of gravity and centre of wave pressure. As Widden et al. [13] however showed, this distance should not be small if reasonable power capture is intended. This is justified by the fact that wave tank experiments indicated that the pitch angle amplitude is subject to a practical limit. From equation (6.117) follows hence, that s needs to be of certain length if $X_{D2} = X_{D2opt}$ is to be achieved.

This is just a quite loose explanation for the issue of unlimited power capture in equation (6.119). Nevertheless, the maximum power capture according to equation (6.35) struggle with the same issue and is despite that used in pertinent literature (e.g. [13],[28]). The derived formulas for power capture and optimum amplitude are based on several assumptions and simplifications. Experiments should be done to investigate the accuracy of these formulas.

6.5 Influence of Diffraction

Diffraction was hitherto either neglected or just considered by a proportionality factor according to the rule of thumb. Diffraction in the sense of reflection will lead to increase in the overall hydrodynamic pressure force; this is simply due to Newton's third law, *actio et reactio*. Highest forces are achieved for perfect reflection of the incident waves, i.e. no energy is absorbed and the diffracted wave progresses in opposite direction to the incident wave. On an ideal stationary wall with infinite depth, placed perpendicular to the wave progression direction, will hence act twice the force as if just under pure consideration of a incident wave. The negligence of diffraction is the explanation why the maximum power capture according to equation (6.100) is limited to half the available wave power (6.101), even if the influence of the reduction due to pure surge motion (according to Figure 6.4) is not considered.

Fortunately found Haskind in 1957, later on reformulated by Newman, an important relation which allows expressing the diffraction problem with the radiation solution. With the use of Green's theorem he derived formulas for the wave-induced forces purely based on

the far-field velocity potential. The far-field velocity potential can also be expressed with the solution of the radiation problem. Hence, for simple problems, Haskind's relation avoids solving the diffraction problem.

The total expression for the excitation force according to the relative motion principle (see [33], equation (670)) is based on the Haskind relation. This total relative motion force, as used in the following, is given by:

$$F_{ID} = A\{\ddot{x}_w - \ddot{x}_D\} + B\{\dot{x}_w - \dot{x}_D\} + C_w\{x_w - x_D\}\,, \tag{6.120}$$

where A is the added mass and B the damping. The subscript of the force, 'ID', stands for 'incident' and 'diffracted'. Writing this equation per unit draught and including the phase amplitude expression for the water particle motion (see equation (6.82) to (6.84)) and the motion of the device (see equation (6.5) to (6.7)) yields:

$$\begin{aligned} dF_{ID} = A^*\{\ddot{x}_w - \ddot{x}_D\} + B^*\{\dot{x}_w - \dot{x}_D\} + C_w^*\{x_w - x_D\} \\ = -\omega^2 A^*\{\left(X_{w2}\mathrm{e}^{ky} - X_{D2}\right)\sin(\omega t) + \left(X_{w1}\mathrm{e}^{ky} - X_{D1}\right)\cos(\omega t)\} \\ + \omega B^*\{\left(X_{w2}\mathrm{e}^{ky} - X_{D2}\right)\cos(\omega t) - \left(X_{w1}\mathrm{e}^{ky} - X_{D1}\right)\sin(\omega t)\} \\ + C_w^*\{X_{w2}\mathrm{e}^{ky} - X_{D2}\}\cos(\omega t)\,. \end{aligned} \tag{6.121}$$

For the time being this formulation is expressed for pure surge motion. Note that the force due to ostensive 'stiffness', C_w^* has just one phase component (see section 6.3). Furthermore the water particle displacement is used as reference for the phase amplitude expressions from which follows by definition that $X_{w1} = 0$.

Force, dF_{ID}, times velocity, $\dot{x}_D$, gives the power capture, which, for lucidity, may again be split into phase components. It follows for the sin²-mode of the power capture:

$$\begin{aligned} dP_{ID}^{\sin^2} = -\omega X_{D1}[-\omega^2 A^*\{X_{w2}\mathrm{e}^{ky} - X_{D2}\} + \omega B^*\{-(-X_{D1})\}] \\ = \omega[\omega^2 A^*(X_{w2}\mathrm{e}^{ky} - X_{D2})X_{D1} - \omega B^* X_{D1}^2] \end{aligned} \tag{6.122}$$

and for the cos²-mode:

$$\begin{aligned} dP_{ID}^{\cos^2} = \omega X_{D2}[-\omega^2 A^*\{-X_{D1}\} + \omega B^*\{X_{w2}\mathrm{e}^{ky} - X_{D2}\} + C_w^*\{X_{w2}\mathrm{e}^{ky} - X_{D2}\}] \\ = \omega\left[\omega^2 A^* X_{D1} X_{D2} + (C_w^* + \omega B^*)\left(X_{w2}\mathrm{e}^{ky} X_{D2} - X_{D2}^2\right)\right]. \end{aligned} \tag{6.123}$$

The mixed sin-cos-mode is not evaluated because it is known that its time average vanishes either way. For the mean power it is considered that the effective value of $\cos^2$ and $\sin^2$ is $\frac{1}{2}$. Adding further the power of both modes and followed by integration over the draught yields:

$$\begin{aligned}\bar{P}_{ID} &= \frac{1}{2}\int_{-l_y}^{0}\left(dP_{ID}^{\sin^2} + dP_{ID}^{\cos^2}\right)dy \\ &= \frac{1}{2}\omega l_y\left[\omega^2 A^* X_{w2}\frac{\left(1-\mathrm{e}^{-kl_y}\right)}{l_y k}X_{D1} - \omega B^* X_{D1}^2\right. \\ &\left. + (C_w^* + \omega B^*)X_{w2}\frac{\left(1-\mathrm{e}^{-kl_y}\right)}{l_y k}X_{D2} - (C_w^* + \omega B^*)X_{D2}^2\right].\end{aligned} \tag{6.124}$$

Setting its differentiation with respect to X_{D1} to zero yields for the optimum in-phase amplitude:

$$X_{D1opt} = \frac{\omega^2 A^*}{2\omega B^*}X_{w2}\frac{\left(1-\mathrm{e}^{-kl_y}\right)}{l_y k}. \tag{6.125}$$

The optimum out-of-phase amplitude is similarly gained by differentiation with respect to X_{D2}. It follows:

$$X_{D2opt} = \frac{X_{w2}}{2}\frac{\left(1-\mathrm{e}^{-kl_y}\right)}{l_y k}. \tag{6.126}$$

Inserting both optimum amplitudes in equation (6.124) leads to the maximum possible power capture:

$$
\begin{aligned}
P_{max} = \frac{1}{2}\omega l_y \Bigg[& \frac{(\omega^2 A^*)^2}{4\omega B^*}\left(X_{w2}^2 \frac{\left(1-\mathrm{e}^{-kl_y}\right)^2}{\left(l_y k\right)^2}\right) \\
& + \frac{(C_w^* + \omega B^*)}{4}\left(X_{w2}^2 \frac{\left(1-\mathrm{e}^{-kl_y}\right)^2}{\left(l_y k\right)^2}\right)\Bigg] \\
& = \frac{1}{8}\omega l_y X_{w2}^2 \frac{\left(1-\mathrm{e}^{-kl_y}\right)^2}{\left(l_y k\right)^2}\left[(C_w^* + \omega B^*) + \frac{(\omega^2 A^*)^2}{\omega B^*}\right] \\
& = \frac{1}{8}\frac{\omega}{k} C_w^* X_{w2}^2 \frac{\left(1-\mathrm{e}^{-kl_y}\right)^2}{l_y k}\left[1 + \frac{\omega B^*}{C_w^*} + \frac{(\omega^2 A^*)^2}{C_w^*\,\omega B^*}\right],
\end{aligned}
\tag{6.127}
$$

where in the last step use of the dispersion equation for deep water was made.

Comparison of this equation with equation (6.99) points out, that diffraction can lead to an increased power capture. The increase comes from the two dimensionless components $\frac{\omega B^*}{C_w^*}$ and $\frac{\left(\omega^2 A^*\right)^2}{C_w^*\,\omega B^*}$. Therefore the radiation damping B^* is from further interest.

Radiation of waves from an oscillating body can be expressed in term of added mass and damping coefficient. The radiated waves transport power which is taken from the oscillating body. This radiated power may be divided into a real part, the "active power" and an imaginary part the "reactive power". The reactive part is associated with the added mass and can be seen as alternating power storage. The active power, related with damping, leads however to power losses due to radiated progressive waves. Falnes deduced in his book: 'Ocean Waves and Oscillating Systems' [34] relations between damping and the motion of any arbitrary wavemaker. The motion of the WaveGyro is here taken to be pure surge of a plate with finite draught l_y. The dimensionless velocity induced into the surrounding water at $x = 0$, the plane about which the plate is oscillating, can be expressed as:

$$
c(y) = \begin{cases} 1, & -l_y \le y < 0 \\ 0, & -l_y \ge y \end{cases}. \tag{6.128}
$$

Where 'dimensionless velocity' simply means that it is expressed per maximum oscillation velocity. In other words, $c(y)$ tells that the water from $x = 0$, down until the lower edge of the plate l_y, moves with the same velocity as the plate whilst the water velocity beneath

the plate is zero. Using this dimensionless velocity in the derivation provided by Falnes (compare [34] equation (5.69), (5.60), (5.69) and (4.79)) yields for the damping:

$$B = R_{11} = \rho\omega l_z 2\frac{\left(1 - e^{-l_y k}\right)^2}{k^2} \ , \tag{6.129}$$

where use of the deep water assumption was made. Using further the dispersion equation, it follows:

$$B^* = \frac{B}{l_y} = 2\frac{g}{\omega}\rho l_z \frac{\left(1 - e^{-l_y k}\right)^2}{l_y k} \ . \tag{6.130}$$

This result can be seen as the maximum damping achievable for the given plate and motion. In other words, this equation is only valid if the plate is a perfect reflector, i.e. does not dissipated energy into heat, and radiates wave just in $-x$ direction.

Calling back the definition $C_w^* = \rho g l_z$ (equation (6.85)), the maximum achievable radiation damping in equation (6.130) may also be expressed as:

$$B^* = \frac{1}{\omega} C_w^* \, 2\frac{\left(1 - e^{-l_y k}\right)^2}{l_y k} \ . \tag{6.131}$$

And rearranging gives:

$$\frac{\omega B^*}{C_w^*} = 2\frac{\left(1 - e^{-l_y k}\right)^2}{l_y k} \ . \tag{6.132}$$

Including this ratio into (6.127) yields:

$$P_{max} = \frac{1}{8}\frac{\omega}{k} C_w^* X_{w2}^2 \frac{\left(1 - \mathrm{e}^{-k l_y}\right)^2}{l_y k}\left[1 + 2\frac{\left(1 - e^{-l_y k}\right)^2}{l_y k} + \frac{(\omega^2 A^*)^2}{C_w^* \, \omega B^*}\right]. \tag{6.133}$$

Using the derivations given by Falnes [34] one could also find a similar relation for the added mass A^*. This would consequently lead to a formulation of the captured power purely in terms of the incident wave properties and the draught l_y of the device. These derivations would go beyond the scope of this thesis and is hence not covered here. One has further to bear in mind that the last derivation for the maximum power was done for

pure surge motion and does hence not account for radiation towards the positive x-direction.

6.6 Resonance Condition

Each harmonic oscillating systems has a natural frequency, also called resonance or eigen-frequency. That is the frequency of the systems when oscillating free, without any externally applied exciting force. If an exciting force is applied on such a system, then the maximum power transmission into it is achieved when the excitation force is oscillating with this natural frequency. That is for the pitch motion:

$$\omega_n^2 = \frac{C_p}{I_p}. \tag{6.134}$$

This condition was already in equation (6.19) used when deriving the optimum power capture. There it was shown, that certain terms in the balance of moment vanish if the resonance condition is applied. This in turn led to a maximisation of the power take-off moment. The general conditions for maximum power capture from waves and the related resonance condition is inter alia deduced by Falnes [34], p51-52.

In the power analysis of the preceding sections it was simply assumed that this resonance condition can be applied. This condition is however not generally given, but requires a sufficient design of the stiffness, C_p and moment of inertia I_p. In the following, both parameters will be treated in more detail.

6.6.1 Hydostatic Stiffness

As yet, the shape respectively hull of the WaveGyro was just assumed to be a 'plate' without further defined properties. To deduce the stiffness against pitch the displacement volume is from greater interest. The 'plate' shall thus now be replaced by a flat ellipsoid. This has the further advantage, that an analytical expression for the added mass can be found.

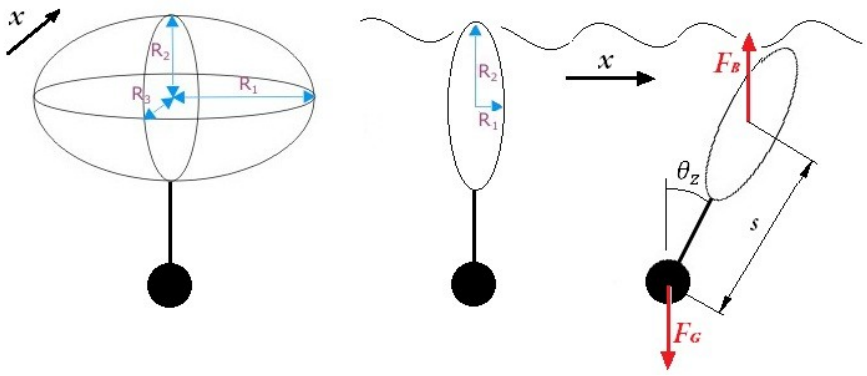

Figure 6.5: Ellipsoidal representation of the WaveGyro device

Figure 6.5 illustrates the ellipsoidal representation of the WaveGyro device. The black cycle beneath the flat plate indicates some kind of ballast mass. The right hand side of the figure shows, how the device is pitching in the x- y-plane and how buoyancy, F_B and gravity F_G balance each other. For simplicity it is assumed that the whole buoyancy is concentrated in the centre of the ellipsoid, whereas the whole mass is concentrated in the ballast. It is further assumed that the device is more or less completely submerged and consequently that the water plane area is negligible and hence not influencing the stiffness. The distance between the point of action of the gravity and the point of action of the buoyancy force is s. The device is clearly supposed to float, thus gravity and buoyancy force are opposite and equal. When the device is subject to a pitch motion, these force are not aligned anymore and a restoration moment originates. Assuming a small pitch angle, this moment is:

$$M_C = -s\theta_z F_B \,. \tag{6.135}$$

With the assumption that the whole mass is concentrated in the ballast, it follows the buoyancy force directly from the displaced volume:

$$F_B = g\rho V_e, \tag{6.136}$$

where V_e is the volume of the ellipsoid. The volume of the ellipsoid can be expressed in terms of its semi-axes:

$$V_e = \frac{4}{3}\pi R_1 R_2 R_3 \,. \tag{6.137}$$

Finally the stiffness constant, which is just the ratio of moment and angle, can be expressed as:

$$C_e = \frac{M_C}{-\theta_z} = sF_B = sg\rho\frac{4}{3}\pi R_1 R_2 R_3 \,. \tag{6.138}$$

Or, when considering the structure just as a 'flat plate' for which width, height and thickness is given by $2R_1$, $2R_2$ and $2R_3$, the stiffness constant may be expressed as:

$$C_p = sg\rho 8 R_1 R_2 R_3 \,. \tag{6.139}$$

Note subscript 'p' is used for the plate and subscript 'e' for the ellipsoid.

6.6.2 Added Moment of Inertia

The added mass is a termination which is commonly used in fluid dynamics. It is called added mass because it leads to a force which is in-phase with the mass-force, respectively acceleration force. To get an idea of this issue one may picture this contribution to the mass-force as a result of surrounding fluid which is accelerated together with the structure. That is simply due to the fact that structure and the fluid can not occupy the same space simultaneously. Actually when the structure is moving, the surrounding fluid will be accelerated to various directions. The added mass can be thought of as to summarization of all those fluid accelerations in one constant; this for each direction of motion. One can thus readily appreciate that the added mass strongly depends on the shape of the structure and analytic description can hence just be made for simple forms.

The motion of the structure in the present work is the angular pitch motion and hence it is the 'added moment of inertia' which is of interest. As mentioned in the previous section, the real body mass of the device is, for simplicity, considered as to be concentrated in the ballast. For this reason the real mass has no contribution to the whole moment of inertia.

The moment of inertia about any axis not passing through the centre of gravity requires consideration of the parallel axis theorem, also called the Huygens-Steiner theorem. That is in general:

$$I = I_{CG} + m \cdot r^2 \tag{6.140}$$

with I_{CG} as the moment of inertia about the centre of gravity, m as the bodies mass and r as the distance between centre of gravity and the axis of rotation. When comparing Figure 6.5 it follows for the added moment of inertia about the ballast, that r is replaced by s, m

by the added mass in surge, A_{11}, and I_{CG} by A_{66}, the added moment of inertia about the centre of the buoy body (i.e. ellipsoid or flat plate). (Bear in mind, that, in the work at hand, pitch is rotation about the z-axis, hence subscribed '66').

Newman [27] (table 4.3, p. 145) gives formulas for the added mass of various two-dimensional bodies. One can put into question if is appropriate to consider the WaveGyro as a two-dimensional body, since its width will be quite comparably to its height. Nevertheless, formulas given by Newman shall initially be used to get estimates for A_{11} and A_{11} and consequently for the dimensions of the body. For a plate of height $2R_2$ the added mass is given by:

$$A_{11} = \pi\rho R_2^2 2R_1 \tag{6.141}$$

and the added moment of inertia is:

$$A_{66} = \frac{1}{8}\pi\rho R_2^4 2R_1\,. \tag{6.142}$$

Note that the width, $2R_1$, is taken as the depth of the two-dimensional body. Insertion into equation (6.140) yields for the moment of inertia of the flat plate:

$$I_p = A_{66} + A_{11}s^2 = \pi\rho R_2^2 2R_1\left(\frac{R_2^2}{8} + s^2\right). \tag{6.143}$$

Using the resonance condition, equation (6.134), and equation (6.139) for the stiffness gives:

$$\omega_n^2 = \frac{C_p}{I_p} = \frac{sg\rho 8R_1R_2R_3}{\pi\rho R_2^2 2R_1\left(\frac{R_2^2}{8} + s^2\right)} = \frac{g4R_3}{\pi R_2\left(\frac{R_2^2}{8s} + s\right)}. \tag{6.144}$$

This can be rewritten to gain the thickness of the plate:

$$l_x = 2\,R3 = \frac{\omega_n^2\pi R_2}{2g}\left(\frac{R_2^2}{s8} + s\right) = \frac{2\pi^3 R_2}{gT^2}\left(\frac{R_2^2}{8s} + s\right). \tag{6.145}$$

Typical dimensions and wave periods are given in equation (6.71) and (6.72). These were: $R_2 = \frac{l_y}{2} = 10m$, $s = 10m$ and $T = 10s$. Using them to gain a first estimate for the thickness yields:

$$l_x = \frac{2\pi^3 10m}{9.81\frac{m}{s^2}10^2 s^2}\left(\frac{10^2 m^2}{8 \cdot 10m} + 10m\right) \approx 7.1m\,. \tag{6.146}$$

For the dimensions given, one readily sees that the added moment of inertia A_{66} plays a minor role. If neglecting it, the estimation of the thickness would just reduce to:

$$l_x = \frac{2\pi^3 R_2}{gT^2}s = \frac{2\pi^3 10m}{9.81\frac{m}{s^2}10^2 s^2}10m \approx 6.3m\,. \tag{6.147}$$

The added mass for a rectangular flat plate as a three-dimensional body is given by Brennan [35] (Table 3). That is in the here used variable description:

$$A_{11} = K\,\pi\rho R_2^2 2R_1\,, \tag{6.148}$$

where, for a ratio of $\frac{R_1}{R_2} = 1$, the constant $K = 0.478$. Without considering A_{66}, this would yield for the thickness:

$$l_x = K\frac{2\pi^3 R_2}{gT^2}s = 0.478\frac{2\pi^3 10m}{9.81\frac{m}{s^2}10^2 s^2}10m \approx 3m\,. \tag{6.149}$$

That tells, if a 3-D flow is considered, the added mass for an equilateral structure will reduce significantly and hence, to keep the resonance condition, also the stiffness which depends on the volume, respectively thickness.

Korotkin [36] gives with his book 'Added Masses of Ship Structures' a compendium of formulas for the added masses of various 2-D and 3-D bodies. For the case $R_1 \geq R_2 \geq R_3$ he states for the added mass of an ellipsoid:

$$A_{11} = \frac{4}{3}\pi\rho R_1 R_2 R_3 \frac{C_0}{2 - C_0}\,, \tag{6.150}$$

where in this formula:

$$C_0 = R_1 R_2 R_3 \int_0^\infty \frac{du}{(R_3^2 + u)\sqrt{(R_1^2 + u)(R_2^2 + u)(R_3^2 + u)}}\,. \tag{6.151}$$

This integral, with the arbitrary integration variable u, is not analytically solvable. Thus the approach used is, to first determine C_0 by the use of the resonance condition (equation (6.134)) and the stiffness for the ellipsoid (equation (6.138)). From equation (6.134) follows:

$$\omega_n^2 = \frac{C_e}{I_e} = \frac{sg\rho\frac{4}{3}\pi R_1 R_2 R_3}{\left(\frac{4}{3}\pi\rho R_1 R_2 R_3 \frac{C_0}{2-C_0}\right)s^2} = \left(\frac{2-C_0}{C_0}\right)\frac{g}{s} = (2/C_0 - 1)\frac{g}{s}, \tag{6.152}$$

where again the assumption is made that the influence of A_{66} is negligible. When rewriting this equation in terms of C_0 one immediately sees that the therewith derived constant is independent of the dimensions. That is:

$$C_0 = \frac{2}{\frac{\omega_n^2 s}{g} + 1} = \frac{2}{\frac{4\pi^2 s}{T^2 g} + 1} \tag{6.153}$$

and, by inserting the values used earlier, this yields:

$$C_0 = \frac{2}{\frac{4\pi^2 10m}{10^2 s^2\ 9.81\frac{m}{s^2}} + 1} \approx 1.43\,. \tag{6.154}$$

Nevertheless, according to equation (6.151), C_0 is also determined by ellipsoid's dimensions. Numerical calculations for C_0 were carried out and curves for C_0 versus the normalised thickness, $\frac{R_3}{R_1}$, are given in Figure 6.6 for various normalised heights, $\frac{R_2}{R_1}$. Where the term 'normalised' just indicates that instead of thickness and height, their dimensionless ratio in respect to the width is taken. Taking now exemplarily the aspect ratio between height and width to be unity (red curve), it follows from the plot of C_0 that $\frac{R_3}{R_1} \approx 0.23$. It follows further, when taking the width, $2R_1$ (or respectively height) to be $20m$ a thickness of $l_x = 2R_3 \approx 4.6m$.

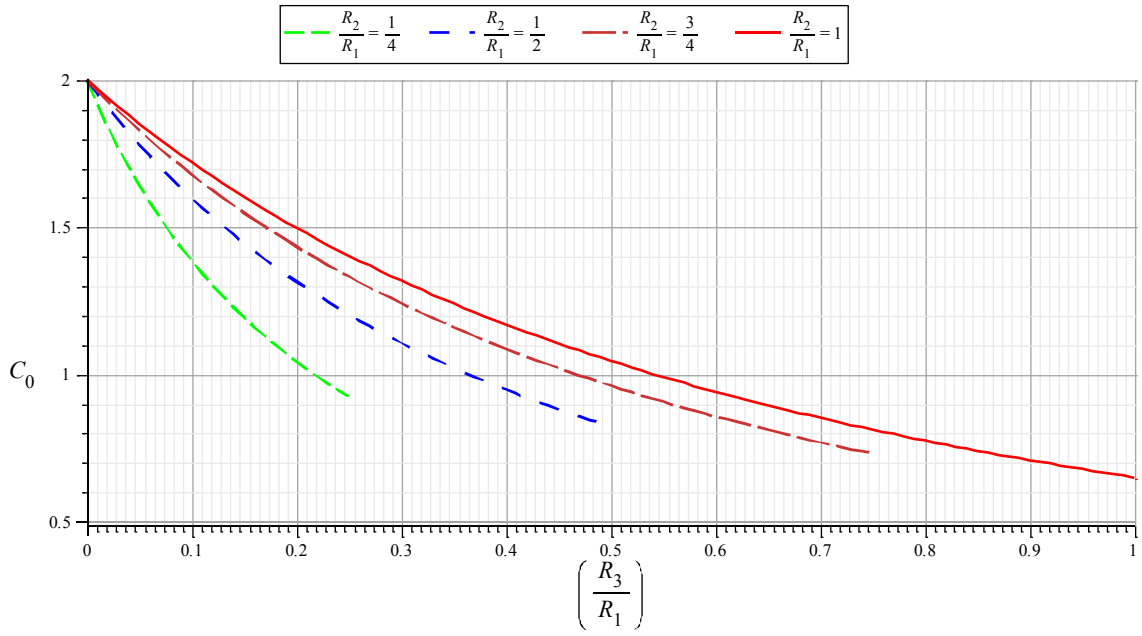

Figure 6.6: C_0 vs. the normalised thickness $\frac{R_3}{R_1}$ for different normalised heights $\frac{R_2}{R_1}$

The last derivation for the dimension of an ellipsoid like device was neglecting the contribution of the added moment of inertia about the centre of the ellipsoid. Korotkin [36] (p. 82) gives also equation for the added moment of inertias, which may now be used to appreciate the difference when neglecting them. The formula he gives may be simplified due to the fact that the ellipsoid considered will be flattened. That is assuming that R_3 is much smaller then R_2 which allows to complete crossing of R_3 from the equations he gives. Likewise it is assumed that the constant B_0 is compared to C_0 negligible, note that B_0 is in heave what C_0 is in surge. The simplified equation for A_{66}, expressed in the nomenclature used here, follows to be:

$$A_{66} = \frac{4\pi\rho R_1 R_2 R_3 (R_2^2 - \cancel{R_3^2})^2 (C_0 - \cancel{B_0})}{15\left(2(R_2^2 - \cancel{R_3^2}) + (\cancel{B_0} - C_0)(R_2^2 + \cancel{R_3^2})\right)} = \frac{4\pi\rho R_1 R_2 R_3 R_2^2 C_0}{15(2 - C_0)} = \frac{4\pi\rho R_1 R_2 R_3 R_2^2}{15}\frac{C_0}{2 - C_0}. \quad (6.155)$$

(An interested readier is advised to consult Korotkin [36] p. 82)

Using further the ellipsoid's added mass in surge, equation (6.150), yields, according to the parallel axis theorem, equation (6.140), for the total added moment of inertia:

$$I_e = A_{66} + A_{11}s^2 = \frac{4\pi\rho R_1 R_2 R_3}{3}\left(\frac{R_2^2}{5} + s^2\right)\frac{C_0}{2 - C_0}. \tag{6.156}$$

By employing the resonance condition, (6.134), together with the formula for the stiffness of the ellipsoid, (6.138), this equation can be reduced to:

$$\frac{sg}{\omega_n^2} = \left(\frac{R_2^2}{5} + s^2\right)\frac{C_0}{2 - C_0} = \left(\frac{R_2^2}{5} + s^2\right)\frac{1}{\frac{2}{C_0} - 1}. \tag{6.157}$$

That is, when rewritten in terms of C_0:

$$C_0 = \frac{2}{\frac{\omega_n^2}{gs}\left(\frac{R_2^2}{5} + s^2\right) + 1} = \frac{2}{\frac{4\pi^2}{T^2 g}\left(\frac{R_2^2}{5s} + s\right) + 1} \tag{6.158}$$

and when inserting the values as before:

$$C_0 = \frac{2}{\frac{4\pi^2}{10^2 s^2\ 9.81\frac{m}{s^2}}\left(\frac{10^2 m^2}{5 \cdot 10m} + 10m\right) + 1} \approx 1.35\,. \tag{6.159}$$

Comparison with the graph given in Figure 6.6 (red curve for $\frac{R_2}{R_1} = 1$) yields finally for the thickness $l_x = 2R_3 \approx 5.6m$.

Different approaches for the relation of the resonance condition to the dimensions of the device were shown. They were based on different simplifications and assumption, such like the type of the hull's shape. But one could see that, regardless which approach were follows, the deduced thickness l_x is quite in the same range. From the derivations which include the whole added moment of inertia (according to the parallel axis theorem), one may summarize that, irrespective of the exact form, a thickness of roughly $6m$ will be appropriate for a l_z, l_y and s as given. With the formulas given, one may also readily calculate the thickness for other given dimensions.

7 Real Sea State

The estimations, based on analysis hitherto, were done for a purely harmonic incident wave of one specific wave period. It is obvious that this is never the case in a real sea. The condition of the free surface in seas and oceans are described by the umbrella term 'sea state'. This includes the distribution and probability of wave height, period and energy, usually based on statistics. The seas state changes significantly with time and location. For the most areas around the world, sets with rough data are freely available and easy accessible via internet (e.g. at: wavelcimate.com). Nevertheless, when designing wave energy converter it is not very convenient to delimitate it by one specific set of data for one specific location. Hence various simplified mathematical formulas to describe the sea states around the world. One of these is the Pierson-Moskowitz Spectrum for a fully developed sea, which is, perhaps due to its simplicity, the most-well known and most used one. The unidirectional spectral function is given by:

$$S(f) = \left(\frac{\alpha}{f^5}\right) e^{-\frac{\beta}{f^4}}, \tag{7.1}$$

where various description for the parameters α and β exist. One, as given by Falnes ([34] p. 86), is:

$$\alpha = \beta \frac{H_S^2}{4}, \quad \beta = \frac{5}{4} f_p^4, \tag{7.2}$$

with f_p the 'peak wave frequency' and H_S the 'significant wave height' which is defined as four times the integral over $S(f)$. The available wave energy per unit area is, with ρg, directly proportional to $S(f)$. For a typical North Atlantic sea state [13] with peak wave period of $T_p = \frac{1}{f_p} = 10s$ and significant wave height of $H_S = 2.2\ m$ the Pierson-Moskowitz Spectrum is given in Figure 7.1 (dashed red line for $T_p = 10s$; dotted blue line for $T_p = 8s$). It can bee readily seen that wave periods which are of interest for energy capture stretch from 5 to 15s (respectively a anfular wave frequency between 0.42s^{-1} and 1.26s^{-1}).

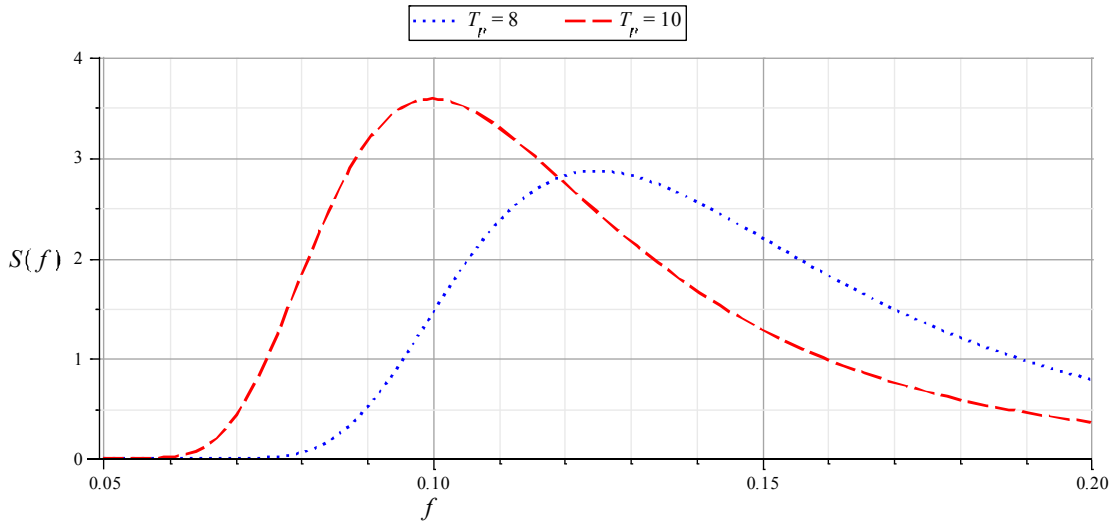

Figure 7.1: Pierson-Moskowitz energy spectrum of a fully developed sea

Bearing in mind that energy transport in waves is just dependent on wave frequency and wave height (compare equation (6.101)) one can appreciate, that it is possible to express the Pierson-Moskowitz Spectrum also as probability distribution of wave height verse wave frequency. Having such a distribution one may call back relations derived for the dimensioning and sizing of the WaveGyro mainly depend on these both parameters. One which is the relation for the dimensioning of the of the gyroscope's angular momentum, $I_{fy}\dot{\varphi}_y$ (see equation (6.78) with (6.77), or respectively equation (6.106) with (6.84) and (6.85)). If I_{fy} and $\dot{\varphi}_y$ are designed invariantly for exact one wave frequency and wave height then they are not perfectly suited for other sea stated.

Considering exemplarily an increased excitation force due to a sea stated with waves higher than the design wave height, leads to a $I_{fy}\dot{\varphi}_y$ smaller than what would be required. This relation was e.g. given in (6.44) (see also (6.45)), which shall thus here be given again:

$$(F_1 - \omega\, B\, X_2)\, s = 2\omega\, I_{fy}\dot{\varphi}_y \Phi_2\, cos(\varphi_x)\,. \tag{7.3}$$

This implies that for a product $I_{fy}\dot{\varphi}_y$, which is to small, other parameters of this equation can not have their designated value. It could be, that e.g. the optimum amplitude condition for X_2 can not be achieved, or that the pitch angle Φ_2 would have to increase. Aside the circumstance that there is for the latter one, for Φ_2, a technical limit, it follows for both that operation outside their optimum value leads to reduced power capture. For X_2, this can be seen by taking a glance back to equation (6.27), the mean power capture (compare also equation (6.35)) and for Φ_2 this follows from the graph given in Figure 6.2. It will

similarly be the case for operation where the designed angular momentum, $I_{fy}\dot{\varphi}_y$ is higher then what would be required for the instantaneous sea state.

To accomplish the resonance condition, as given in equation (6.134), it was mentioned that the national frequency of the device has to be equal to the wave frequency. As the wave frequency is subject to change, this condition may not be achieved for all times. This condition was however in each of the power analysis used to cancel the influence of the device's angular moment of inertia and stiffness from the moment balance equations (see e.g. equation (6.17) and (6.18)). It follows, that these terms will generally, for varying wave frequencies, not vanish and that hence the power capture will not reach its optimum.

Having described the influence of a varying sea on the captured power, the logical next step would be to deduce equations for the optimum design dimensions when subject to a varying, real sea state. If a data set of sea state measurements is available this can be done numerically. The probably more general and direct way is, to generate weighting by the Pierson-Moskowitz Spectrum. The weighting accounts for the reduction in power capture, which appears for operation in any sea conditions differing from the design sea condition. In doing so one can gain the optimum design parameters for maximum mean power capture over the whole range of prevailing sea states for given locations. Derivations required for this are beyond the scope of this work and thence here not covered.

It shall however be mentioned that the gyroscopic momentum $I_{fy}\dot{\varphi}_y$ as well as the device's moment of inertia I_p and stiffness C_p do not necessarily have to be constant. The moment of inertia can quite easily be adjusted by varying the flywheel's spin rate $\dot{\varphi}_y$. And, whilst it is constructional difficult to adjust the stiffness continuously, this can quite easily be done for the moment of inertia I_p, e.g. by internal movable masses or even simpler by pumping water over into internal reservoirs. It is an economical question if it is worth to implement these tuning functions into the design or not. In order to answer this question, investigation of the power lost, when operating without a possibility of instantaneous tuning, has to be investigated. Whereas the adjustment of I_p is probably easy to realise in a cost-effective way, there will be a upper limit for the spin rate $\dot{\varphi}_y$, given by technological issues.

8 Spin-Up Mechanism

The spin-up mechanism is the technical apparatus which converts the precession moment to a moment applied on the spin-axis of the gyroscope. A generator is attached on this axis, which is thought to withdraw the applied moment. One may thus argue that the termination 'spin-up' is a bit misleading because the spin velocity is actually supposed to stay constant. How the conversion of the moment is generally supposed to work was outlined earlier in section 4.2. It was explained how common cogwheel in combination with sprag clutches could be used for this conversion but planetary gearings have been mentioned as well. To the former it was stated that issues may arise due to the necessity of cogwheels with very small diameters. This issue is due to a velocity-diameter constriction and shall now be treated a bit more in depth.

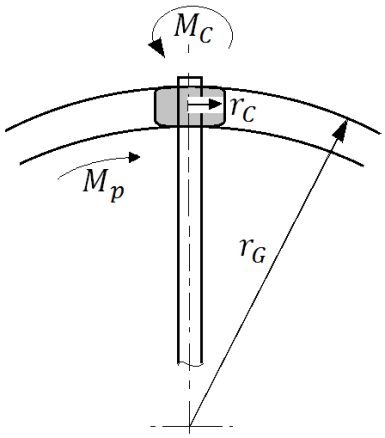

Figure 8.1: Sketch of the simplest cogitable spin-up mechanism

The velocity with which the cogwheel will run in the groove depends on its radius, r_C and its spin rate which is clearly just the spin rate of the flywheel, $\dot{\varphi}_y$. The same velocity may however also be expressed in terms of the radius of the groove, r_G and the precession speed of the gyroscope, $\dot{\varphi}_x$. This may be followed on the sketch presented in Figure 8.1. Expressing this velocity relation in formulas gives:

$$r_G|\dot{\varphi}_x| = r_C|\dot{\varphi}_y|\,, \tag{8.1}$$

which more conveniently may be expressed as the ratio:

$$\frac{r_G}{r_C} = \frac{|\dot{\varphi}_y|}{|\dot{\varphi}_x|}. \tag{8.2}$$

One issue arising directly from this formula is, that r_C, r_G and $\dot{\varphi}_y$ are constants (at least considered over one wave period) whereas the precession rate $\dot{\varphi}_x$ was as yet treated a harmonically varying angular velocity (see e.g. equation (6.12)). In other words, having a spin-up mechanism which is purely designed with simple cogwheels will lead to a, at least piecewise, rectangular pulse-like oscillation of the precession motion. Calling back that the power analysis, given in chapter 6, is based on a harmonic precession, such a rectangular oscillation is clearly not desirable; even so this does not mean it is unfeasible. But the effect would be an also rectangular characteristic for the varying power take of moment and pitch moment. This in turn leads to higher technical demands on the structure and to deviations from the conditions for maximum power capture.

Nevertheless, further constrictions which follow from equation (8.2) shall now be discussed. The precession velocity is therefore theoretically taken to be constant with $\dot{\varphi}_x = \omega\Phi_2$, where $\Phi_2 \approx 1.3\,rad$ (respectively $75°$ according to Figure 8.1). The power take-off moment, M_p is converted to the acceleration moment applied on the cogwheel, M_C. This conversion is via the force, which acts between the cogwheel teeth and the groove. When expressing this force in terms of moment and leaver it follows:

$$\frac{M_p}{r_G} = \frac{M_C}{r_C}, \tag{8.3}$$

which may also be expressed in the radii ratio:

$$\frac{r_G}{r_C} = \frac{M_p}{M_C}. \tag{8.4}$$

Combination with the first radii ratio (equation (8.2)) yields for the cogwheel moment:

$$M_C = M_p \frac{|\dot{\varphi}_x|}{|\dot{\varphi}_y|} = M_p \frac{\omega\Phi_2}{\dot{\varphi}_y}. \tag{8.5}$$

The power take-off moment was given in equation (6.42) in a relation with the maximum power capture. A symmetrical WEC can maximally capture half of the wave power avail-

able, as inter alia explained by Falnes [34], section 6.1. For simplicity this fact may be used to write equation (6.42) as follows:

$$M_p \Phi_2 \omega = \frac{1}{2} P_{ave} \,, \tag{8.6}$$

which then allows to rewrite equation (8.5) as:

$$M_C = \frac{1}{2} \frac{P_{ave}}{\dot{\varphi}_y} \,. \tag{8.7}$$

The available wave power, P_{ave} is given by equation (6.101) in dependents on the wave height and frequency. Because the formula for M_C is either way a really rough estimation, just the typical wave height and frequency for the North Atlantic (as given in section 6.2.3) may be used to calculate P_{ave}. Considering further a spin rate $\dot{\varphi}_y$ of 10,000 rpm (see also section 6.2.3) gives for the cogwheel moment:

$$M_C = \frac{1}{2} l_z \frac{\rho g^2 H^2}{16 \omega \dot{\varphi}_y} = \frac{1}{2} 20m \frac{1025 \frac{kg}{m^3} 9.81^2 \frac{m}{s^2} 2.2^2 m^2}{16 \cdot 0.63 \frac{rad}{s} 10{,}000 \cdot 2\pi \frac{rad}{60s}} \approx 450Nm \,. \tag{8.8}$$

The torsional stress in the flywheel axis is given by:

$$\tau = \frac{M_C}{S_p} \,, \tag{8.9}$$

with S_p as the 'polar section modulus'. The polar section modulus for a solid circular axis is given by:

$$S_p = \frac{\pi \, r_A^3}{2^7} \,, \tag{8.10}$$

where r_A is the radius of the axis. Replacing now τ by the maximal permitted torsional stress $\tau = \tau_{per}$ allows writing for the radius of the axis:

$$r_A = \sqrt[3]{\frac{2^7 M_C}{\pi \, \tau_{per}}} = 4 \sqrt[3]{\frac{2 \, M_C}{\pi \, \tau_{per}}} \,. \tag{8.11}$$

Taking $\tau_{per} = 440 \frac{N}{mm^2}$, which is half (for safety) the value of the critical stress for a common high quality steel (16MnCr5) [37], and using the deduced moment according to equation (8.8) gives for the radius:

$$r_A = 4 \cdot \sqrt[3]{\frac{2 \cdot 450Nm}{\pi \, 440 \frac{N}{mm^2}}} \approx 35mm \, . \tag{8.12}$$

This value gives more something like the minimum value required. Assuming in a next step that it is technically somehow possible to manufacture a cogwheel with more or less the same radius then the radius of the axis, $r_C = r_A$, then it follows from equation (8.2) for the radius of the groove:

$$r_G = \frac{|\dot{\varphi}_y|}{|\dot{\varphi}_x|} \, r_C = \frac{\dot{\varphi}_y}{\omega \Phi_2} \, r_A = \frac{10{,}000 \cdot 2\pi \, \frac{rad}{60s}}{0.63 \frac{rad}{s} \cdot 1.3 \, rad} \, 35mm \approx 45m \, , \tag{8.13}$$

which is at the first glance clearly unfeasible. Using just in a second trial jus half the spin rate $\dot{\varphi}_y = 5{,}000rpm$ gives a axis radius $r_A \approx 44mm$ and a groove radius of $r_G \approx 28m$. Even with this very rough estimation it follows quite clear that a simple spin-up mechanism, only consisting of a cogwheel, sprag clutch and toothed groove is not sufficient enough.

Some kind of gearbox or other kind of conversion will be required. An epicyclic gear set could provide a transmission ratio, lowering the velocity ratio of equation (8.2), and would further permit a harmonic precession motion. Latter one can be achieved by control of the planet-carrier's speed. However any other kind of gearing, preferable continuously variable, could be envisaged as well, also a multistage epicyclic gear does not need to be precluded from consideration.

Even an electric transmission could be a solution. This would admit maximum capability of control and performance of the moment conversion. It entails that a high torque generator is mounted on the precession axis and a smaller but fast motor/generator is attached to the spin axis. Power electronics would manage the power and hence moment transmission from one to the other. Having such two generator (respectively motor) design means actually nothing other than the spin-up of the gyroscope is just for interim power storage. In other words the first, high torque generator could also be used alone, if, via

power electronics directly connected to the grid. This would lead to an extreme fluctuation of the fed-in-power. The use of the second generator/motor on the spin axis gives an inertial energy buffer which allows smooth power output. This can be seen as to be quite similar to the usual hydraulic conversion and buffering used in other WEC. Further investigation would be required to tell, if such a system would be cost-effective. Regarding the spin-up mechanism there is generally the need fro further investigations. This is however beyond the scope of the present work. This chapter shall be stint to show that a more complex moment conversion is necessary.

9 Model Considerations

Initially there was the intention to design and built a model of the WaveGyro device within this project followed by wave tank tests. As time progressed it got more and more obvious that this is just impossible in the fairly short time frame given. The WaveGyro was a completely novel idea for which no preceding work was done. A lot of considerations have to be made before one should build a model. At least if the model shall lead to reasonable ratification and improvement of the analytics which it underlies. Hence the work at hand focused on the analytical description and derivation of the WaveGyro. This chapter shall just give briefly some considerations, which in successional work should be borne in mind when actually dealing with the design of a model.

9.1 Design Advices

Necessary simplifications have to be considered. Therefore one needs to query the purpose of a WaveGyro model. Two purposes can be identified, that is on the one hand the verification of the gyroscopic reaction moment (as treated in chapter 5) and on the other hand the verification of the hydrodynamic behaviour (as treated in chapter 6). Both could be tested with one and the same model in just one kind of test routine. This would however be rather complicated and not really target-oriented. Latter, because it would be hard, until impossible, to allot causes and effects to gyroscopic and hydrodynamic behaviours.

It is probably most convenient to have model which allows testing of both behaviour independently as well as together. That could be a modular design composed of a supporting frame structure, a hull, a ballast mass and a unit for the gyroscope. Analytical derivations for optimum dimension were given, it is however reasonable to have model which can be adjusted. This allows beside verification of the mathematical description the opportunity to find ways of further improvement and to investigate the level of influence of each dimension. The main frame therefore could just be build up with off-the-shelf aluminium profiles, detachable connected to allow alteration. The lower end of this frame provides some kind of fixation for ballast mass. The ballast mass is composed of several small masses, to allow adjustment. This could be simply realized by a vertical rail on which steel discs can be slipped on, where the suspension of the vertical rail itself is adjustable in height. Simple polyurethane foam can be used for the construction of the hull (respectively buoy). Incorporation of a frame or profile rail would easily allow exchange of the hull. Sev-

eral different hull shapes, including the 'flat plate' and the 'ellipsoid' should be made, tested and compared.

The gyroscopes for the reaction need to be extremely simplified. Most convenient is a pure disk as flywheel, mounted on a small DC-motor. Both together are suspended in a gimbal, which is allowing precession motion. A further motor, perhaps a high-torque or stepper motor, acts on the precession axis to simulate the power take of moment. Concerning speed and moment, both motors should be oversized to allow alternation of the operation conditions in a broad range. The flywheel should, like the ballast mass, be built up of several discs in order to carry out tests for different gyroscope momentums. The whole gyroscope assembly should, for the issue of protection and safety, be enclosed in sealed housing. The housing needs to be easily mountable on different positions on the main frame, while it has to be considered that the housing has to convey the moment introduced by the gyroscopes. It should be possible to put the whole gyroscope assembly into a test bed where its performance can be tested separately.

9.2 Model Scaling

If one wants to build a model, then the proportions between the real device and the model are of essential interest. The dimensions of the real device can be drawn from the optimum power analysis done in chapter 6. The subsequent scaling of the model needs to account for several issues. Generally one may say, as smaller the scaling ratio is, as more accurate will the results be and as better comparable with expectations for a real device. Availability of means, time, and test facilities give however a limiting factor. To the latter one, the availability of facilities one has to mention the two towing tanks readily available, one in the Solent University and a smaller one directly in the University of Southampton. The first one with a length of 60m, width of 3.7m and depth of 1.8m, while the second one has a length of 30m, width of 2.4m and a water depth of 1.2m. These dimensions give a general limit to the feasible sizes of model and wavelength, which can be used without major disturbances. The wavelength is more or less limited by the deep water assumption, that is roughly $\lambda < 3d$. It follows for the Solent wave tank, a wavelength of less then 5.5m, which gives, compared to a common wavelength of 160m in the North Atlantic, a minimum scaling ratio of 1:30.

The dimensional proportions of real device to a model may be expressed with the scaling ratio R_L, where the subscript 'L' is a indication for the dimension length. The same

ratio needs to be applied to all other essential quantities with the dimension length (e.g. wavelength). The ratio necessary for different dimensions is not that straightforward. Sorensen[38] states in his book relations between the length ratio and ratios of other dimensions. The hydrodynamic important dimensionless Froude, Reynolds, Euler, Cauchy and Weber numbers are, what he used to derive these ratios. Arguing that it is impossible to satisfy simultaneously the Froude and Reynolds number when using the same fluid (water), he chooses the wave related and thus more significant Froude number to deduce scaling ratios for other units. That is:

$$\begin{aligned} Time\ ratio &= R_T = R_L^{0.5} \\ Pressure\ ratio &= R_P = R_L \\ Force\ ratio &= R_F = R_L^3 \end{aligned} \tag{9.1}$$

Especially the force ratio needs to be considered when scaling the flywheels of the gyroscopes; in a wider sense the mass of the flywheels represents nothing else then a gravity or respectively inertia force. The gyroscopes of the model do not need to have the correct length ratio, as long as their momentum is scaled correctly. This allows a more freely choice of speed and size of flywheel and motor.

10 Conclusion

This work dealt with a novel concept for wave energy conversion, the so-called WaveGyro. In the first chapters it was explained how this innovative concept arose step by step. Reasons for the new concept, related with its advantages, were given. One main advantage, which was pointed out, is the internal reaction moment which allows construction of a completely enclosed and rigid device. This leads to robustness, an essential factor in the harsh sea environment. It was further emphasized why gyroscopes are intended to provide the reaction moment rather then huge masses. This was reasoned with the much lower moving mass and less space required, as well as the higher capability of control.

Basic physics and mechanics were employed in chapter 5 to derive the kinetic behaviour of the gyroscopes. First, a simplified approach was given, followed by a more holistic approach, showing influence of parameters and simplifications. Subsequently, in chapter 6, these derivations were extended to include the wave hydrodynamics. Optimum dimensions and parameters, in order to capture maximum wave power, have been deduced in this chapter. This was done in consideration of simplifications and assumptions. These simplifications were justified and their influence on the accuracy was estimated. Several approaches for the determination of the maximum power capture, according to different assumptions, were presented. The influence of a real sea state into the analysis for optimum conditions was briefly addressed in chapter 7.

The mechanism which is intended to convert the high pitch moment, introduced by the waves, into a more small and handy moment about the flywheel axis was examined in chapter 8. The related factor of power storage and levelling was touched and with the realisation related difficulty and complexity was outlined. The spin-up mechanism will probably be the main crux towards a realisation of the WaveGyro. Further work in this matter will be required, including technical and economical investigations of different solutions.

As a general conclusion it can be said that results from first estimates of dimensions and operation parameters of the gyroscope look promising. The overall dimensions of the WaveGyro are in a feasible range and it was shown that the shape of the hull is not of primarily concern. Even so an improved hull may tease out the absolute maximisation of the power capture. Further work is recommended regarding the actualisation of the gyroscope assembly, as well as for the determination of the best hull. Motion in the heave mode could be included into the power analysis, because motion in two modes gives the possibility to

capture theoretically 100% of the wave power available (compare [34], section 6.1). A power capture up to 100% is otherwise just possible if the device is asymmetric. Both objectives require further theoretical investigation of the hulls shape and the device's motions in view of the power capturable.

Additional to extension of the theory done in the work at hand, would practical wave tank test lead to deeper insight. Chapter 9 gave basic recommendations for the construction of a model. This included guidance for the configuration and assembly as well as basic rules which need to be considered when scaling. The author of this thesis would welcome future work and further investigation in the presented novel concept of the WaveGyro.

11 Bibliography

[1]. **BBC News Glasgow & West Scotland.** Islay to get major tidal power scheme. [Online] 17 03 2011. www.bbc.co.uk/news/uk-scotland-glasgow-west-12767211.

[2]. **Department of Enegry & Climatechange.** *The UK wave energy resource.* [Online] [Cited: 19 03 2011.] www.decc.gov.uk/en/content/cms/what_we_do/uk_supply/energy_mix/renewable/explained/wave_tidal/wave_tech/wave_tech.aspx.

[3]. *Fifth European Wave Energy Conference - (Offshore Power generation by magneto hydro dynamical tidal current conversion).* **Berkel, J.van and Roman, Y.** s.l. : Neptune Systems, 16 Sep 2003.

[4]. **Neptune Systems; Yvette Roman, Jacob van Berkel; .** *Final report Neptune Systems tidal converter.* 07/09/2004. Projectnummer: 0351-03-03-11-013, Report number: R.04.09,.

[5]. **T. Heath.** *Realities of Wave Technology.* UK : Wavegen Ltd, [date not known]. ART1727.

[6]. **Scott David, Bortman Adolph.** Wave-tuned plates - harness sea power. *Popular Science.* May 1979.

[7]. **Farley, J.** The Triplate Wave Energy Converter. [ed.] Department of Energy. London-Heathrow : (Royal Military College of Science, Shrivenham), 22-23 Nov 1978. pp. 129-133. ISBN 0-70-58075 1 -7.

[8]. **Chris, Budd.** *Porject Description - Stabilised Two Wall Wave Energy Device.* 24. Jan 2011.

[9]. **Budd, Chriss.** *Meeting and discussion about the Ampere Wave concept.* University of Southamtpon, 22 Feb 2011.

[10]. **Bracewell, R.H.** FROG and PS FROG: A Studay of Two Reacionless Ocean Wave Enery Converters (PhD Thesis). Lancaster : Lancaster University, 30 Sep 1990.

[11]. **French M.J., Bracewell R.H.** Latest Developments in Wave Energy at Lancaster. Lancaster University : Department of Engineering, before 1999.

[12]. **McCabe, A.P., et al.** Developments in the design of the PS Frog Mk 5 wave energy converter. [ed.] Elsevier Ltd. *Renewable Energy.* 2006, Vol. 31, pp. 141–151. (available online 22.09.2005).

[13]. **Widden M B, French M J , Aggidis G A,.** Analysis of a pitching-and-surging wave-energy converter that reacts against an internal mass, when operating in regular sinusoidal waves. *Proc. IMechE.* 29 04 2008, Vols. 222, Part M: J. Engineering for the Maritime Environment, pp. 153-161.

[14]. **Babarit A., Clément A., Ruer J., Tartivel C.,.** SEAREV : A FULLY INTEGRATED WAVE ENERGY CONVERTER. ca.2008.

[15]. **Gemmell, R.E. and Muetze, A.** Discussion of a New Rocking Buoy Reaction Based Wave Energy Converter Topology. XIX International Conference on Electrical Machines - ICEM 2010, Rome : IEEE, 2010. 978-1-4244-4175-4/10.

[16]. **Laithwaite, E. R. and Salter, S. H.** *Method of, and apparatus for, extracting energy from waves. US Patent 4300871;* United Kingdom Atomic Energy Authority, 11 Charles II St., London SW1Y 4QP, GB2, 17 11 1981.

[17]. **Bracco G., Giorcelli E., Mattiazzo G., Pastorelli M., Taylor J,.** ISWEC: design of a prototype model with gyroscope. Torino (Italy) and Edinburgh (UK) : IEEE, 2009. 978-1-4244-2544-0/08.

[18]. **Sachs, et al.** *Mechanism for generating power from wave motion on a body of water. US Patent 4 352 023;* 28 Sep. 1982 .

[19]. **Townsend, N.C.** ENERGY HARVESTING UTILISING THE GYROSCOPIC EFFECT; FSI Away Day 2011;. Fluid Structure Interactions Research Group, School of Engineering Science, University of Southampton : [not published], 2011. (Poster).

[20]. **Kanki H., et al.** Development of a Highly Efficient Wave Energy Converter Applying Gyroscopic Moments to Produce Electricity. [ed.] The International Society of Offshore and Polar Engineers (ISOPE). Beijing, China : [publisher not known], 2010. ISBN 978-1-880653-77-7.

[21]. **Mishler, L.A.** *Gyroscopic Device. US Patent 3726146,* 10 Apr 1973.

[22]. **Ucke, C. and Schlichting, H.J.** Faszinierendes Dynabee. *Physik in unserer Zeit.* 33. Jahrgang 2002, pp. 230, 231.

[23]. **Cooper, Bell.** Dynabee Dynamics. Oklahoma State University, Stillwater, OK 74078 : Department of Physics.

[24]. **Townsend, Nicholas C. and Shenoi, Ramanand. A.** Gyrostabiliser Vehicular Technology. University of Southampton : [not yet published], 2011.

[25]. **Gross, D., et al.** *Technische Mechanik - Band 3: Kinetik.* 9. Berlin Heidelberg : Springer-Verlag, 2006. p. 177. ISBN-13 978-3-540-34084-3.

[26]. A Matrix-Algebra; p. 18. [Online] 2011. http://www.stat.uni-muenchen.de/~kneib/regressionsbuch/download/matrixanhang.pdf.

[27]. **Newman, J. N.** *Marine Hydrodynamics.* [ed.] Massachusetts Institute of Technology. Cmabridge, Massachusetts, London : The MIT Press, 1977. ISBN 0-262-14026-8.

[28]. **Falnes, Johannes.** *Ocean Waves and Oscillaiting Systems.* [ed.] Department of Physics Norwegian University of Science and Technology NTNU. United Kingdom : Cambridge University Press, 2002. pp. 52, eq. 3.45. ISBN 0-521-78211-2.

[29]. **Hudspeth, Robert T.** WAVES AND WAVE FORCES ON COASTAL AND OCEAN STRUCTURES. [ed.] USA Oregon State University. Singapore : World Scientific Publishing Co. Pte. Ltd, 2006. Vol. 21, p. 560. ISBN 981-238-612-2.

[30]. **Spyrides, Costas.** Design of an energy harvesting device for use on a sailing yacht; (not yet published). *Master Thesis.* September 2011.

[31]. **Beacon Power.** FACT SHEET; Frequency Regulation and Flywheels. 2009.

[32]. **Seakeeper, Inc.** Seakeeper Gyro Stabilization System. *Seakeeper Brochure.* 2008.

[33]. **Journée, J.M.J. and Massie, W.W.** *OFFSHORE HYDROMECHANICS.* 1. Delft : Delft University of Technology, Jan. 2001. pp. 6- 19 ff.

[34]. **Falnes, Johannes.** *Ocean Waves and Oscillaiting Systems.* [ed.] Department of Physics Norwegian Universtiy of Science and Technology NTNU. Cambridge : Cambridge University Press, 2002. ISBN 0-521-78211-2.

[35]. **Brennen, C.H.** *A Review of Added Mass and Fluid Inertial Forces.* Port Hueneme, California : Naval Civil Engineering Laboratory, 1982. Report No.: CR 82.010.

[36]. **Korotkin, Alexandr I.** *Added Masses of Ship Structures.* [ed.] Krylov Shipbuilding Research Institute. UK : Springer, 2009. ISBN 978-1-4020-9431-6.

[37]. **Heinzler, M.** *Tabellenbuch Metall.* Haan-Gruiten, Germany : Verlag Europa-Lehrmittel, 2002. ISBN 3-8085-1722-0.

[38]. **Sorensen, Robert M.** *Basic Wave Mechanics: for Costal and Ocean Engineers.* USA : John Wiley & Sobs, Inc., 1993. ISBN 0-471-55165-1.

[39]. **Gulick D. W., O'Reilly O. M.,.** On the Dynamics of the Dynabee. *Journal of Applied Mechanics.* 06 2000, Vol. 67, pp. 321-325.

[40]. **Herbert K. Sachs, George A. Sachs,.** *Mechanism for generating power from wave motion on a body of water. US Patent 4352023;* 28 09 1982.

[41]. **Evans, D. E.** A theory for wave-power absorption by oscillating bodies. [ed.] Universtiy of Bristol Department of Mathematics. *J. Fluid Mech.* 1, 19 12 1975, Vol. 77, pp. 1-25.

[42]. **Newman, J.N.** Absorption of wave energy by elongated bodies. *Applied Ocean Research.* 1979, Vol. 1, 4, pp. 189-196.

[43]. **McCormick, Michael E.** *Ocean Engineering Mechanics.* [ed.] United States Naval Academy. New York : Cambridge University Press, 2009. ISBN-13 978-0-511-64188-6.

12 Appendices

Appendix A

```
> restart
> with(LinearAlgebra):
> interface(typesetting=extended):
```

Derivation of the gyroscopic moment, considering all angular velocites (no simplification due to neglection). The nomeclature is not completely consistent with the one used in the thesis!

Angular velocity of the flywheel has to be expressed in respect to the inertial frame:

Therfore rotation matrices needed as follows:

```
> A_dg := Matrix([[1, 0, 0], [0, cos(φ_x(t)), sin(φ_x(t))], [0, -sin(φ_x(t)), cos(φ_x(t))]])
```

$$A_{dg} := \begin{bmatrix} 1 & 0 & 0 \\ 0 & \cos(\varphi_x(t)) & \sin(\varphi_x(t)) \\ 0 & -\sin(\varphi_x(t)) & \cos(\varphi_x(t)) \end{bmatrix}$$

```
> A_gf := Matrix([[cos(φ_y(t)), 0, -sin(φ_y(t))], [0, 1, 0], [sin(φ_y(t)), 0, cos(φ_y(t))]])
```

$$A_{gf} := \begin{bmatrix} \cos(\varphi_y(t)) & 0 & -\sin(\varphi_y(t)) \\ 0 & 1 & 0 \\ \sin(\varphi_y(t)) & 0 & \cos(\varphi_y(t)) \end{bmatrix}$$

And the angular velocities defined in different frames(the subscript 'dot' indicates a time derivative, hence angular velocity):

Pitch:

```
> θ_zdot := Vector([0, 0, θ̇_z(t)])
```

$$\theta_{zdot} := \begin{bmatrix} 0 \\ 0 \\ \dot{\theta}_z(t) \end{bmatrix}$$

Precession:

```
> φ_xdot := Vector([φ̇_x(t), 0, 0])
```

$$\varphi_{xdot} := \begin{bmatrix} \dot{\varphi}_x(t) \\ 0 \\ 0 \end{bmatrix}$$

Spin:

```
> φ_ydot := Vector([0, φ̇_y(t), 0])
```

$$\varphi_{ydot} := \begin{bmatrix} 0 \\ \dot{\varphi}_y(t) \\ 0 \end{bmatrix}$$

Rotation of the gimbal frame:

> $\omega_g := \varphi_{xdot} + A_{dg} \cdot \theta_{zdot}$

$$\omega_g := \begin{bmatrix} \dot{\varphi}_x(t) \\ \sin(\varphi_x(t))\,\dot{\theta}_z(t) \\ \cos(\varphi_x(t))\,\dot{\theta}_z(t) \end{bmatrix}$$

Rotation of the flywheel frame:

> $\omega_f := \varphi_{ydot} + A_{gf} \cdot \omega_g$

$$\omega_f := \begin{bmatrix} \cos(\varphi_y(t))\,\dot{\varphi}_x(t) - \sin(\varphi_y(t))\cos(\varphi_x(t))\,\dot{\theta}_z(t) \\ \dot{\varphi}_y(t) + \sin(\varphi_x(t))\,\dot{\theta}_z(t) \\ \sin(\varphi_y(t))\,\dot{\varphi}_x(t) + \cos(\varphi_y(t))\cos(\varphi_x(t))\,\dot{\theta}_z(t) \end{bmatrix}$$

Angular moment of inertia. Due to symetry is $II_{zz} = II_{xx}$, and hence :

> $II_g := Matrix([[II_{xx}, 0, 0], [0, II_{yy}, 0], [0, 0, II_{xx}]])$

$$II_g := \begin{bmatrix} II_{xx} & 0 & 0 \\ 0 & II_{yy} & 0 \\ 0 & 0 & II_{xx} \end{bmatrix}$$

Moment expressed in the flywheel frame:

> $M_f := simplify(II_g \cdot map(diff, (\omega_f), t) + CrossProduct(\omega_f, (II_g \cdot \omega_f)))$

$$\begin{aligned} M_f := \Big[& \big[II_{xx}\cos(\varphi_y(t))\,\ddot{\varphi}_x(t) + 2\,II_{xx}\sin(\varphi_y(t))\sin(\varphi_x(t))\,\dot{\varphi}_x(t)\,\dot{\theta}_z(t) \\ & - II_{xx}\sin(\varphi_y(t))\cos(\varphi_x(t))\,\ddot{\theta}_z(t) \\ & + II_{xx}\sin(\varphi_x(t))\,\dot{\theta}_z(t)^2\cos(\varphi_y(t))\cos(\varphi_x(t)) - II_{yy}\sin(\varphi_y(t)) \\ & \dot{\varphi}_y(t)\,\dot{\varphi}_x(t) - II_{yy}\cos(\varphi_y(t))\,\dot{\varphi}_y(t)\cos(\varphi_x(t))\,\dot{\theta}_z(t) \\ & - II_{yy}\sin(\varphi_y(t))\sin(\varphi_x(t))\,\dot{\varphi}_x(t)\,\dot{\theta}_z(t) \\ & - II_{yy}\sin(\varphi_x(t))\,\dot{\theta}_z(t)^2\cos(\varphi_y(t))\cos(\varphi_x(t))\big], \\ & \big[II_{yy}\left(\ddot{\varphi}_y(t) + \cos(\varphi_x(t))\,\dot{\varphi}_x(t)\,\dot{\theta}_z(t) + \sin(\varphi_x(t))\,\ddot{\theta}_z(t)\right)\big], \\ & \big[II_{xx}\sin(\varphi_y(t))\,\ddot{\varphi}_x(t) - 2\,II_{xx}\cos(\varphi_y(t))\sin(\varphi_x(t))\,\dot{\varphi}_x(t)\,\dot{\theta}_z(t) \\ & + II_{xx}\cos(\varphi_y(t))\cos(\varphi_x(t))\,\ddot{\theta}_z(t) + II_{yy}\cos(\varphi_y(t))\,\dot{\varphi}_y(t)\,\dot{\varphi}_x(t) \\ & + II_{yy}\cos(\varphi_y(t))\sin(\varphi_x(t))\,\dot{\varphi}_x(t)\,\dot{\theta}_z(t) - II_{yy}\sin(\varphi_y(t)) \\ & \dot{\varphi}_y(t)\cos(\varphi_x(t))\,\dot{\theta}_z(t) \\ & - II_{yy}\sin(\varphi_y(t))\cos(\varphi_x(t))\,\dot{\theta}_z(t)^2\sin(\varphi_x(t)) \\ & + II_{xx}\sin(\varphi_y(t))\cos(\varphi_x(t))\,\dot{\theta}_z(t)^2\sin(\varphi_x(t))\big]\Big] \end{aligned}$$

where the contribution of the first term is:

> $simplify(II_g \cdot map(diff, (\omega_f), t))$

$$\left[\left[-II_{xx}\left(\sin\left(\varphi_y(t)\right)\right)\dot{\varphi}_y(t)\,\dot{\varphi}_x(t)-\cos\left(\varphi_y(t)\right)\ddot{\varphi}_x(t)+\cos\left(\varphi_y(t)\right)\dot{\varphi}_y(t)\cos\left(\varphi_x(t)\right)\dot{\theta}_z(t)-\sin\left(\varphi_y(t)\right)\sin\left(\varphi_x(t)\right)\dot{\varphi}_x(t)\,\dot{\theta}_z(t)+\sin\left(\varphi_y(t)\right)\cos\left(\varphi_x(t)\right)\ddot{\theta}_z(t)\right)\right],\left[II_{yy}\left(\ddot{\varphi}_y(t)+\cos\left(\varphi_x(t)\right)\dot{\varphi}_x(t)\,\dot{\theta}_z(t)+\sin\left(\varphi_x(t)\right)\ddot{\theta}_z(t)\right)\right],\left[II_{xx}\left(\cos\left(\varphi_y(t)\right)\dot{\varphi}_y(t)\,\dot{\varphi}_x(t)+\sin\left(\varphi_y(t)\right)\ddot{\varphi}_x(t)-\sin\left(\varphi_y(t)\right)\dot{\varphi}_y(t)\cos\left(\varphi_x(t)\right)\dot{\theta}_z(t)-\cos\left(\varphi_y(t)\right)\sin\left(\varphi_x(t)\right)\dot{\varphi}_x(t)\,\dot{\theta}_z(t)+\cos\left(\varphi_y(t)\right)\cos\left(\varphi_x(t)\right)\ddot{\theta}_z(t)\right)\right]\right]$$

and the contribution of the second term is:

> $simplify\left(CrossProduct\left(\omega_f,\left(II_g\cdot\omega_f\right)\right)\right)$

$$\left[\left[\left(-II_{yy}+II_{xx}\right)\left(\sin\left(\varphi_y(t)\right)\right)\dot{\varphi}_y(t)\,\dot{\varphi}_x(t)+\cos\left(\varphi_y(t)\right)\dot{\varphi}_y(t)\cos\left(\varphi_x(t)\right)\dot{\theta}_z(t)+\sin\left(\varphi_y(t)\right)\sin\left(\varphi_x(t)\right)\dot{\varphi}_x(t)\,\dot{\theta}_z(t)+\sin\left(\varphi_x(t)\right)\dot{\theta}_z(t)^2\cos\left(\varphi_y(t)\right)\cos\left(\varphi_x(t)\right)\right)\right],\left[0\right],\left[-\left(-II_{yy}+II_{xx}\right)\left(\cos\left(\varphi_y(t)\right)\dot{\varphi}_y(t)\,\dot{\varphi}_x(t)+\cos\left(\varphi_y(t)\right)\sin\left(\varphi_x(t)\right)\dot{\varphi}_x(t)\,\dot{\theta}_z(t)-\sin\left(\varphi_y(t)\right)\dot{\varphi}_y(t)\cos\left(\varphi_x(t)\right)\dot{\theta}_z(t)-\sin\left(\varphi_y(t)\right)\cos\left(\varphi_x(t)\right)\dot{\theta}_z(t)^2\sin\left(\varphi_x(t)\right)\right)\right]\right]$$

Convertion of the moment into the gimbal frame:

> $M_g := simplify\left(A_{gf}^{-1}\cdot M_f\right)$

$$M_g := \left[\left[II_{xx}\ddot{\varphi}_x(t)+II_{xx}\sin\left(\varphi_x(t)\right)\dot{\theta}_z(t)^2\cos\left(\varphi_x(t)\right)-II_{yy}\dot{\varphi}_y(t)\cos\left(\varphi_x(t)\right)\dot{\theta}_z(t)-II_{yy}\sin\left(\varphi_x(t)\right)\dot{\theta}_z(t)^2\cos\left(\varphi_x(t)\right)\right],\left[II_{yy}\left(\ddot{\varphi}_y(t)+\cos\left(\varphi_x(t)\right)\dot{\varphi}_x(t)\,\dot{\theta}_z(t)+\sin\left(\varphi_x(t)\right)\ddot{\theta}_z(t)\right)\right],\left[-2\,II_{xx}\sin\left(\varphi_x(t)\right)\dot{\varphi}_x(t)\,\dot{\theta}_z(t)+II_{xx}\cos\left(\varphi_x(t)\right)\ddot{\theta}_z(t)+II_{yy}\dot{\varphi}_y(t)\dot{\varphi}_x(t)+II_{yy}\sin\left(\varphi_x(t)\right)\dot{\varphi}_x(t)\,\dot{\theta}_z(t)\right]\right]$$

Convertion of the moment into the device frame:

> $M_d := simplify\left(A_{dg}^{-1}\cdot M_g\right)$

$$M_d := \left[\left[II_{xx} \ddot{\varphi}_x(t) + II_{xx} \sin\left(\varphi_x(t)\right) \dot{\theta}_z(t)^2 \cos\left(\varphi_x(t)\right) - II_{yy} \right.\right.$$
$$\left. \dot{\varphi}_y(t) \cos\left(\varphi_x(t)\right) \dot{\theta}_z(t) - II_{yy} \sin\left(\varphi_x(t)\right) \dot{\theta}_z(t)^2 \cos\left(\varphi_x(t)\right) \right],$$
$$\left[\cos\left(\varphi_x(t)\right) II_{yy} \ddot{\varphi}_y(t) + 2 \cos\left(\varphi_x(t)\right)^2 II_{yy} \dot{\varphi}_x(t) \dot{\theta}_z(t) \right.$$
$$+ \cos\left(\varphi_x(t)\right) II_{yy} \sin\left(\varphi_x(t)\right) \ddot{\theta}_z(t) + 2 II_{xx} \dot{\varphi}_x(t) \dot{\theta}_z(t) - 2 II_{xx} \dot{\varphi}_x(t)$$
$$\dot{\theta}_z(t) \cos\left(\varphi_x(t)\right)^2 - \sin\left(\varphi_x(t)\right) II_{xx} \cos\left(\varphi_x(t)\right) \ddot{\theta}_z(t)$$
$$\left. - \sin\left(\varphi_x(t)\right) II_{yy} \dot{\varphi}_y(t) \dot{\varphi}_x(t) - II_{yy} \dot{\varphi}_x(t) \dot{\theta}_z(t) \right],$$
$$\left[\sin\left(\varphi_x(t)\right) II_{yy} \ddot{\varphi}_y(t) + 2 \sin\left(\varphi_x(t)\right) II_{yy} \cos\left(\varphi_x(t)\right) \dot{\varphi}_x(t) \dot{\theta}_z(t) \right.$$
$$+ II_{yy} \ddot{\theta}_z(t) - II_{yy} \ddot{\theta}_z(t) \cos\left(\varphi_x(t)\right)^2 - 2 \cos\left(\varphi_x(t)\right) II_{xx} \sin\left(\varphi_x(t)\right)$$
$$\left. \dot{\varphi}_x(t) \dot{\theta}_z(t) + II_{xx} \cos\left(\varphi_x(t)\right)^2 \ddot{\theta}_z(t) + \cos\left(\varphi_x(t)\right) II_{yy} \dot{\varphi}_y(t) \dot{\varphi}_x(t) \right] \right]$$

> *With constant spin rate* :

> $M_{dl} := subs\left(\ddot{\varphi}_y(t) = 0, M_d\right)$

$$M_{dl} := \left[\left[II_{xx} \ddot{\varphi}_x(t) + II_{xx} \sin\left(\varphi_x(t)\right) \dot{\theta}_z(t)^2 \cos\left(\varphi_x(t)\right) - II_{yy} \right.\right.$$
$$\left. \dot{\varphi}_y(t) \cos\left(\varphi_x(t)\right) \dot{\theta}_z(t) - II_{yy} \sin\left(\varphi_x(t)\right) \dot{\theta}_z(t)^2 \cos\left(\varphi_x(t)\right) \right],$$
$$\left[2 \cos\left(\varphi_x(t)\right)^2 II_{yy} \dot{\varphi}_x(t) \dot{\theta}_z(t) + \cos\left(\varphi_x(t)\right) II_{yy} \sin\left(\varphi_x(t)\right) \ddot{\theta}_z(t) \right.$$
$$+ 2 II_{xx} \dot{\varphi}_x(t) \dot{\theta}_z(t) - 2 II_{xx} \dot{\varphi}_x(t) \dot{\theta}_z(t) \cos\left(\varphi_x(t)\right)^2$$
$$- \sin\left(\varphi_x(t)\right) II_{xx} \cos\left(\varphi_x(t)\right) \ddot{\theta}_z(t) - \sin\left(\varphi_x(t)\right) II_{yy} \dot{\varphi}_y(t) \dot{\varphi}_x(t)$$
$$\left. - II_{yy} \dot{\varphi}_x(t) \dot{\theta}_z(t) \right],$$
$$\left[2 \sin\left(\varphi_x(t)\right) II_{yy} \cos\left(\varphi_x(t)\right) \dot{\varphi}_x(t) \dot{\theta}_z(t) + II_{yy} \ddot{\theta}_z(t) - II_{yy} \right.$$
$$\ddot{\theta}_z(t) \cos\left(\varphi_x(t)\right)^2 - 2 \cos\left(\varphi_x(t)\right) II_{xx} \sin\left(\varphi_x(t)\right) \dot{\varphi}_x(t) \dot{\theta}_z(t)$$
$$\left. + II_{xx} \cos\left(\varphi_x(t)\right)^2 \ddot{\theta}_z(t) + \cos\left(\varphi_x(t)\right) II_{yy} \dot{\varphi}_y(t) \dot{\varphi}_x(t) \right] \right]$$

Considering a second gyroscope with counterwise spinning rate and counterwise precession:

> $A_{2dg} := Matrix\left(\left[\left[1, 0, 0\right], \left[0, \cos\left(-\varphi_x(t)\right), \sin\left(-\varphi_x(t)\right)\right], \left[0, -\sin\left(-\varphi_x(t)\right), \cos\left(-\varphi_x(t)\right)\right]\right]\right)$

$$A_{2\,dg} := \begin{bmatrix} 1 & 0 & 0 \\ 0 & \cos\left(\varphi_x(t)\right) & -\sin\left(\varphi_x(t)\right) \\ 0 & \sin\left(\varphi_x(t)\right) & \cos\left(\varphi_x(t)\right) \end{bmatrix}$$

> $A_{2gf} := Matrix\left(\left[\left[\cos\left(-\varphi_y(t)\right), 0, -\sin\left(-\varphi_y(t)\right)\right], \left[0, 1, 0\right], \left[\sin\left(-\varphi_y(t)\right), 0, \cos\left(-\varphi_y(t)\right)\right]\right]\right)$

$$A_{2\,gf} := \begin{bmatrix} \cos\left(\varphi_y(t)\right) & 0 & \sin\left(\varphi_y(t)\right) \\ 0 & 1 & 0 \\ -\sin\left(\varphi_y(t)\right) & 0 & \cos\left(\varphi_y(t)\right) \end{bmatrix}$$

And the angular velocities for the second gyroscope, defined in different frames:

> $\varphi_{2xdot} := Vector\left(\left[-\dot{\varphi}_x(t), 0, 0\right]\right)$

$$\varphi_{2\,xdot} := \begin{bmatrix} -\dot{\varphi}_x(t) \\ 0 \\ 0 \end{bmatrix}$$

> $\varphi_{2ydot} := Vector\left(\left[0, -\dot{\varphi}_y(t), 0\right]\right)$

$$\varphi_{2\,ydot} := \begin{bmatrix} 0 \\ -\dot{\varphi}_y(t) \\ 0 \end{bmatrix}$$

Angular velocity of the second gimbal frame:

> $\omega_{2g} := \varphi_{2xdot} + A_{2dg} \cdot \theta_{zdot}$

$$\omega_{2\,g} := \begin{bmatrix} -\dot{\varphi}_x(t) \\ -\sin\left(\varphi_x(t)\right)\dot{\theta}_z(t) \\ \cos\left(\varphi_x(t)\right)\dot{\theta}_z(t) \end{bmatrix}$$

Angular velocity of the second flywheel frame:

> $\omega_{2f} := \varphi_{2ydot} + A_{2gf} \cdot \omega_{2g}$

$$\omega_{2\,f} := \begin{bmatrix} -\cos\left(\varphi_y(t)\right)\dot{\varphi}_x(t) + \sin\left(\varphi_y(t)\right)\cos\left(\varphi_x(t)\right)\dot{\theta}_z(t) \\ -\dot{\varphi}_y(t) - \sin\left(\varphi_x(t)\right)\dot{\theta}_z(t) \\ \sin\left(\varphi_y(t)\right)\dot{\varphi}_x(t) + \cos\left(\varphi_y(t)\right)\cos\left(\varphi_x(t)\right)\dot{\theta}_z(t) \end{bmatrix}$$

And with the same moment of inertia : $II_g = Matrix\left(\left[\left[II_{xx}, 0, 0\right], \left[0, II_{yy}, 0\right], \left[0, 0, II_{xx}\right]\right]\right)$

>

Gives the moment of the second gyroscope in the flywheel frame:

> $M_{2f} := simplify\left(II_g \cdot map\left(diff, \left(\omega_{2f}\right), t\right) + CrossProduct\left(\omega_{2f}, \left(II_g \cdot \omega_{2f}\right)\right)\right)$

$$
\begin{aligned}
M_{2f} := \Big[\Big[& -II_{xx}\cos\left(\varphi_y(t)\right)\ddot{\varphi}_x(t) - 2\,II_{xx}\sin\left(\varphi_y(t)\right)\sin\left(\varphi_x(t)\right)\dot{\varphi}_x(t)\,\dot{\theta}_z(t) \\
& + II_{xx}\sin\left(\varphi_y(t)\right)\cos\left(\varphi_x(t)\right)\ddot{\theta}_z(t) \\
& - II_{xx}\sin\left(\varphi_x(t)\right)\dot{\theta}_z(t)^2\cos\left(\varphi_y(t)\right)\cos\left(\varphi_x(t)\right) + II_{yy}\sin\left(\varphi_y(t)\right) \\
& \dot{\varphi}_y(t)\,\dot{\varphi}_x(t) + II_{yy}\cos\left(\varphi_y(t)\right)\dot{\varphi}_y(t)\cos\left(\varphi_x(t)\right)\dot{\theta}_z(t) \\
& + II_{yy}\sin\left(\varphi_y(t)\right)\sin\left(\varphi_x(t)\right)\dot{\varphi}_x(t)\,\dot{\theta}_z(t) \\
& + II_{yy}\sin\left(\varphi_x(t)\right)\dot{\theta}_z(t)^2\cos\left(\varphi_y(t)\right)\cos\left(\varphi_x(t)\right)\Big], \\
& \Big[-II_{yy}\left(\ddot{\varphi}_y(t) + \cos\left(\varphi_x(t)\right)\dot{\varphi}_x(t)\,\dot{\theta}_z(t) + \sin\left(\varphi_x(t)\right)\ddot{\theta}_z(t)\right)\Big], \\
& \Big[II_{xx}\sin\left(\varphi_y(t)\right)\ddot{\varphi}_x(t) - 2\,II_{xx}\cos\left(\varphi_y(t)\right)\sin\left(\varphi_x(t)\right)\dot{\varphi}_x(t)\,\dot{\theta}_z(t) \\
& + II_{xx}\cos\left(\varphi_y(t)\right)\cos\left(\varphi_x(t)\right)\ddot{\theta}_z(t) + II_{yy}\cos\left(\varphi_y(t)\right)\dot{\varphi}_y(t)\,\dot{\varphi}_x(t) \\
& + II_{yy}\cos\left(\varphi_y(t)\right)\sin\left(\varphi_x(t)\right)\dot{\varphi}_x(t)\,\dot{\theta}_z(t) - II_{yy}\sin\left(\varphi_y(t)\right) \\
& \dot{\varphi}_y(t)\cos\left(\varphi_x(t)\right)\dot{\theta}_z(t) \\
& - II_{yy}\sin\left(\varphi_y(t)\right)\cos\left(\varphi_x(t)\right)\dot{\theta}_z(t)^2\sin\left(\varphi_x(t)\right) \\
& + II_{xx}\sin\left(\varphi_y(t)\right)\cos\left(\varphi_x(t)\right)\dot{\theta}_z(t)^2\sin\left(\varphi_x(t)\right)\Big]\Big]
\end{aligned}
$$

And gimbal frame:

> $M_{2g} := simplify\left(A_{2gf}^{-1} \cdot M_{2f}\right)$

$$
\begin{aligned}
M_{2g} := \Big[\Big[& -II_{xx}\ddot{\varphi}_x(t) + II_{yy}\dot{\varphi}_y(t)\cos\left(\varphi_x(t)\right)\dot{\theta}_z(t) \\
& + II_{yy}\sin\left(\varphi_x(t)\right)\dot{\theta}_z(t)^2\cos\left(\varphi_x(t)\right) \\
& - II_{xx}\sin\left(\varphi_x(t)\right)\dot{\theta}_z(t)^2\cos\left(\varphi_x(t)\right)\Big], \\
& \Big[-II_{yy}\left(\ddot{\varphi}_y(t) + \cos\left(\varphi_x(t)\right)\dot{\varphi}_x(t)\,\dot{\theta}_z(t) + \sin\left(\varphi_x(t)\right)\ddot{\theta}_z(t)\right)\Big], \\
& \Big[-2\,II_{xx}\sin\left(\varphi_x(t)\right)\dot{\varphi}_x(t)\,\dot{\theta}_z(t) + II_{xx}\cos\left(\varphi_x(t)\right)\ddot{\theta}_z(t) + II_{yy}\dot{\varphi}_y(t) \\
& \dot{\varphi}_x(t) + II_{yy}\sin\left(\varphi_x(t)\right)\dot{\varphi}_x(t)\,\dot{\theta}_z(t)\Big]\Big]
\end{aligned}
$$

And *device frame*:

> $M_{2d} := simplify\left(A_{2dg}^{-1} \cdot M_{2g}\right)$

$$M_{2\,d} := \left[\left[-II_{xx}\,\ddot{\varphi}_x(t) + II_{yy}\,\dot{\varphi}_y(t)\cos\left(\varphi_x(t)\right)\dot{\theta}_z(t) + II_{yy}\sin\left(\varphi_x(t)\right)\dot{\theta}_z(t)^2\cos\left(\varphi_x(t)\right) - II_{xx}\sin\left(\varphi_x(t)\right)\dot{\theta}_z(t)^2\cos\left(\varphi_x(t)\right)\right],\right.$$
$$\left[-\cos\left(\varphi_x(t)\right)II_{yy}\,\ddot{\varphi}_y(t) - 2\cos\left(\varphi_x(t)\right)^2 II_{yy}\,\dot{\varphi}_x(t)\,\dot{\theta}_z(t) - \cos\left(\varphi_x(t)\right)II_{yy}\sin\left(\varphi_x(t)\right)\ddot{\theta}_z(t) - 2\,II_{xx}\,\dot{\varphi}_x(t)\,\dot{\theta}_z(t) + 2\,II_{xx}\,\dot{\varphi}_x(t)\right.$$
$$\dot{\theta}_z(t)\cos\left(\varphi_x(t)\right)^2 + \sin\left(\varphi_x(t)\right)II_{xx}\cos\left(\varphi_x(t)\right)\ddot{\theta}_z(t) + \sin\left(\varphi_x(t)\right)II_{yy}\,\dot{\varphi}_y(t)\,\dot{\varphi}_x(t) + II_{yy}\,\dot{\varphi}_x(t)\,\dot{\theta}_z(t)\Big],$$
$$\left[\sin\left(\varphi_x(t)\right)II_{yy}\,\ddot{\varphi}_y(t) + 2\sin\left(\varphi_x(t)\right)II_{yy}\cos\left(\varphi_x(t)\right)\dot{\varphi}_x(t)\,\dot{\theta}_z(t) + II_{yy}\,\ddot{\theta}_z(t) - II_{yy}\,\ddot{\theta}_z(t)\cos\left(\varphi_x(t)\right)^2 - 2\cos\left(\varphi_x(t)\right)II_{xx}\sin\left(\varphi_x(t)\right)\right.$$
$$\left.\dot{\varphi}_x(t)\,\dot{\theta}_z(t) + II_{xx}\cos\left(\varphi_x(t)\right)^2\ddot{\theta}_z(t) + \cos\left(\varphi_x(t)\right)II_{yy}\,\dot{\varphi}_y(t)\,\dot{\varphi}_x(t)\right]\Big]$$

Combing both moments expressed in the device frame gives then:

> $M_{\mathrm{D}} := M_d + M_{2d}$

$$M_{\mathrm{D}} := \left[\left[0\right],\left[0\right],\right.$$
$$\left[2\sin\left(\varphi_x(t)\right)II_{yy}\,\ddot{\varphi}_y(t) + 4\sin\left(\varphi_x(t)\right)II_{yy}\cos\left(\varphi_x(t)\right)\dot{\varphi}_x(t)\,\dot{\theta}_z(t) + 2\,II_{yy}\,\ddot{\theta}_z(t) - 2\,II_{yy}\,\ddot{\theta}_z(t)\cos\left(\varphi_x(t)\right)^2\right.$$
$$\left.- 4\cos\left(\varphi_x(t)\right)II_{xx}\sin\left(\varphi_x(t)\right)\dot{\varphi}_x(t)\,\dot{\theta}_z(t) + 2\,II_{xx}\cos\left(\varphi_x(t)\right)^2\ddot{\theta}_z(t) + 2\cos\left(\varphi_x(t)\right)II_{yy}\,\dot{\varphi}_y(t)\,\dot{\varphi}_x(t)\right]\Big]$$

And with constant spinnrate, $\ddot{\varphi}_y(t) = 0$:

> $M_{D1} := subs\left(\ddot{\varphi}_y(t) = 0, M_{\mathrm{D}}\right)$

$$M_{D1} := \left[\left[0\right],\left[0\right],\right.$$
$$\left[4\sin\left(\varphi_x(t)\right)II_{yy}\cos\left(\varphi_x(t)\right)\dot{\varphi}_x(t)\,\dot{\theta}_z(t) + 2\,II_{yy}\,\ddot{\theta}_z(t) - 2\,II_{yy}\right.$$
$$\ddot{\theta}_z(t)\cos\left(\varphi_x(t)\right)^2 - 4\cos\left(\varphi_x(t)\right)II_{xx}\sin\left(\varphi_x(t)\right)\dot{\varphi}_x(t)\,\dot{\theta}_z(t)$$
$$\left.+ 2\,II_{xx}\cos\left(\varphi_x(t)\right)^2\ddot{\theta}_z(t) + 2\cos\left(\varphi_x(t)\right)II_{yy}\,\dot{\varphi}_y(t)\,\dot{\varphi}_x(t)\right]\Big]$$

END